

# Origins, Behavior, and Sedimentology of Lahars and Lahar-Runout Flows in the Toutle-Cowlitz River System

LAHARS AND LAHAR-RUNOUT FLOWS IN THE TOUTLE-COWLITZ RIVER  
SYSTEM, MOUNT ST. HELENS, WASHINGTON

---

U.S. GEOLOGICAL SURVEY PROFESSIONAL PAPER 1447-A



# Origins, Behavior, and Sedimentology of Lahars and Lahar-Runout Flows in the Toutle-Cowlitz River System

By KEVIN M. SCOTT

LAHARS AND LAHAR-RUNOUT FLOWS IN THE TOUTLE-COWLITZ RIVER SYSTEM, MOUNT ST. HELENS, WASHINGTON

---

U. S. GEOLOGICAL SURVEY PROFESSIONAL PAPER 1447-A

*Analyses of modern flows  
lead to greater understanding  
of ancient flow deposits*



---

UNITED STATES GOVERNMENT PRINTING OFFICE, WASHINGTON : 1988

**DEPARTMENT OF THE INTERIOR**

**DONALD PAUL HODEL, *Secretary***

**U.S. GEOLOGICAL SURVEY**

**Dallas L. Peck, *Director***

**Library of Congress Cataloging-in-Publication Data**

Scott, Kevin M., 1935-

Lahars and lahar-runout flows in the Toutle-Cowlitz River system, Mount St. Helens, Washington.

(U.S. Geological Survey professional paper ; 1447-A- )

Includes bibliographies.

Contents: [1] Origins, behavior, and sedimentology of Lahars and Lahar-Runout flows in the Toutle-Cowlitz River System — [2] Magnitude and frequency of Lahars and Lahar-Runout flows in the Toutle-Cowlitz River System.

Supt. of Docs. no.: I 19.16:1447-A-B

1. Lahars—Washington (State)—Toutle River Watershed. 2. Lahars—Washington (State)—Cowlitz River Watershed. 3. Sediments (Geology)—Washington (State)—Toutle River Watershed. 4. Sediments (Geology)—Washington (State)—Cowlitz River Watershed. I. Title. II. Series: Geological Survey professional paper ; 1447-A, etc.

QE598.2.S38 1988

551.3

86-600198

---

For sale by the Books and Open-File Reports Section, U.S. Geological Survey,  
Federal Center, Box 25425, Denver, CO 80225

# CONTENTS

	Page		Page
Abstract .....	A1	Clast lithology— <i>Continued</i>	
Introduction .....	2	Pumice .....	A42
Definitions and concepts .....	2	Low-density rock types from domes .....	42
Lahar-runout flows .....	5	Juvenile dacite derived from facies of the debris avalanche .....	42
Lahar in the strict and general senses .....	5	Eroded soil .....	42
Flow transformations .....	5	Lahar boundary features .....	43
Flow bulking .....	6	Lahar-abraded pavement .....	43
Levels of particle support .....	6	Sole layer .....	44
Boundary features .....	6	Type I—sandy sole layers lacking dispersed coarse	
Acknowledgments .....	6	clasts .....	44
Lahars and lahar-runout flows of the modern eruptive period	7	Type II—sole layers with dispersed coarse clasts ..	45
Lahars and lahar-runout flow of May 18–19, 1980 .....	7	Type III—sole layers of clast-supported gravel; the	
Lahar and lahar-runout flow of March 19–20, 1982 .....	8	“ball-bearing bed” .....	46
Phases, flow types and divisions, and facies models .....	8	Inverse grading .....	46
Phases of the 1980 South Fork lahar .....	8	Origin and relations of the boundary features .....	47
Proximal phase .....	9	Flow transformations .....	51
Medial phase .....	11	Pyroclastic surge and avalanche to debris flow .....	51
Distal phase .....	12	Temperature of the pyroclastic surge .....	54
Lahar-runout phase .....	12	Origin of water in the lahar .....	55
Flow types and divisions .....	13	Comparison with other pyroclastic surge and flow	
Longitudinal flow transformations .....	13	deposits .....	55
Flow divisions at a section—basal flow and the whale-		Comparison with Kalama- and post-Kalama-age deposits	56
back bars .....	13	Flood surge to debris flow .....	57
Lahar and lahar-runout facies models .....	16	Debris flow to hyperconcentrated streamflow .....	57
Lahar channel facies .....	17	Evidence for transformation .....	57
Lahar flood-plain facies .....	19	Characteristics of deposits of hyperconcentrated lahar-	
Lahar-runout facies .....	19	runout flows .....	60
Transition facies .....	19	Lack of stratification in particle- and clast-	
Lahar-related steamflow deposits .....	20	supported deposits .....	61
Facies of the largest lahar in the river system .....	21	Inverse grading .....	61
Size distributions of the lahars .....	21	Coarse-tail grading of low-density clasts .....	62
North Fork lahar—peak-flow deposits of the flood-plain		Concentration of low-density clasts near lateral	
facies .....	23	flow boundaries .....	62
North Fork lahar—basal-flow deposits of the channel		Sorting .....	62
facies .....	25	Transitional cumulative curves .....	62
North Fork lahar—sole layer of the channel facies .....	26	Lack of coarse inflection point in cumulative curves	63
South Fork lahar—peak-flow deposits of the flood-plain		Sediment transport in the lahar-runout flow of March	
facies .....	27	19–20, 1982, and correlation with deposit characteris-	
South Fork lahar—avalanche deposits of the deflating		tics .....	63
pyroclastic surge and basal-flow deposits of the channel		Effect of postdepositional drainage on deposit texture	66
facies .....	29	Origin and evolution of lahar-runout flows .....	66
South Fork lahar—sole layer of the channel facies .....	30	Conclusions on lahar texture as related to origin and behavior	69
Lahars of previous eruptive stages and periods .....	32	Lahars formed by flow transformations .....	69
Large lahar of the Pine Creek eruptive period .....	32	Flood surges transformed to lahars .....	69
“Ball-bearing bed” .....	32	Catastrophically ejected surges and avalanches trans-	
Alluvium—source of sediment in lahars of the Pine		formed to lahars .....	70
Creek eruptive period .....	34	Lahars formed from failure of volcanic deposits not selec-	
Clast roundness and the lahar bulking factor .....	35	tively sorted .....	70
Roundness in the 1980 lahars .....	36	Summary of the general relation of lahar origin to mag-	
Bulking factors of the 1980 lahars .....	37	nitude .....	71
Roundness in the pre-1980 lahars .....	38	Interpretations of dynamics based on texture .....	71
Bulking factors of the pre-1980 lahars .....	39	References cited .....	72
Roundness in the sole layers .....	40	Appendix—Equations used in calculating lahar velocity and	
Abrasion and cataclasis in lahars .....	40	statistics of grain size distributions .....	76
Clast lithology .....	41	Velocity .....	76
Pyroxene andesite and olivine basalt .....	41	Grain size statistics .....	76

## ILLUSTRATIONS

	Page
FIGURE 1. Map showing the major streams draining Mount St. Helens .....	A3
2. Graph of stage and recession sediment concentrations in the Cowlitz River at Castle Rock, May 18-19, 1980 .....	7
3. Photograph showing surface of the debris avalanche approximately 18 km downstream from the 1980 crater .....	8
4. Photograph of pyroclastic flow formed by collapse of the Plinian eruption column .....	9
5. Photograph showing uppermost part of watershed of South Fork Toutle River, and tributary Sheep Canyon .....	10
6. Profile of the South Fork Toutle River, showing longitudinal phases of the main lahar occurring on May 18, 1980 .....	11
7. Diagram portraying origin of the 1980 South Fork lahar as the transformation of a pyroclastic surge .....	14
8. Photograph showing longitudinal view of whaleback bar in South Fork Toutle River .....	16
9. Photograph showing transverse view of whaleback bar in South Fork Toutle River .....	17
10. Diagrams portraying facies types described in table 4 .....	19
11. Cross section of Cowlitz River showing deposits of North Fork lahar of May 18, 1980, and subsequent streamflow .....	20
12. Diagrams of channel and flood-plain facies of 1980 North Fork lahar at Coal Bank Bridge and of lahars of Pine Creek age near the Green Mountain Mill .....	22
13. Graphs showing downstream changes in particle-size distribution characteristics in peak-flow deposits of 1980 North Fork lahar .....	23
14. Cumulative curves and histograms of peak-flow deposits of the North Fork lahar .....	24
15. Photograph of bar deposits of North Fork lahar at confluence of forks of Toutle River .....	26
16. Photograph showing channel facies of the North Fork lahar at Kid Valley .....	27
17. Cumulative curves of sole layer, bar, and peak-flow deposits of the North Fork lahar near Kid Valley .....	28
18. Photograph showing two subunits in sole layer of North Fork lahar at the Highway 99 bridge .....	29
19. Graphs showing downstream changes in mean size, sorting, skewness and percent clay in peak-flow deposits of the 1980 South Fork lahar .....	30
20. Cumulative curves of the distal phase of the South Fork lahar and the lahar-runout flow derived from that lahar .....	31
21. Graphs showing downstream changes in mean size and sorting of the avalanche and bar deposits of the South Fork pyroclastic surge and lahar .....	32
22. Cumulative curves and histograms for first lahar of Pine Creek age, including channel and flood-plain facies, the "ball-bearing bed," and alluvium in a megaclast .....	34
23. Photograph of "ball-bearing bed" at base of first lahar of Pine Creek age .....	35
24. Photograph of megaclast in the first lahar of Pine Creek age .....	36
25. Graph showing mean roundness of particles in first lahar of Pine Creek age, alluvium in a megaclast in that lahar, and bar and flood-plain deposits of 1980 North Fork lahar .....	37
26. Histograms showing distribution of clast roundness in Pine Creek age and 1980 deposits .....	38
27. Graph showing clast roundness in sole layer, bar deposits, and flood-plain deposits of 1980 North and South Fork lahars .....	39
28. Graph showing downstream variations in percentages of andesite, basalt, and pumice in peak-flow deposits of the 1980 North and South Fork lahars .....	41
29. Photograph of surface formed by compaction and truncation at contact of two units of the bar deposits of North Fork lahar .....	44
30. Photograph showing flood-plain facies of three older lahars .....	45
31. Photograph showing sole layer of first lahar of Pine Creek age on valley side slope near Kid Valley Bridge .....	47
32. Diagrammatic cross section showing distribution of sole layer and inverse grading in North Fork lahar near Tower Bridge .....	48
33. Photograph showing lateral margin of lahar deposit on surface of the debris avalanche near Elk Rock .....	51
34. Graph showing discharge and velocity of pyroclastic surge and main lahar in South Fork Toutle River .....	52
35. Photograph of pyroclastic surge descending southwest flank of Mount St. Helens 2 min after beginning of the May 18, 1980, eruption .....	53
36. Diagrammatic sections of depositional units of 1980 South Fork lahar, 1982 lahar, and runout flows evolved from those lahars .....	58
37. Diagram showing downstream change in texture resulting from transformation of debris flow to hyperconcentrated streamflow .....	60
38. Photograph of deposits of the main peak of 1982 runout flow at Kid Valley, near downstream end of the transition interval .....	60
39. Diagram showing textural change in transition facies of 1982 lahar, just upstream from Kid Valley .....	61
40. Cumulative curves of inversely graded part of transition facies of 1982 lahar .....	61
41. Cumulative curves of 1982 lahar and lahar-runout flow deposits, compared with modern and ancient streamflow deposits .....	63
42. Graphs of discharge and sediment concentration of 1982 lahar-runout flow at Tower Road .....	64
43. Sediment transport curve of the 1982 lahar-runout flow at Tower Road .....	65

## TABLES

	Page
TABLE 1. Known lahars and lahar-runout flows in the Toutle-Cowlitz River system . . . . .	A4
2. Interpreted characteristics of at-a-section flow subdivisions in lahars . . . . .	13
3. Dimensions of whaleback bars formed by the 1980 lahar in the South Fork Toutle River . . . . .	14
4. Facies characteristics of large lahars and associated flows from Mount St. Helens . . . . .	18
5. Textures of selected pre-1980 lahars and lahar-runout flow deposits . . . . .	33
6. Clast roundness in pre-1980 lahars . . . . .	38
7. Characteristics of the sole layers of the 1980 North Fork and South Fork lahars . . . . .	49
8. Measured peak sediment concentration and adjusted mean size and sorting values for the lahar-runout flow of March 19-20, 1982 . . . . .	67
9. Sequential changes in flow type and particle-support mechanisms during the transformation from lahar, to lahar-runout flow, to normal streamflow . . . . .	68

## GLOSSARY

**Andesite.** Fine-grained volcanic rock characteristically medium dark in color and containing 54 to 62 percent silica.

**Ash.** Fine pyroclastic particles less than 4.0 mm in diameter.

**Ash cloud.** Turbulent cloud of fine material rising above the main body of a pyroclastic flow.

**Antidune.** A wave of cohesionless sediment that is in phase with the overlying water-surface wave (standing wave).

**Bagnold effect.** The displacement in the direction of least shear of particles within a body of sheared, mainly cohesionless sediment.

**Basalt.** Fine-grained volcanic rock characteristically dark in color and containing less than 54 percent silica.

**Base surge.** An expanding basal cloud of particles that travels outward from a large explosion.

**Bayonet trees.** Trees inclined to a low angle and sharpened to smooth spikes by lahar erosion.

**Bed load.** Material moved in traction along the bed of a river.

**Berm.** A nearly flat-topped, terracelike body of sediment deposited along the side of a channel.

**Boulder.** A sediment particle with a diameter greater than 256 mm.

**Bulking.** The addition of significant amounts of sediment to a flow by erosion.

**Celerity.** The velocity of a flood wave.

**Clast-supported.** Having a texture in which the gravel-size particles are mainly in contact.

**Clay (size).** A sediment particle with a diameter less than 0.004 mm.

**Cobble.** A sediment particle with a diameter of 64-256 mm.

**Competence.** The transporting ability of a current, expressed in terms of the maximum particle size of a given density that can be transported.

**Critical diameter.** In a lahar, the diameter above which most particles are dispersed in the finer grained matrix.

**Cross strata, beds, or laminae.** Sets of strata (beds if >1 cm; laminae if <1 cm) that are not parallel to the main layers within which they occur.

**Dacite.** Volcanic rock that characteristically is light in color and contains 62-69 percent silica.

**Debris avalanche.** A rapid flow of unsorted masses of rock and other material including, in the 1980 example in the North Fork Toutle River valley, water, snow, ice, and vegetation.

**Dispersive stress or pressure.** Stress caused by shearing of a static grain bed and resulting in dilation or dispersion that selectively moves particles upward within the flowing mass.

**Dome.** A steep-sided mass of viscous lava extruded from a volcanic vent.

**Drumlin.** Hill molded into a streamline form by glacial action.

**Fabric.** The arrangement of particles in a sedimentary deposit.

**Facies.** The characteristics of a sedimentary deposit that are imparted by the depositional environment.

**Flood plain.** A low, flat, valley-bottom area inundated by overbank flood flow.

**Flood surge.** Water wave with a steep rising limb. Also called "water surge" and "streamflow surge." Types include snowmelt and lake-breakout surges.

**Graded layer.** A deposit in which the particle sizes show a systematic vertical size change. A unit with particles systematically finer upward has normal grading or is normally graded; one with particles systematically coarser upward has inverse grading or is inversely graded. The terms may be applied to parts of a flow unit.

**Grain.** In a general sense, a synonym of particle when used as an adjective, as in grain size or coarse-grained deposit.

**Grain flow.** Flow of particles with little or no cohesion, which are not suspended by turbulence but are supported by momentum provided by interactions with other particles in the flow.

**Granule.** A sedimentary particle from 2 to 4 mm in diameter.

**Gravel.** A collective term for sedimentary particles coarser than 2 mm.

**Inverse grading.** See graded layer.

**Kinematic wave.** A wave in which the material forming the crest moves bodily forward.

**Lahar.** Volcanic debris flow and its deposits.

**Lahar-abraded pavement.** Nearly planar surface cut by a lahar, most commonly near channel thalweg.

**Lahar bulking factor (LBF).** Proportion of sediment in a lahar that can be shown to have been introduced by erosion during flow.

**Lahar-runout flow.** Hyperconcentrated streamflow mainly evolved directly from a distal lahar.

**Laminar flow.** Fluid flow in which there is sliding within the fluid along surfaces nearly parallel to the flow boundary.

**Matrix-supported.** Containing dispersed coarse clasts.

- Mud.** All material in the clay and silt size ranges.
- Particle-supported.** Having a texture in which particles are mainly in contact. A lahar may have a particle-supported matrix, yet as a whole may be characterized as matrix-supported because the gravel-size particles are dispersed. When the gravel-size particles are in contact, the unit is described as clast-supported.
- Pebble.** A sediment particle having a diameter from 4 to 64 mm.
- Phi scale.** A geometric grade scale of particle size with class boundaries based on negative logarithms to base 2,  

$$\phi = -\log_2 \text{ size (mm)}$$
- Plug.** Rigid core of a debris flow, formed in region of flow where yield strength of debris exceeds shear stress; velocity distribution in plug is nearly constant with depth.
- Pumice.** Light-colored, low-density, frothy volcanic rock (of dacite composition at Mount St. Helens) formed by the expansion of gas in erupting lava.
- Pyroclastic.** Pertaining to fragmental rock material formed by a volcanic explosion or ejection from a vent.
- Pyroclastic flow.** A flowing mixture of hot gases and pyroclastic material.
- Pyroclastic surge.** A flow that is more dispersed and less likely to approximate steady-state conditions than a pyroclastic flow. Types include the ground, base, and ash-cloud surges discussed in the text section "Comparison with other pyroclastic surge and flow deposits."
- Reach.** A length of channel with relatively uniform characteristics.
- Recession.** Falling discharge, or downward trending limb of hydrograph.
- Rosin's law.** A probability distribution produced by crushing of isotropic material:  

$$y = 100(1 - e^{-bx^n})$$
 where  $y$  is weight percent sediment passing a sieve of mesh size  $x$ ,  $b$  is the reciprocal of mean size, and  $n$  is a numerical coefficient analogous to the standard deviation of a normal distribution.
- Sand.** Sediment particles having diameters between 2.0 and 0.0625 mm.
- Sediment-transport curve.** A plot of sediment discharge and water discharge.
- Silt.** Sediment particles having diameters between 0.0625 and 0.004 mm.
- Sole layer.** Texturally distinct basal sublayer of a lahar.
- Sorting.** The dispersion of particle sizes about the mean. The term is also used to express the selective transport of different particle sizes.
- Stage.** Level above a datum of a lahar or water flood.
- Surge.** See *pyroclastic surge* and *flood surge*. Used singly, the term refers to one or the other, in context, or to an ongoing wave of turbulent flow in the process of transforming from one to the other.
- Suspended sediment.** Sediment in transport whose immersed weight is supported by the fluid.
- Tephra.** Material erupted from a volcanic crater or vent and deposited from the air.
- Thalweg.** The deepest line along a stream channel.
- Turbulent flow.** Flow that is characterized by vortices and eddies.

---

**ORIGINS, BEHAVIOR, AND SEDIMENTOLOGY OF LAHARS AND  
LAHAR-RUNOUT FLOWS IN THE TOUTLE-COWLITZ RIVER SYSTEM**

---

By KEVIN M. SCOTT

---

ABSTRACT

In the 50,000-yr history of Mount St. Helens more than 35 lahars (volcanic debris flows and their deposits) and lahar-runout flows (hyperconcentrated streamflow evolved directly from a distal lahar) have inundated flood plains more than 50 km away in the river system draining the northwest sector of the volcano. At least six of the largest lahars or their runout phases probably inundated flood plains near the Columbia River, more than 100 km downstream. Characteristics of the 1980 flow deposits were compared to those of deposits from previous eruptive stages and periods to obtain a long-term perspective of lahar origins and behavior.

Several kinds of flow transformations were associated with lahar origin and evolution: (1) Pyroclastic surge to lahar. Deflation of a catastrophically ejected, lithic pyroclastic surge directly formed the 1980 lahar in the South Fork Toutle River and is a mode of lahar genesis inferred to have occurred in at least one other eruptive period. (2) Avalanche to lahar. Catastrophically ejected avalanches, possibly also associated with pyroclastic surges or flows to varying degrees, yielded downstream lahars in older eruptive periods. (3) Flood surge to lahar. The largest two lahars in the history of the river system formed by bulking of stream alluvium in flood surges from lake breakouts through volcanically initiated natural dams. Other flows of intermediate size were formed from meltwater surges initiated by pumiceous pyroclastic flows in the oldest eruptive stage, and subsequently by lithic pyroclastic flows. The relatively small 1982 lahar also formed from a volcanically induced meltwater surge. (4) Lahar to hyperconcentrated streamflow. Lahar debulking and change to lahar-runout flow occurred in the distal phases of most of the ancient and modern flows that could be traced downstream. The most common lahars in the river system were really, therefore, the middle segments of flood waves beginning and ending as streamflow surges.

The formation of lahar-runout flows involved the progressive incorporation of streamflow overrun by the leading part of the debris flow. The change occurred over a channel distance of as much as 19 km, producing an inversely graded transition facies in which runout deposits appear as a thickening wedge at the base of a flow unit and are transitionally overlain by debris flow deposits that thin

progressively and disappear downstream. As water content increased downstream, two decrements contributed to the change from poorly sorted, mainly matrix-supported debris flow deposits to granular, particle-supported runout sand with sorting in the range of 1.1-1.6  $\phi$ : (1) dispersed coarse clasts were deposited because of loss of yield strength, and (2) some silt and clay were lost from runout deposits by rapid drainage of interstitial fluids as flow receded.

The less pronounced textural change in the few lahars with relatively more clay (3 to 5 percent) shows that formation of lahar-runout flows was in part a function of low clay content (<3 percent) and a consequent low cohesiveness that facilitated miscibility with streamflow. The lahars with more clay are inferred to have formed mainly by slumping of hydrothermally altered material, as was most of the 1980 lahar in the North Fork Toutle River. That flow extended more than 100 km with gradual textural change tending toward a hyperconcentrated runout flow, but it did not complete the transformation.

Most of the lahars in the system are relatively granular, have silty sand matrices, and contain more regions of particle support than many other reported debris flows. Particle interaction was important during flow, locally to the point of cataclasis. Distinctive flow divisions and boundary features were formed, some of which are evidence of dilatant fluid behavior. A bed-load-analog basal carpet of interacting coarse clasts developed by settling of the coarsest clasts in the lahar and by erosion of coarse alluvium from the flow boundary, at which shear was locally so concentrated that in reaches with rapid energy loss a pavement similar to a glacial pavement was cut. Pulses of basal flow formed whaleback bars during a brief period near the lahar peak. Other boundary features included a texturally distinct basal subunit described as the sole layer, and nearly universal inverse grading. The inversely graded lower part of each unit is commonly overlain by an ungraded or poorly graded core, which is in turn overlain by a normally graded upper part that was produced by settling within the intralahar "plug." The boundary features reflect variations in the intensity of shear-induced particle interactions, as well as migration of the boundary of the intralahar "plug" and development of an accretionary, roughness-reducing coating of the boundary during the flood wave rise.

## INTRODUCTION

Modern and ancient lahars and their runout phases have inundated flood plains for long distances from Mount St. Helens periodically throughout the history of the volcano. The lahars that formed during the major eruption on May 18, 1980, reached down the Toutle and lower Cowlitz Rivers as far as the Columbia River, more than 100 km away. The cost of the resulting damage and remedial engineering work in the succeeding two years exceeded 300 million dollars. The flows were spectacular in their impact on the natural landscape and in the diversity of sedimentologic features preserved in the deposits (Janda and others, 1981). Deposits from older eruptive periods reveal a history of older flows that were as extensive as the modern flows and more diverse in origin. One ancient flow was substantially more than an order of magnitude larger than the largest 1980 flow. The purpose of this report is to analyze the 1980 and subsequent lahar deposits in the Toutle-Cowlitz River system and relate the character of those flows to their observed flow behavior. The results are then applied to the older flows to interpret their origin and behavior. A companion report (Scott, in press) investigates the size and recurrence probabilities of these flows.

Field study began on the east and south sides of the volcano (fig. 1) because of the sequence of different flow types related to the May 18, 1980, eruption. There the largest lahars had originated almost synchronously with the lateral blast as the downstream continuations of a pyroclastic surge. That behavior has subsequently been quantified by Pierson (1985). In the fall of 1980, storm runoff rapidly began to erode the flow deposits in the Toutle and Cowlitz Rivers, so study was shifted to that drainage. The main lahar in the South Fork of the Toutle River had an origin like that of the large flows on the opposite side of the volcano and was the only major 1980 flow with deposits exposed through the runout phase. Although the larger lahar of May 18 in the North Fork Toutle River had a different origin, mainly by slumping of surficial parts of the debris avalanche, it shows many flow features surprisingly similar to those of the South Fork lahar. As the runoff season of 1980-81 progressed, each flood flow revealed a new erosional "slice" of the 1980 lahars and also exposed new stratigraphic sections of the older lahars (table 1). The sedimentary features of both the modern and ancient flows were then observed in three dimensions as erosion progressed.

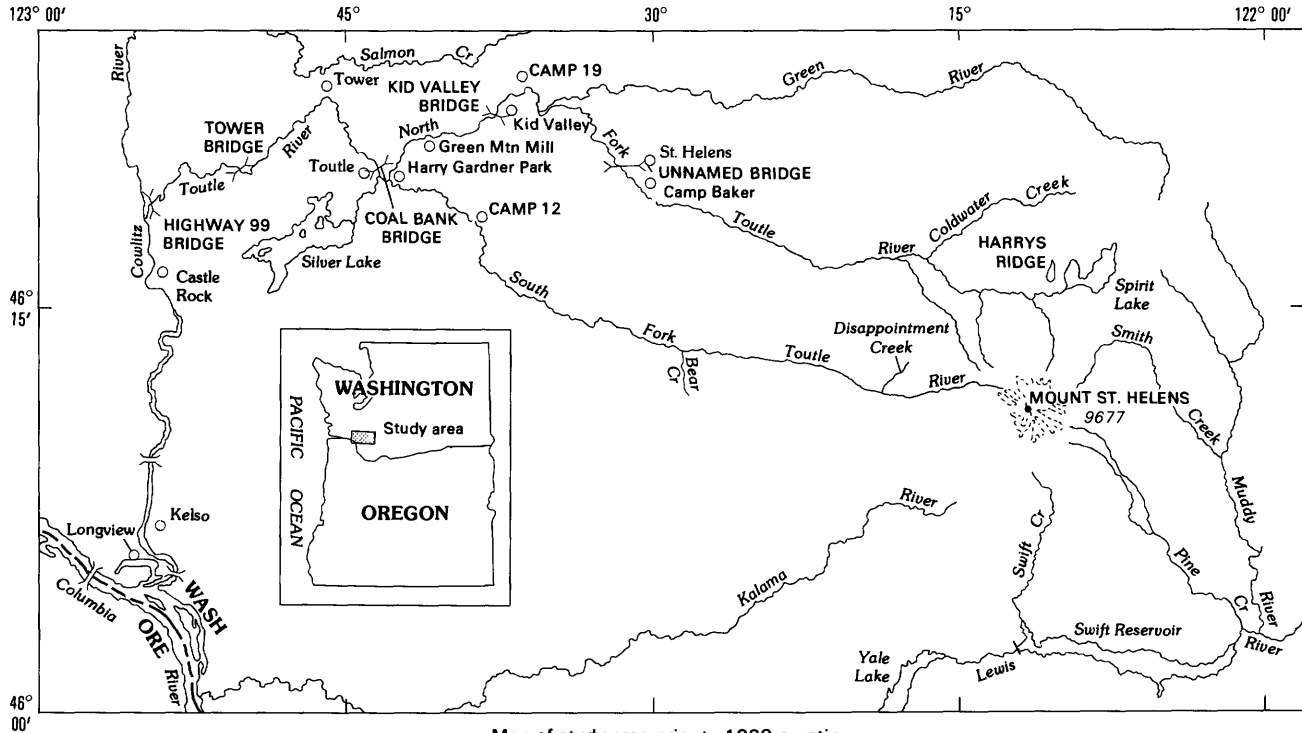
The use of the term "lahar" for both volcanic debris flows and volcanic mudflows, as well as for their deposits, avoids some problems in terminology. The 1980 lahars have been commonly described in popular and scientific reports as mudflows, a category of debris flows in which mud (the total of silt- and clay-size sediment)

is a significant part of the deposits. A widely accepted practical definition used here is that of Varnes (1978, p. 18), who defined mudflows as those debris flows with deposits containing at least 50 percent sand, silt, and clay. Some definitions place greater emphasis on the clay content; for example, mudflows commonly contain 25 percent or more clay according to Friedman and Sanders (1978). A mudflow differs generally from other debris flows by having enough silt and clay to give the deposit a muddy appearance. On this subjective distinction, the peak-flow deposits of the 1980 lahars qualify as mudflows. They also qualify on a specific textural basis according to Varnes (1978). However, most of the clast-supported bar deposits (having mainly gravel-size clasts in contact) do not meet the Varnes criteria for a mudflow and also lack the characteristic matrix-supported texture (clasts "float" in matrix) of typical debris flow deposits.

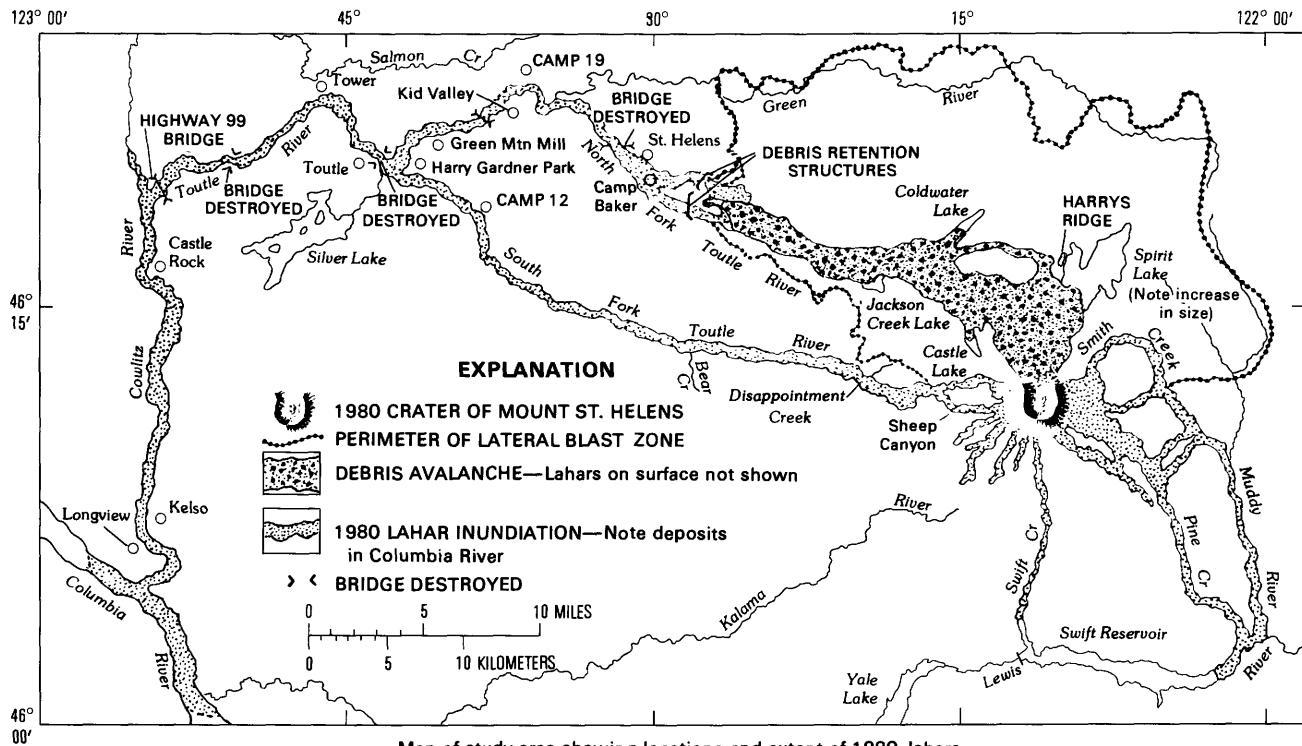
Worldwide, lahars had taken lives numbered in the tens of thousands by 1976 (Neall, 1976a, b). Then, in 1985, a single eruption in Colombia produced lahars that killed more than 20,000 people. "Lahar" is an Indonesian term for a debris flow containing angular volcanic blocks (van Bemmelen, 1949), but is of diverse application there and elsewhere. Some subsequent definitions have expanded the term to include torrential waterflows (Schieferdecker, 1959) or hyperconcentrated streamflows (Fisher and Schmincke, 1984), whereas others have limited it to a specific composition (Schmid, 1981) or an origin on the flank of a volcano (Crandell, 1971; Bates and Jackson, 1980). The term "lahar" is applied here to flows and deposits equivalent in most respects to those described by D. R. Crandell and D. R. Mullineaux at several Cascade Range volcanoes. (See References Cited.) Although relatively small debris flows may be a daily occurrence on active and some inactive volcanoes, any magnitude distinction for a lahar should remain subjective. Usage of the term has generally implied a flow large enough to pose a hazard, as well as one that is the direct or indirect result of volcanic activity (rather than a product of the alpine environment, as in the case of small, snowmelt-induced debris flows). The variety of compositions and textures of lahars documented at Mount St. Helens, and the variety of origins of the lahars on and beyond the base of the mountain, emphasize that the term is most useful if not qualified beyond the definition of a debris flow related (even indirectly) to volcanic activity.

## DEFINITIONS AND CONCEPTS

Several undescribed lahar features and debris-flow behavior modes came to light during the study. These are described at appropriate locations in the text, but



Map of study area prior to 1980 eruption



Map of study area showing locations and extent of 1980 lahars

FIGURE 1.—Major streams draining Mount St. Helens. The Toutle-Cowlitz River system drains most of northwest half of the volcano. The natural flow of Spirit Lake into the North Fork Toutle River is now blocked by the debris avalanche.

## LAHARS AND LAHAR-RUNOUT FLOWS, TOUTLE RIVER, WASHINGTON

TABLE 1.—Occurrence and extent of known lahars and lahar-runout flows in the Toutle-Cowlitz River system

[Eruptive history of Mount St. Helens after Crandell (1987, and written commun., 1984) and Mullineaux (1986); tephra units from Mullineaux and Crandell (1981) and Mullineaux (1986). The number of flows large enough to have inundated flood plains at the confluence of the forks of the Toutle River is indicated for each eruptive period. Dating and stratigraphy of the flows are discussed in Scott (in press)]

Eruptive stages and periods	Approximate age <sup>1</sup>	Tephra set	No. of overbank flows	Occurrence and extent
<b>SPIRIT LAKE ERUPTIVE STAGE:</b>				
Period beginning in 1980	Modern	1980	2	1980 lahar in South Fork Toutle R. extended to confluence of forks (a second, non-overbank lahar also reached confluence). Runout phase reached the Cowlitz R. 1980 lahar in North Fork Toutle R. extended to Columbia R. 1982 lahar in North Fork extended to Kid Valley. Runout phase reached Cowlitz R.
-----Dormant interval of 123 yr-----				
Goat Rocks eruptive period	150-93	T	0	No lahars extended significant distances past base of cone.
-----Dormant interval of about 200 yr-----				
Kalama eruptive period	470-320	W, X	3	Avalanches and coarse rubbly lahars buried forests in upper South Fork, may correlate with 2 downstream overbank lahars that extend to confluence. 3 lahars probably of this age in North Fork; at least 1 was overbank and extended to confluence.
-----Dormant interval of about 700 yr-----				
Sugar Bowl eruptive period	1,200	---	0	No lahars extended significant distances past base of cone.
-----Dormant interval of about 500 yr-----				
Castle Creek eruptive period	2,200-1,700	B	0	Lahar probably of this age in North Fork extended in paleo-channel at least to Camp Baker. Lahars of this period are unlikely to be preserved in stratigraphic record because of the erosional regime that probably existed after emplacement of the voluminous Pine Creek lahar deposits.
-----Dormant interval of about 300 yr-----				
Pine Creek eruptive period	3,000-2,500	P	5	At least 2 initial lahar-runout flows, 1 overbank, extended to confluence. 1 huge lahar followed by 3 smaller flows in North Fork extended to confluence. At least the first and third lahars in this sequence reached Cowlitz R. and probably extended to Columbia R.
-----Dormant interval of about 300 yr-----				
Smith Creek eruptive period	4,000-3,300	Y	5	3 lahars and at least 2 overbank runout flows extended at least to confluence. Youngest 2 lahars originated in North Fork. Largest lahar probably reached Columbia R.
-----Dormant interval of about 5,000 yr-----				
SWIFT CREEK ERUPTIVE STAGE	13,700->9,200	S, J	11	10 lahars and 1 overbank runout flow extended at least to confluence.
-----Dormant interval of about 5,000 yr-----				
COUGAR ERUPTIVE STAGE	20,400-19,200	M, K	1	At least 1 large lahar extended to Cowlitz R. and probably to Columbia R.
-----Dormant interval of about 15,000 yr-----				
APE CANYON ERUPTIVE STAGE	50,000(?) to ~36,000	C	>8	At least 5 lahars and several overbank runout flows extended at least to confluence. At least 2 lahars probably extended to Columbia R.

<sup>1</sup> Years before 1950. Based on radiocarbon dates, except for ages of Goat Rocks period (based on tree rings and historic records) and Kalama period (based on tree rings and radiocarbon dates).

an introduction to some concepts and terminology is a necessary preliminary to the discussion.

#### LAHAR-RUNOUT FLOWS

The lahar-runout flows consisted of hyperconcentrated streamflow, defined as flow containing from 40 to 80 percent sediment by weight (Beverage and Culbertson, 1964), which corresponds to 20 to 60 percent by volume or to concentrations of 400,000 to 800,000 ppm or 530,000 to 1,590,000 mg/L. Hyperconcentrated streamflow of three separate origins has been documented by measurements of suspended sediment in the river system: (1) recession streamflow associated with the two largest lahars in 1980, (2) a small lake-breakout flood surge in August 1980 on the surface of the 1980 debris avalanche, and (3) the runout phase of the 1982 lahar. Further study of the 1980 and 1982 runout flow deposits and of sediment transport in the 1982 flow yields a more specific description. The vertical textural sequences in a facies transitional between the lahars and lahar-runout flows show that the change occurred through progressive loss of sediment concomitant with dilution by streamflow that was overrun by the leading edge of the lahar. Thus most of the hyperconcentrated runout flow evolved directly from the leading edge and peak of the lahar. Unlike the runout flow, the recession hyperconcentrated flow did not leave significant deposits. As a practical matter, though, beyond the zone of transition, hyperconcentrated flow derived from the recessional limb of the lahar flood wave cannot be differentiated from that produced by transformation of the peak and leading edge. Therefore, the definition of a lahar-runout flow advanced here embraces all hyperconcentrated streamflow downstream from a lahar, regardless of origin. Recognizing that most such streamflow will have evolved directly from the distal part of the lahar emphasizes the importance of the dilution process.

The hyperconcentrated flows evolved to normal streamflow with further dilution downstream. That streamflow can be considered the distal part of the lahar-runout flow but did not differ significantly from normal flood flow in the river system. Because this report focuses on the hyperconcentrated flows and the characteristics of their deposits, lahar-runout flows are described as the hyperconcentrated portion of the downstream flow wave. Discovering the unique characteristics of modern lahar-runout deposits leads to the recognition of ancient lahars and thus to the inclusion of those events in analyses of magnitude and frequency.

#### LAHAR IN THE STRICT AND GENERAL SENSES

The recognition of lahar-runout flows raises the question of whether the hyperconcentrated runout flow and the normal streamflow that evolves farther downstream should be considered parts of the lahar. The most common usage of "lahar" is for a rheologically obvious debris flow. That usage describes a lahar in the strict sense. A more general description would include downstream flows and deposits of flows transformed from—but not part of—a debris flow (the usage of Crandell and others, 1984). A complication is the fact that, over the interval of transformation from lahar to runout flow, which may extend for many kilometers, the single depositional unit consists of debris-flow deposits overlying streamflow deposits. The front of the single flood wave is hyperconcentrated streamflow; the tail consists of debris flow. The segment of channel where this occurs is called the transition interval and is included in the runout phase; the depositional unit is called the transition facies.

#### FLOW TRANSFORMATIONS

The lahars in the river systems of Mount St. Helens differ significantly from most nonvolcanic debris flows. (See Costa, 1984.) Major differences are their magnitude, the distance traveled, their very low clay content (less than 1 percent in some cases), and the systematic downstream textural changes. The textural changes reflect the long distances traveled and the flow transformations by which the lahars formed from previously sorted materials that had lost much of their fine sediment (Scott, 1984; 1985a). The most common origin, and that forming the largest flows (Scott, 1985b), was the transformation of a water flood to a lahar through the incorporation of eroded sediment. The consequently granular, noncohesive texture of most of the lahars was the main factor contributing to the downstream transformations to lahar-runout flows by mixing of the leading edges of the lahars with perennial streamflow. In contrast, many debris flows of alpine and semiarid areas rapidly lose water as they move across permeable alluvial fans or through ephemeral channels.

Many features of the lahars in the river system are similar to the features of sediment gravity flows (fluids driven by gravity acting on sediment) in subaqueous settings. To emphasize the importance of sediment concentration on the behavior of those flows, Fisher (1983) developed the concept of flow transformation and defined it as the change between laminar and turbulent behavior involving (1) change without much variation in water content (body transformations), (2) separations resulting from gravity (gravity transformations), and

(3) separations by turbulent mixing with the ambient fluid above the flow surface (surface transformations). This general concept is extended to the changes by which the lahars and their runout flows formed and evolved. Their forms of transformations also include (1) change from the turbulent behavior of a flood surge to the mainly laminar behavior (see Enos, 1977) of a debris flow because of sediment added at the flow boundary and, conversely, (2) change from a mainly laminar debris flow back to turbulent behavior as sediment concentrations were diluted into the lower part of the hyperconcentrated range by streamflow that had been overrun. The formation of a lahar from a pyroclastic surge and the segregation of basal avalanches from the surge represent gravity transformations. The continuing flow of avalanches as lahars is included here as a category of transformation, although it does not involve as radical a change in behavior.

The flows and deposits recording the transformation from a lahar to hyperconcentrated flow show a transition in which, although normal debris-flow characteristics and the ability to suspend gravel-size clasts were lost, grain contact and interaction were important and turbulence was not well developed. This intermediate type of behavior is that of a dilatant fluid that has some of the characteristics of grain flow (Bagnold, 1954, 1956; Lowe, 1976, 1979). Sediment support in grain flow is in part by particle-to-particle contact that, in a sheared, normally distributed mixture, can move larger particles in the direction of least shear (generally upward and inward). Dilatant fluid behavior also was characteristic of the lahars in the system (Denlinger and others, 1984); that behavior is presented as a general model of debris flow by Takahashi (1981).

#### FLOW BULKING

The term "bulking" is used as a general term for the incorporation of sediment in a flow by erosion at the flow boundary, as in the case of a flood surge adding sediment to the point that the flow is transformed to a lahar. Although not in common use (see Costa, 1984), the term has been applied in the same general sense to the incorporation of large amounts of sediment in flood flows in mountain watersheds (for example, Flaxman, 1974), irrespective of whether the bulked flow was Newtonian or non-Newtonian. A lahar bulking factor (LBF) is defined as the proportion of the sediment in a lahar that was demonstrably incorporated through bulking of alluvium, leading in combination with other evidence to the recognition of lahars formed by transformation of flood surges in channels beyond the base of the volcano.

#### LEVELS OF PARTICLE SUPPORT

Particle or clast support in the lahars may exist at three levels: (1) Locally in some lahars, megaclasts form an intact framework with normal laharic sediment as the matrix. (2) Clasts forming the normal coarse mode of the lahar commonly develop an intact framework in the bar deposits. (3) The matrices of all types of lahar deposits in the river system are commonly supported by sand (particles 0.0625–2.0 mm in contact). The view of a lahar as consisting of a continuous or matrix phase and a dispersed phase (Fisher, 1971) could be replaced by a description of the sediment as a matrix phase and a coarse-grained phase. The latter phase may or may not be dispersed.

#### BOUNDARY FEATURES

A group of distinctive boundary features provides evidence for interpreting flow behavior. A zone or carpet of boulder-size clasts near or at the base of the lahars was formed by settling of coarse material initially dispersed in the flow and by the erosion of coarse streambed alluvium. Lahar-abraded pavements beneath the flows record intensely concentrated shear and boulder impacts on the bed even at flow depths of only several meters. The amount of shear has implications for dam and spillway design in potentially lahar-impacted watersheds. A related feature is the sole layer, defined as a texturally distinct basal sublayer in a lahar, typically 10–25 cm thick and, in the 1980 examples, characterized by compaction and primary foliation. The sole layer formed during the rising and peak stages of flow and is characteristic of preexisting channels and other locations where shear was concentrated at the flow boundary. The remarkable "ball-bearing bed" is a sole layer of concentrated fine pebbles sorted, abraded, and fractured near the flow boundary of the first lahar of Pine Creek age, a huge lahar that formed by bulking of a flood surge released from an ancestral Spirit Lake.

#### ACKNOWLEDGMENTS

I am indebted to the staff of the U.S. Geological Survey's David A. Johnston Cascades Volcano Observatory for many helpful discussions. Individuals are cited in the text. Wayne Steuben performed or supervised the size analyses, solving the analytical problems presented by variable particle density and angularity. A number of local residents provided important information, among them Ted Conradi, whose observations of the 1980 flows as they inundated his property near

Tower verified the identification of the transition facies of the South Fork lahar-runout flow in that area. The study of the largest lake-breakout lahar of Pine Creek age was a cooperative project with the Cowlitz County Department of Community Development. S. L. Deatherage of that organization greatly facilitated that aspect of the work.

Drafts of several sections of the report benefited from discussion with or review by R. J. Janda and T. C. Pierson of the U.S. Geological Survey, and R. H. Dott, Jr., University of Wisconsin; R. V. Fisher, University of California at Santa Barbara; M. F. Sheridan, Arizona State University; and J. F. Hubert, University of Massachusetts.

## LAHARS AND LAHAR-RUNOUT FLOWS OF THE MODERN ERUPTIVE PERIOD

### LAHARS AND LAHAR-RUNOUT FLOW OF MAY 18-19, 1980

The first modern lahar in the Toutle River system was observed in the South Fork Toutle River 8 km west of the crater of Mount St. Helens less than 10 minutes after the eruption at 0832 P.d.t. on May 18, 1980 (eyewitness account reported by Rosenbaum and Waitt, 1981). The flow (hereafter called the South Fork lahar) began as a pyroclastic surge that deflated at the base of the cone and continued as a debris flow, with overbank depths commonly in the range of 4-18 m, to the confluence of the forks of the Toutle River. Shortly below that point the flow mixed with streamflow of the main Toutle River and continued mainly as a runout phase that was only locally overbank. The runout flow was in turn diluted to normal streamflow at the confluence with the Cowlitz River, causing a rise in stage of only 1.0 m at Castle Rock (fig. 2). Peak flow velocity (mean velocity at peak stage, in most cases corresponding to peak discharge) of the lahar decreased from more than 30 m/s upstream to less than 10 m/s near the confluence of the forks (Fairchild and Wigmosta, 1983).

The largest lahar of the present eruptive period at Mount St. Helens occurred in the North Fork Toutle River. That flow (hereafter called the North Fork lahar) formed mainly by dewatering of the debris avalanche deposit (fig. 3) and consequent slumping and erosion of its surface, after a relaxation time of about 5 hours on May 18 (Janda and others, 1981). Part of the lahar probably formed by bulking of large spring discharges on the erodible avalanche surface (R. J. Janda and Harry Glicken, oral commun., 1982). The devastating, broadly peaked flow (fig. 2) covered the flood plains of the North Fork and the main Toutle River to depths commonly

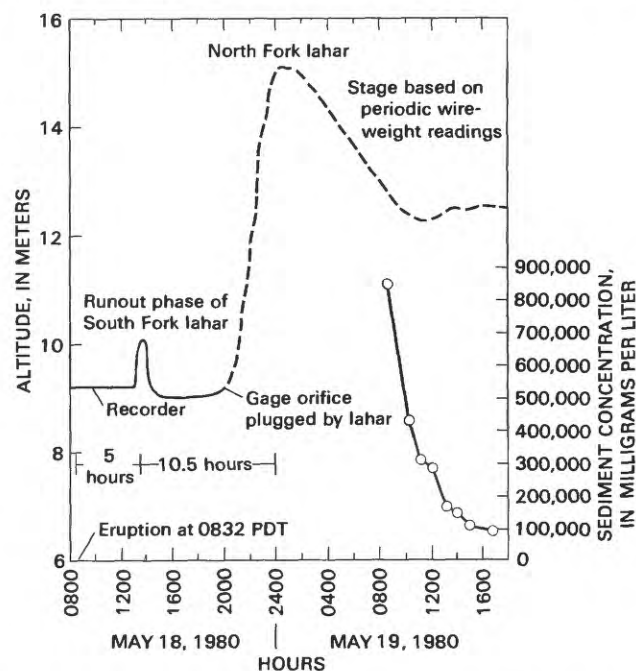


FIGURE 2.—Stage and recession sediment concentrations in the Cowlitz River at Castle Rock, May 18-19, 1980 (data from Lombard and others, 1981, and Dinehart and others, 1981). The earliest measured concentration of recession flow is in the hyperconcentrated range.

between 2 and 6 m. The flow inundated flood plains only locally in the upstream part of the Cowlitz River. Without existing levees, though, overbank areas as far as the confluence with the Columbia River would have been inundated. Flow velocity, ranging between 6 and 12 m/s, and peak discharge, ranging between 6,000 and 8,500 m<sup>3</sup>/s, declined only gradually downstream in the Toutle River system (Fairchild and Wigmosta, 1983).

Both the North Fork and South Fork lahars caused significant channel modification and instability. The changes reflect lahar deposition, mainly on flood plains but also as bars in the channel, as well as erosion of alluvium, mainly from the preexisting active channel. The overall change was in most cases one of net fill and significant loss of channel capacity. The reduction in channel roughness may have contributed to the more peaked discharge of subsequent flows (Orwig and Mathison, 1982), but the effects are difficult to separate from those of the changed rainfall-runoff relations. In the main Toutle River, channel change caused by the runout flow of the South Fork lahar appears to have been locally pronounced, but could not be separated from the larger changes associated with the succeeding North Fork lahar because of the thick deposits from that flow that covered those of the runout flow. Changes at cross sections on the North Fork, South Fork, and main Toutle River are shown in Janda and others (1981);



FIGURE 3.—Surface of the debris avalanche approximately 18 km downstream from the 1980 crater. Smooth areas are underlain by deposits of the 1980 North Fork lahar. Photograph by Austin Post, June 30, 1980.

subsequent adjustments in channel geometry are discussed by Lisle and others (1983).

The final lahar of May 18 began about 1400 P.d.t. and was a much smaller flow seen in the upper South Fork by the observer who reported the initial large flow. This lahar formed high on the flanks of the cone and was highly pumiceous, suggesting an origin connected with the loading and icemelt or snowmelt effects of small pumiceous pyroclastic flows like the one shown in figure 4. As suggested by flow tracks extending continuously from the crater rim (fig. 5), the lahar probably formed directly from a pyroclastic flow interacting with the

muddy (13–22 percent silt and clay) deposits of the earlier pyroclastic surge and the surge-scoured surfaces of the Toutle and Talus Glaciers. The second flow generally was confined to the channel except (1) in the uppermost reaches a short distance from the base of the cone (fig. 5), and (2) at its downstream end, where it inundated a large area of flood plain after being dammed at Harry Gardner Park by the earlier deposits of the North Fork and South Fork lahars.

#### LAHAR AND LAHAR-RUNOUT FLOW OF MARCH 19–20, 1982

A lahar was produced in the North Fork Toutle River from a flood surge formed by melting of a thick snowpack by hot eruption products during the dome-building eruption of March 19, 1982 (Waitt and others, 1983). The main flood surge transformed to a lahar by sediment bulking as the flow left the crater and crossed the debris avalanche surface (Pierson and Scott, 1985). An initial peak that could be traced in its runout phase for more than 80 km was followed by a second, lower peak that could not be traced beyond 50 km from the crater. The 1982 lahar is significant because its origin—by bulking of a flood surge—is similar to that of the largest older lahar in the watershed and because it transformed downstream to a runout flow that extended to the Cowlitz River. The peak velocities of the lahar and lahar-runout flow ranged between 8 and 15 m/s and 4 and 7 m/s, respectively (Pierson and Scott, 1985).

The progressive changes in the 1982 runout flow and deposits and the associated hydrologic and sediment data are discussed in the section on flow transformations. Another interpretation of the lahar and lahar-runout flow (Harrison and Fritz, 1982) is discussed in the section on lahar and lahar-runout facies models.

### PHASES, FLOW TYPES AND DIVISIONS, AND FACIES MODELS

#### PHASES OF THE 1980 SOUTH FORK LAHAR

Most ancient and modern lahars in the river system changed markedly downstream. The South Fork lahar was studied in detail because many of the longitudinal changes in the texture and behavior of that flow (fig. 6) were seen in other 1980 lahars and the March 1982 lahar. Similar changes in texture and, by inference, in behavior were observed in older flows that could be traced downstream for a significant distance. In contrast, the damaging North Fork lahar was unusual in that its deposits show only a slight yet systematic

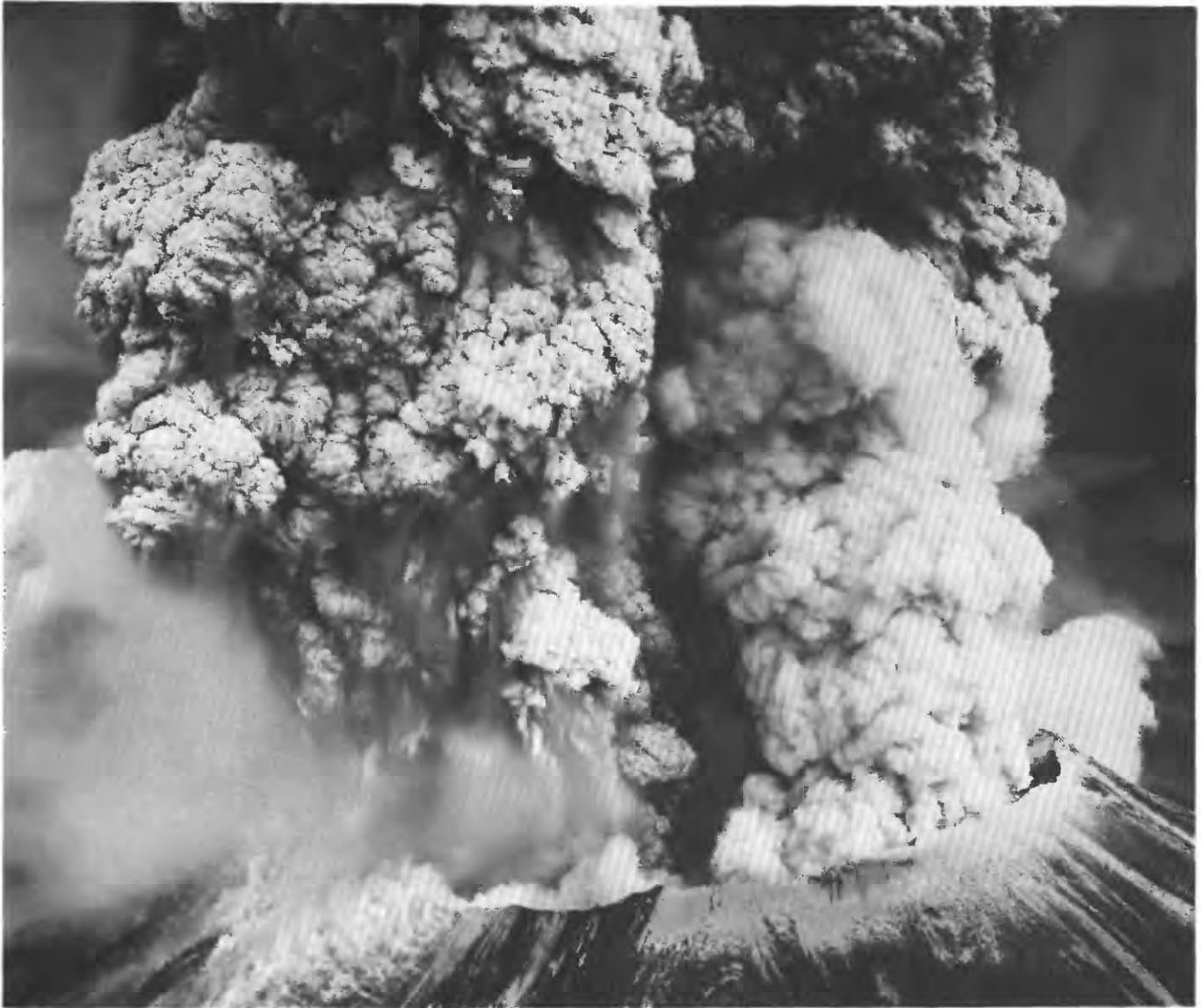


FIGURE 4.—Pyroclastic flow (on left) formed by marginal collapse of the Plinian eruption column, entering the watershed of the South Fork Toutle River. Photograph by Robert M. Krimmel at approximately 1100 P.d.t. on May 18, 1980.

textural change downstream, and the main flood wave moved continuously as a mudflow from the debris avalanche to the Columbia River. That lahar did not exhibit the pronounced phases of the South Fork lahar, a difference that relates to the relatively high clay content of the North Fork lahar.

#### PROXIMAL PHASE

The South Fork lahar (fig. 6) began as the direct transformation of a voluminous macroturbulent flow, as shown by the continuity of flow deposits and by the accompanying textural and behavioral evidence that is described in the section on flow transformations. The

flow originated in the first minutes of the May 18 eruption, was initially highly inflated by air and gas, and had many of the characteristics of a pyroclastic surge. Flow velocities of the surge measured in confined channels on the middle slopes of the cone were at least 60 m/s.<sup>1</sup> As the flow gradually settled and progressively lost air and gas, velocity declined to the range of 30–37 m/s.

<sup>1</sup>A comprehensive study of the dynamics of the 1980 South Fork lahar was not made because of other concurrent studies on the subject (for example, Fairchild and Wigmosta, 1983). Most of the measurements given herein were made upstream from those by Fairchild and Wigmosta, to illustrate the dynamic changes of the South Fork flow in the zone of rapid deflation and change from an air- and gas-mobilized surge to a water-mobilized lahar. (See data in section on flow transformation.) The data are compatible with those of Fairchild and Wigmosta in the zone of overlap. See the appendix for an explanation of the methods used in calculating flow velocity at peak stage.



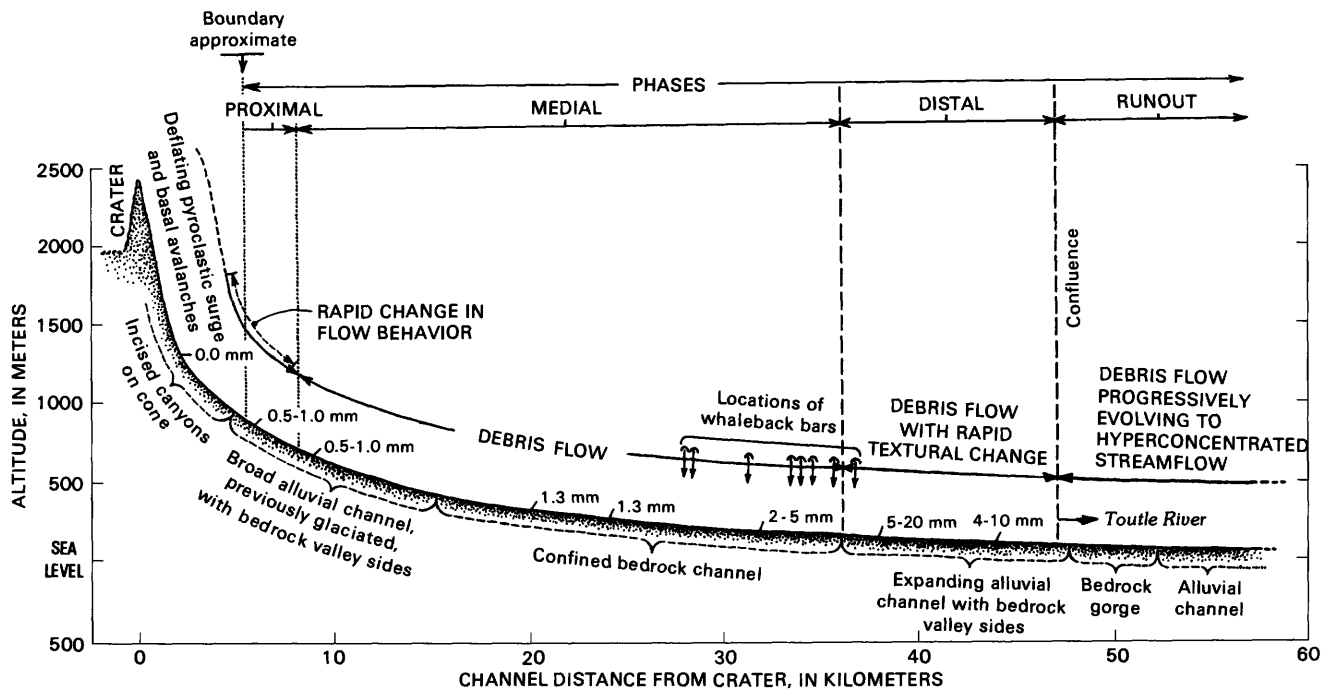


FIGURE 6.—Profile of the South Fork Toutle River from the crater rim to the confluence with the North Fork, showing longitudinal phases of the main lahar of May 18, 1980. Thicknesses of mud coatings on trees are shown in millimeters.

Peak discharge attenuated very rapidly, declining from 1,100,000 m<sup>3</sup>/s on the middle slopes to 120,000 m<sup>3</sup>/s near the start of the water-mobilized phase, over a distance of 3.3 km.

The deposits of both the pyroclastic surge and the proximal lahar are characterized by textural variability. Coarse rubbly deposits settled from the surge in canyon bottoms, whereas thin, silty, locally pebble-rich deposits accreted to canyon sides at flow depths that exceeded 100 m in some places. As water mobilization increased downstream, coarse muddy bars formed in channels, and muddy peak-flow deposits with sorting as poor as 4.4  $\phi$  (graphic standard deviation<sup>2</sup>) coated valley sides. The proximal phase of the South Fork lahar can be considered to include the deflating part of the

surge or, as in figure 6, to include only the part of the flow that shows clear evidence of being dominantly water mobilized. The boundary between the surge and lahar is transitional and is located in figure 6 at the approximate point where water mobilization clearly dominated, although much deflation had occurred upstream. Both the surge and the lahar removed trees and scoured stumps except near the flow margins or in protected areas. The effects on vegetation as they pertain to flow behavior are also discussed in the section on flow transformations.

#### MEDIAL PHASE

The medial phase of the South Fork lahar is characterized by only slight changes in texture of the peak-flow deposits, in a series of channel reaches extending from slightly beyond the base of the cone, 5.5 km from the crater, to a distance of 36 km. Flow velocity declined from near 30 m/s near the beginning of the phase to 7 m/s just beyond the downstream transition

FIGURE 5 (facing page).—Uppermost watershed of the South Fork Toutle River and tributary Sheep Canyon. Velocity and discharge of first May 18 surge and flow (dark deposits) were determined at points indicated by arrows. Note light-colored deposits of the lateral blast (a), flow tracks of May 18 flows extending to crater rim (b), deposits of the second, pumice-rich lahar (light-colored deposits in channel) (c), and confluence with Sheep Canyon (d). Photograph by Austin Post, May 19, 1980.

<sup>2</sup>The statistics of the grain size distributions are described by the graphically derived measures of Folk (1980). See the appendix for a fuller description of these measures.

to the distal phase. The celerity of the medial-phase lahar wave was approximately 7.0 m/s (Cummins, 1981) over most of the channel reach upstream from Weyerhaeuser Camp 12. Throughout the 30.5-km distance traversed by the medial phase, sorting of the peak debris flow deposits remains in the narrow range of 2.6–3.3  $\phi$ , with a mean grain size of 0.7–1.7  $\phi$  (0.31–0.61 mm).

The changing character of the flow is illustrated by the thicknesses of mud coatings on trees that remained standing on the flood plain and in protected areas (fig. 6). The increasing thicknesses of these coatings downstream do not correspond to a proportional enrichment of mud content in the peak-flow deposits; silt and clay make up a relatively uniform 15–20 percent (5 samples) of those deposits throughout the medial phase. The increase in coating thickness reflects the increased duration of the lahar flood wave and the lower velocity of flow caused by increased hydraulic roughness associated with vegetation on the downstream flood plain. Trees on the flood-plain surface locally remained standing; those at channel margins and in the mainly confined reaches traversed by this phase of the lahar were either removed or knocked down and scoured into “bayonet” trees (Janda and others, 1981, fig. 278).

The deposits of the medial phase are divided into a channel facies and a flood-plain facies, which are progressively more distinct with greater distance from the volcano. Also during this phase a coarse basal carpet of flow developed, as evidenced by clast-supported bar deposits. The whaleback bars formed from the basal flow are most abundant in the downstream part of the medial phase but extend into the upstream part of the distal phase (fig. 6).

#### DISTAL PHASE

During the final debris flow phase, the rate of change of flow texture accelerated as the peak discharge attenuated. The phase began at the head of a broad, expanding reach in which flow volume was progressively lost through deposition and in which the rate of flow was consequently reduced. Flow velocity declined downstream to less than 7 m/s, measured 0.3 km below the start of the distal phase. The celerity of the distal-phase lahar wave was about 3.7 m/s (Cummins, 1981) for the channel interval between Weyerhaeuser Camp 12 and the Coal Bank Bridge.

Deposits of the distal phase show a rapid downstream decline in mean size and an improvement in sorting. Upstream from the point where transformation to the runout phase began, sorting declines (improves) to 2.2  $\phi$  or lower, as mean grain size declines to smaller than 2.3  $\phi$  (0.20 mm). The change from distal phase to runout

phase is defined by the beginning of the transformation to hyperconcentrated streamflow, at the upstream start of the transition interval.

The differences between the channel and flood-plain facies are less distinct than in the medial phase. Whaleback bars, with a single exception near the head of the distal reach, are not well developed. The flood-plain facies is widely distributed throughout the inundated area and thus has a high likelihood of preservation in the stratigraphic record. The channel facies, however, was not well developed, and has been largely removed by subsequent stream erosion. Trees marginal to channels were felled, but high-velocity flow was not of sufficient duration to form well-developed “bayonet” trees.

#### LAHAR-RUNOUT PHASE

The end of debris flow transport in the distal phase marked the end of the lahar in the strict sense and the beginning of the runout phase. The debris flow debulked over at least 9 km at the beginning of this phase, during which the leading edge of the flow was progressively transformed to hyperconcentrated streamflow. The transition interval is included in the lahar as defined in the general sense, and the deposits are described as the transition facies in the section on facies models. The hyperconcentrated flow was identified on the basis of eyewitness descriptions, evidence of high sediment concentrations from the deposits, and by analogy and deposit identity with the runout phase of the lahar of March 19–20, 1982. Actual sediment concentrations in that flow were measured and are described in the section on flow transformations.

The 1980 runout phase extended from the vicinity of Harry Gardner Park, just upstream from the confluence of the forks of the Toutle River, to the Cowlitz River (fig. 2). Flow velocities of the 1980 runout flow were probably comparable to those measured directly in the 1982 runout flow, which were in the range of 4–7 m/s. Celerity of the 1980 flood wave between the Coal Bank Bridge and the gaging station at Castle Rock was 3.3 m/s (Cummins, 1981).

As in the 1982 runout flow, hyperconcentrated flow ceased upon dilution with streamflow at the confluence of the Toutle and Cowlitz Rivers. The deposits recording that change were buried within hours by the North Fork lahar, but observers reported (Cowlitz County Sheriff's log) that sediment concentrations in the flow in the Cowlitz River did not appear high.

Sorting of the massive or crudely stratified runout deposits of the South Fork flow (3 samples), as well as the March 1982 runout flow (12 samples), is characteristically in the range of 1.1–1.6  $\phi$ . Mean grain size of

the South Fork flow deposits is in the range of 1.7–3.3  $\phi$  (0.10–0.31 mm). Another general characteristic of the South Fork runout deposits is a concentration at or near the flow boundary of abrasion-rounded wood fragments transported from the lateral-blast zone (fig. 1). An analogous feature locally present in the 1982 runout flow units and some of the ancient runout deposits is pumice concentrated at or near the base and flow boundaries of the units (the South Fork lahar deposits contain only a small amount of eroded older pumice). These and other characteristics of the runout-phase deposits are discussed in detail in the section on flow transformations.

## FLOW TYPES AND DIVISIONS

### LONGITUDINAL FLOW TRANSFORMATIONS

The evolution from a lahar to hyperconcentrated streamflow is the most commonly observed longitudinal change of flow type. Recognition of this process increases the accuracy with which individual flows can be traced over long distances, and provides evidence of upstream lahars from their downstream runout equivalents. Even the largest lahar in the 50,000-year history of the watershed (PC 1; Scott, 1985b, in press) showed evidence of this same kind of round-trip transformation: initial bulking to form a lahar followed by the beginning of debulking in the direction of a runout flow. The second largest lahar in the system (PC 3) formed the same way and underwent even more complete debulking.

### FLOW DIVISIONS AT A SECTION—BASAL FLOW AND THE WHALEBACK BARS

The deposits and boundary features of the South Fork and North Fork lahars show the same evidence of a local division of flow mode in a vertical profile. The two divisions, described informally as the peak flow and the basal flow (table 2), became more pronounced with increasing distance from the volcano (fig. 7). They are comparable in geometry and partly in process to the upper part of normal streamflow, containing suspended sediment only, and the basal part, which transmits the bed load. Coarse clasts were dispersed in the matrix of the peak debris flow, like the grains in streamflow suspension. Coarse clasts were in greater concentration in the basal debris flow, with the clast-to-clast contact and interaction with the flow boundary that characterize bed-load transport. The movement of coarse clasts in a debris flow by a different mechanism than that transporting the remainder of the flow is considered by Daido (1971) and Lowe (1979).

TABLE 2.—*Interpreted characteristics of at-a-section flow divisions in lahars in the Toutle-Cowlitz River system*

Characteristic	Peak flow	Basal flow
Geometry-----	Main part of lahar flood wave.	Carpet at base of flow, mainly in channels; variable in thickness.
Relation to peak.	Composes most of lahar flood wave except for waves of basal flow.	Moves as kinematic waves during rise of lahar and near peak stage/discharge. Levels of bar crests show deposition began near peak
Flow type-----	Debris flow-----	Basal part of debris flow, with some characteristics of grain flow or noncohesive debris flow.
Shear distribution.	Less concentrated than in basal flow.	Local extreme concentration at channel boundary, producing lahar-abraded pavement, grain cataclasis, and truncation of size distributions.
Erosive character.	Low; flow commonly passive on flood plains.	Locally highly erosive.
Deposit framework.	Coarse clasts dispersed in flow or buoyed at flow surface.	Coarse clasts in contact.
Facies-----	Forms flood-plain facies.	Forms most of channel facies (with sole layer formed mainly during rising stage).
Lahar-bulking factor.	Low; 15 percent in deposits of North Fork lahar.	High; 48 percent in deposits of North Fork lahar.

That the basal carpet of coarse clasts was transported during rising and peak debris flow discharge is shown by the extension of the crests of the clast-supported bar deposits to near the level of the peak stage. Basal concentrations of coarse clasts, moving in waves or pulses, are indicated by the periodic intervals of sound reported by R. L. Dinehart (written commun., 1980) during the rise of the North Fork lahar at the Highway 99 Bridge. The sound was the same as that of "boulder movement in a glacial outwash river." Additional evidence of the basal flow is a high content of alluvium bulked into the bar deposits and a relatively small amount of alluvium present in the peak-flow deposits. Other aspects of the behavior of the basal flow are discussed in the section on lahar boundary features.

Peak-flow deposits contain dispersed, matrix-supported clasts with a mode in the pebble size range. The basal-flow deposits contain clasts with a mode in the cobble size range, are mainly clast supported, and have an interstitial matrix like that supporting the dispersed clasts in the peak-flow deposits. The matrices

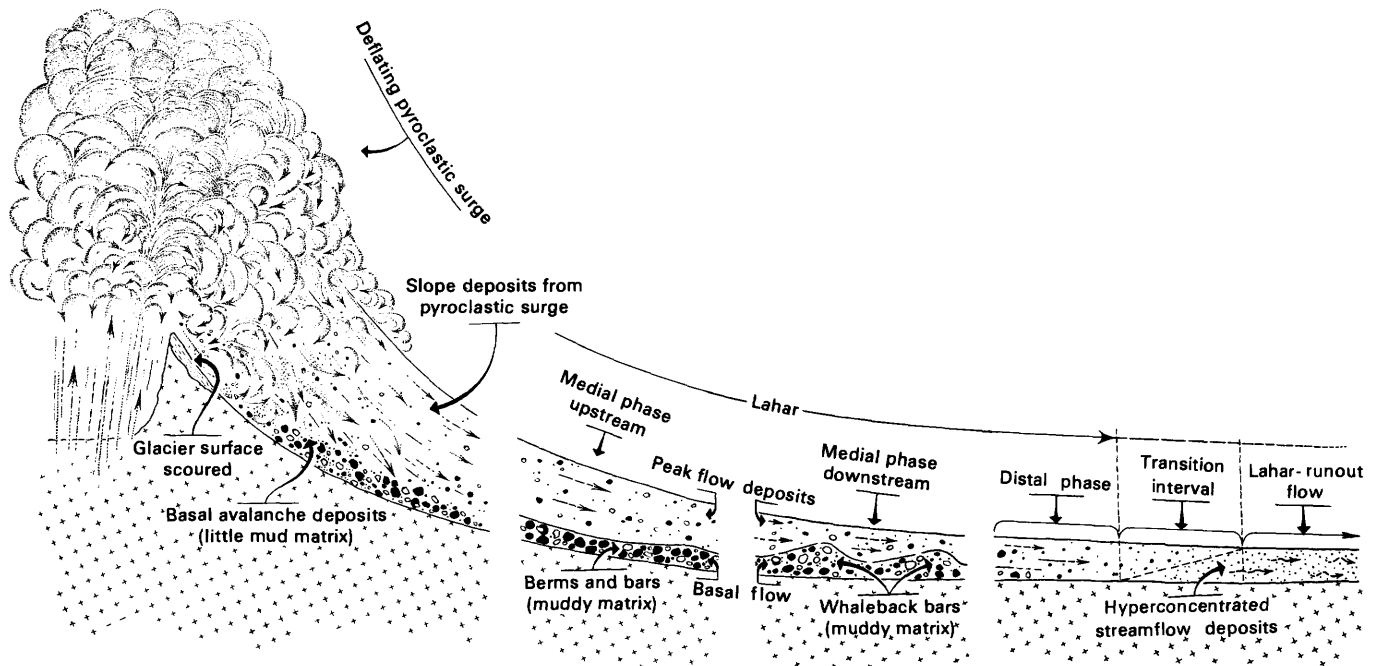


FIGURE 7.—Diagrammatically portrayed origin of the 1980 South Fork lahar as the transformation of a pyroclastic surge.

of both types of deposits are particle supported. The locally preserved boundary between the deposit types is a discrete, dynamically shaped surface that forms the whaleback bars (figs. 6, 7).

The whaleback bars are as much as 150 m in length and resemble drumlins, the bars formed by Pleistocene floods from breakouts of glacial lakes (Malde, 1968; Baker, 1978), and the bars formed by a flood surge from a breached dam (Scott and Gravlee, 1968). The bars formed by the South Fork lahar (table 3, figs. 8, 9) have shapes generally similar in plan view to that of an air-foil, as do drumlins (Chorley, 1959). A degree of lateral asymmetry reflects flow deflected by the channel side. The crest and the widest point of the whaleback bars occur most commonly downstream of the midpoint, unlike the crests and widest points of drumlins, which are generally up-glacier of the midpoint. In that respect the bars are similar to large gravel dune forms observed in the Kenai River in Alaska (Scott, 1982, fig. 12). The term "whaleback" has been applied to similarly shaped, smaller bedrock features formed by glacial abrasion (Flint, 1971, p. 97); use of the term as an adjective with "bar" yields an apt description of the lahar depositional features.

Although the whaleback bars of the North Fork lahar were not measured, because of their rapid erosion, they were clearly larger and more irregularly shaped than those in the South Fork. The main characteristics of the

TABLE 3.—Dimensions of whaleback bars formed by the 1980 lahar in the South Fork Toutle River

[Shape measurements were taped in reference to the lowest closed contour line around the features. For example, height is the vertical distance from that contour to the crest of the bar. Confidence limits at 95 percent level are shown with mean values]

Number of bars measured.....	6
Mean length.....	79.3±34.1 m
Mean width.....	23.4±11.3 m
Mean length/width ratio.....	3.48±0.70
Mean height.....	2.5±1.0 m
Range of flow depth at peak stage above bar crest.....	1.7-14.6 m
Range of percentages of cross-sectional area of flow, at peak stage, above the level of bar crest.....	15-70 pct
Position of crest, in percentage of length from upstream end of bar.....	61±10 pct

features were the same, however; this similarity in the bars formed by lahars differing in origin and dynamics suggests that the features are normal products of large lahars extending beyond the vicinity of the volcano. Incipient whaleback bars were present in other channels conveying 1980 lahars, but these features were fully developed only in the forks of the Toutle River. In both forks, full development occurred only after approximately 25-30 km of flow, the distance apparently

needed for the segregation by settling within the flow, and for the introduction of enough eroded material to create the basal carpet of coarse clasts from which the bars were formed. Lahars in other drainages of the volcano did not extend this far because of impoundment in reservoirs.

The bars consist typically of poorly stratified gravel, and most have well-developed normal grading throughout most of the unit. In some, the normally graded part overlies a massive ungraded zone of variable thickness, or a thin, inversely graded basal zone, or both. The deposit is mainly clast supported, and both texture and structure generally indicate emplacement in a brief time interval. In this respect the forms are different from the similarly shaped but larger bars produced by glacier outburst floods. Those forms, described as longitudinal or pendant bars, are commonly internally stratified (Malde, 1968, fig. 5). They form downstream from bedrock projections by the accretion of foreset strata from pulses of sediment moving as current ripples (Baker, 1978). Among the whaleback bars of the Toutle River drainage, multiple overlapping pulses of basal flow were preserved only locally along the North Fork.

The level of the crests of the whaleback bars, close to peak stage, shows that the bars formed near the lahar flood peak and locally were developed at the peak. An analogy with bar formation during a water flood suggests that the whaleback bars were forming rapidly during earliest recession flow. The upper, normally graded parts of the bars of the North Fork lahar culminate in a mud-rich surface layer, the cohesive nature of which locally prevented erosion from the overriding recession flow. Boulders deposited from recession flow on bar surfaces and crests have a much higher proportion of weak, hydrothermally altered rock types than those within the bars. The bars of the South Fork lahar, although having upper, normally graded zones, do not have muddy surfaces; surficial boulders were also deposited locally from recession flow.

The basal flow apparently consisted of kinematic waves of coarse sediment at the base of the North Fork lahar and did not cause major fluctuations in stage (fig. 2). Small-scale surface wave movement, which may have been related to the basal-flow waves, formed steplike terraces 20–30 cm apart. The terraces are present in the upper 3–4 m of peak-flow deposits upstream from the confluence of the forks of the Toutle River. The features correspond to regular, successively lower oscillations or stillstands in stage, which were also shown by mudlines inside inundated houses. These early recession fluctuations were best developed near Kid Valley but were also present on the surface of the debris

avalanche, where incipient bars and berms formed but significant pulses in the basal flow were not evident. Thus they may represent either fluctuations resulting from the anastomosing of flow on the avalanche, or the intermittent surging that has been observed in smaller scale debris flows. The most suggestive evidence of wave movement is the striking similarity in stage fluctuations shown by the features.

Most of the largest whaleback bars were formed in unconfined expanding reaches of both the North and South Forks of the Toutle River. The thickest bar deposits of the North Fork lahar, where the forms locally consisted of several flow units, are in the constricted reach at Coal Bank Bridge, where the flow may have been slightly ponded. A common denominator of the sites of bar deposition is rapid energy loss.

Within the confined channel, the bars occupy positions strictly analogous to those of bars formed by a catastrophic flood flow. The bars downstream from lateral bedrock projections resemble lobate pendant bars (for example, see Scott and Gravlee, 1968, fig. 15), in that they have the same morphology and a generally similar internal structure. This similarity supports the analogy of the basal flow in the lahars to the boulder-size bed load in a catastrophic flood flow. The bed load in rivers is a traction carpet of particles supported, according to Bagnold (1973), by dispersive pressure from particle collisions. Although clast interaction was intense in the basal flow, the bars locally contain a few clasts of weak, altered rock types could have survived extended transport only in the normal dispersed state. Thus the intense clast interaction in the flow was mainly a local phenomenon in areas of low energy, with clasts moving in contact as grain flow or noncohesive debris flow, probably for discontinuous intervals. The areas of lahar-abraded pavement generally coincide with, or lie just upstream from, the coarsest bar deposits (reflecting the “grinding to a stop” of the basal flow). This association suggests that extreme shearing of the channel boundary was only local. Under a constant energy gradient, coarser clasts would normally be moved away from the boundary by size-dependent particle interactions, as probably occurred during much of the transport. Thus, the basal flow consists of coarse sediment at or near the base of the lahar, in which the degree of clast interaction is highly variable. The coarse sediment apparently moved through areas of constant energy gradient at least partly in a dispersed state, and this was a more common boundary condition than was the intense particle interaction responsible for the abraded pavement. This conclusion explains why the sole layer was preserved in most reaches, but not all.



FIGURE 8.—Longitudinal view of whaleback bar in the South Fork Toutle River 28.4 km from the crater of Mount St. Helens. Flow direction was from right to left. Although normal grading is present in the deposit, the basal third of the cutbank consists of coarse pre-lahar alluvium, thereby exaggerating the amount of apparent grading.

#### LAHAR AND LAHAR-RUNOUT FACIES MODELS

In the dynamic river regime that accompanies and follows volcanic eruptions, accurate process-response models can be generated with data gathered over time spans much briefer than those that separate the major channel-forming events. A facies model is a set of generalizations derived from comparison of several modern and ancient deposits of a particular process or environment. Certain depositional units of lahars and their associated flows are sufficiently distinctive to serve as facies models representing specific flow processes and environments in the river system. The characteristics listed in table 4 and figure 10 are based primarily on the 1980 lahars in both forks of the Toutle River and on the runout flows of the 1980 South Fork lahar and the 1982 lahar. The table includes, however, only those characteristics that are likely to be preserved and which can be extrapolated to older units, based on

extensive observations of older flows at Mount St. Helens and other Cascade Range volcanoes.

With the exception of the transition facies, each facies is specific to a single flow process or type. The lahar channel facies consists of deposits of the basal debris flow and includes, locally, a well-developed sole layer. The lahar flood-plain facies represents the extensive sheets of peak-flow deposits on the flood-plain surface. The lahar-runout facies consists of the deposits of hyperconcentrated streamflow that evolved directly from debris flow. The lahar-related streamflow deposits—not distinguished as a facies because of their similarity to normal flood deposits—were deposited from streamflow that clearly had less than 40 percent sediment by weight (the lower limit of hyperconcentrated flow), based on comparison with 1982 deposits of flows with known sediment concentrations.

Although the 1980 North Fork lahar originated by dewatering of an avalanche deposit and did not have an identifiable runout phase, its at-a-section flow



FIGURE 9.—Transverse view of the whaleback bar in the preceding figure, looking downstream. Apparent horizontal stratification reflects erosional flow lines formed during lahar recession.

divisions and the resulting channel and flood-plain facies were closely similar to those of the medial phase of the South Fork lahar. The only significant difference was in the presence of mud “skins” on the whaleback bars of the North Fork lahar. The more common mechanisms for generating lahars in the river system are flood surge bulking and pyroclastic surge deflation. The sedimentologic evidence for this conclusion, based on textures of the complete record of lahars in the river system (table 1), is discussed in the Conclusions section of this report.

#### LAHAR CHANNEL FACIES

Initially, the channel facies of the 1980 flows was widely present in and adjacent to preexisting stream channels, but it was mainly eroded from confined reaches by 1985. In broad valley areas the post-eruption shifting of channels was extensive as streams adjusted to the higher post-eruption flow regime (U.S. Army Corps of Engineers, 1984), but the vagaries of the lateral

migration allowed the lahar channel facies to be at least temporarily preserved. The greater the valley width the more likely is the preservation of the facies in the stratigraphic record.

Recognition of ancient channel facies permits the determination of locations and relative ages of paleochannels that conveyed significant volumes of flow. The lateral transition to the flood-plain facies can be seen in some exposures, thereby revealing the paleochannel configuration. Flow depths and cross sectional areas can be determined where the channel facies can be correlated with the peak-flow deposits of the same older lahar (see Scott, 1985a, in press). In the North Fork Toutle River, channel facies of the older lahars are present in stratigraphic sections in the valley areas between the downstream end of the debris avalanche and the community of St. Helens, and from the confluence of the forks to a point 6.2 km upstream. A lahar of probable Castle Creek age (about 2,000 years old) locally forms the basal part of a channel unit that can be traced in the vicinity of Camp Baker for about 2 km.

TABLE 4.—Facies characteristics of large lahars and associated flows from Mount St. Helens in the Toutle-Cowlitz River system

[Includes flows extending tens of kilometers from Mount St. Helens]

Characteristic	Lahar facies		Transition facies	Lahar-runout facies	Lahar-related streamflow deposits
	Lahar channel facies	Lahar flood-plain facies			
Agent of deposition.	Debris flow. Basal part of lahar; locally has coarse clasts in contact and some characteristics of grain flow and noncohesive debris flow. Sole layer accreted at debris flow boundary.	Debris flow. Peak flow of lahar flood wave.	Combined hyperconcentrated streamflow (front of wave) and debris flow (tail of wave); debris flow deposits overlies streamflow deposits in a single unit.	Hyperconcentrated streamflow; grain flow and/or noncohesive debris flow in upper part of hyperconcentrated range.	Streamflow with sediment concentrations mainly below hyperconcentrated range, formed by debulking of hyperconcentrated flow or by erosion of a lahar.
Form of top surface.	Locally forms whaleback bars.	Nearly planar.	Nearly planar.	Nearly planar.	Fluvial bar morphology.
Particles on or near surface.	Wood debris and normal- and low-density boulders on surface or slightly embedded.	Local concentrations of wood debris, pumice, and low-density clasts.	Wood debris and pumice common on surface; low-density clasts embedded.	Wood debris and pumice common on surface; low-density clasts embedded locally.	Local concentrations of wood fragments.
Particle support.	Mainly clast-supported with grain-supported silty sand matrix.	Mainly matrix-supported; local clast support in lower part and at level of maximum clast size.	Clast support at base transitional to matrix support in upper part.	Granular, noncohesive; mainly has openwork structure.	Granular and noncohesive except for surficial silt layer.
Grading.	Normal in upper 10-80 pct of unit; commonly ungraded in central zone; inverse in basal 20 pct or less.	Normal in upper 50-75 pct of unit; central ungraded zone; basal 15-50 pct inverse (more pronounced than in channel facies).	Commonly inverse in most of unit; commonly normal in uppermost part.	Poorly developed; inverse in subunits or in most of unit; grading may be progressively lost downstream.	Not distinct.
Stratification.	Poor, except for contact with sole layer and local strata within sole layer.	None.	Mostly massive, except for local crude stratification in lower part and local pumice lenses near flow boundaries.	Appears massive, but may be crudely stratified into inversely graded subunits. Pumice layers seen commonly near lateral flow boundary and locally at base of unit.	Good. Cross strata common. Silt layer 5-60 cm thick common at top; silt layer may show convolute lamination.
Modal size class.	Commonly in cobble or boulder size range.	Commonly in pebble size range.	Like lahar flood-plain facies in upper part; like lahar-runout facies in lower part.	Sand size range, commonly 0.2-2.0 $\phi$ .	Sand size range.
Sorting.	3.0-4.5 $\phi$ (main deposit), 3.1-4.3 $\phi$ (sole layer); matrix also poorly sorted; 2.5 $\phi$ .	2.0-4.5 $\phi$ (1.8 $\phi$ is approximate lower limit approached near point of transition to hyperconcentrated runout flow).			
Wood content	Uprooted trees form subhorizontal molds in older deposits; wood rarely preserved.	Standing trees form vertical molds in older deposits; wood rarely preserved.	Wood preserved in some older deposits, but was originally less abundant than in lahar facies.	Wood commonly preserved in older deposits.	Wood abundant and well preserved in older deposits; charred wood locally abundant.
Sole layer.	Commonly forms basal 10-25 cm; compacted and shows primary foliation in 1980 units.	Poorly developed or absent in 1980 flows, but common in older units.	None.	None.	None.
Erosion at base.	Common; local lahar-abraded pavement.	Rare.	Common.	Common.	Common, but usually slight.

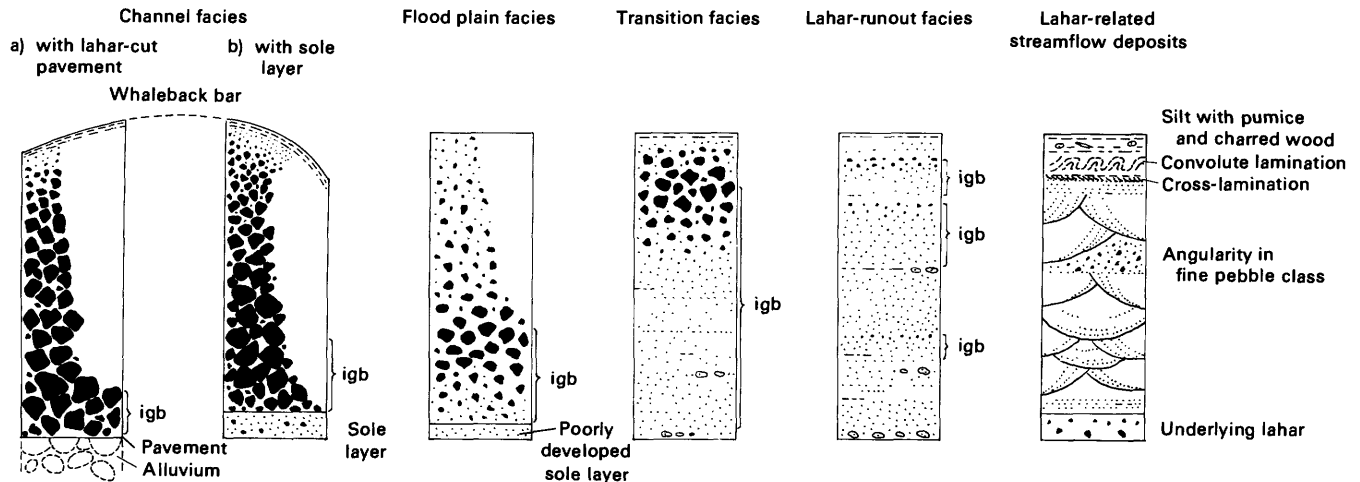


FIGURE 10.—Portrayal of the facies types described in table 4. igb=Inversely graded bedding.

LAHAR FLOOD-PLAIN FACIES

The lahar flood-plain facies is the most widespread of the lahar facies and is formed by relatively uniform deposition of the peak debris flow on the modern active flood plain. The broad distribution of this facies obviously gives it a high probability of preservation in the stratigraphic record. At the Coal Bank Bridge section (Scott, in press), in which 15 flows from 4 eruptive stages or periods are recorded, 1 flow deposit represents the lahar channel facies, 1 is present as both a channel and flood-plain facies, and 11 are examples of the flood-plain facies. The remaining 2 deposits represent the runout facies.

LAHAR-RUNOUT FACIES

Runout flows associated with the 1980 and 1982 lahars resulted in little overbank deposition. Older deposits with the same characteristics are interbedded with units of the flood-plain facies in the stratigraphic record, as at the Coal Bank Bridge section, showing that the runout phases of some older lahars were large enough to inundate flood plains more than 80 km from the volcano. The characteristics of the modern flows that were most definitive for identification of the facies in previous eruptive periods were (1) a massive or crudely stratified structure, (2) inverse grading in most of the depositional unit, (3) the local occurrence of pumice or wood fragments at or near the flow boundaries (contrasting with the concentrations of pumice commonly found near the tops of other units), and (4) a texture of granular, openwork sand with sorting in the range of 1.1–1.6  $\phi$ .

TRANSITION FACIES

The intervals of transition of the 1980 South Fork lahar and the 1982 lahar to lahar-runout flows were characterized by a basal granular deposit consisting of sand and fine gravel, like that of lahar-runout facies, commonly grading (inversely) upward to muddier, coarser, more poorly sorted debris flow deposits. Similar inversely graded transitional units were seen in the deposits of previous eruptive periods at Mount St. Helens and at other Cascade Range volcanoes. This vertical sequence within a single flow unit apparently represents a common, but not exclusive, transition mode from lahar to lahar-runout flow in confined channels. The relation of the transition to sediment-transport dynamics is discussed in the section on flow transformations.

A generalized three-part sequence was presented as a model of the 1982 sediment flows at Mount St. Helens by Harrison and Fritz (1982), but it mainly represents the transition facies. Their model consisted of a lower unit of gravel, a middle unit of crudely laminated sand or granules, and a thinner upper, muddy unit supporting boulder-size clasts. Extensive observations of the 1982 lahar and runout deposits indicate that the upper two units describe the 19-km interval in which the first, higher peak of the lahar was transitional to lahar-runout flow, and the 9-km transition interval of the second peak of the flow. At the farthest upstream locality of Harrison and Fritz, the coarse basal unit consists of gravel transported by the March 19–20 flow but artificially concentrated behind a sediment-retention dam on the North Fork. At their intermediate localities, the basal unit of the model sequence commonly consists either

of deposits of the channel facies of the 1980 North Fork lahar or of normal pre-1980 channel alluvium. Both types of deposits underlie the 1982 flows near their study sites, commonly with a sharp contact separating units 1 and 2, as they observed. Although rare gravel bars were formed downstream from channel obstructions and bridge piers during the runout of the 1982 lahar, the forms are highly localized and do not constitute a uniform basal unit of the flow deposit. The bars and isolated coarse clasts correlate with reaches where coarse material was derived from highly erodible dredge-spoil piles. Finally, farther downstream, the deposits at the Harrison and Fritz locality on the lower Cowlitz River consist of flood deposits formed during February 1982.

#### LAHAR-RELATED STREAMFLOW DEPOSITS

Streamflow deposits directly associated with a lahar, other than the hyperconcentrated lahar-runout flows, include (1) those of flood surges in the process of undergoing bulking to lahars, as in the formation of the 1982 lahar; (2) those resulting from downstream dilution of a lahar-runout flow, as occurred in the 1980 and 1982 runout flows; and (3) those formed from streamflow during or shortly after lahar recession.

A flow undergoing bulking is by definition mainly erosional, and thus its deposits are unlikely to be widely preserved in the stratigraphic record. At Mount St. Helens the bulking process generally has been rapid throughout the mountain's history because of the abundance of erodible pyroclastic debris. At some other Cascade Range volcanoes pyroclastic detritus is relatively scarce, and some flood surges, particularly those originating from glacier outbursts or moraine-lake breakouts, have bulked only to the point of hyperconcentrated flow. These flows constitute a locally significant hazard, and their deposits are preserved in downstream valley fills. An example of a flow at Mount St. Helens that may not have completed the transformation to a lahar but did attain a sediment content in the range of hyperconcentration was the relatively small flood surge that resulted from failure of a natural dam on the avalanche surface on August 27, 1980. Deposits of that flow were not preserved. Because no other incompletely bulked flows have been observed at Mount St. Helens, a corresponding facies model is not shown in table 4.

The downstream deposits representing diluted runout flows are like the deposits of normal flood flows, but may contain angular particles from the associated lahar, charred wood, or uncommonly large amounts of pumice (table 4; fig. 10).

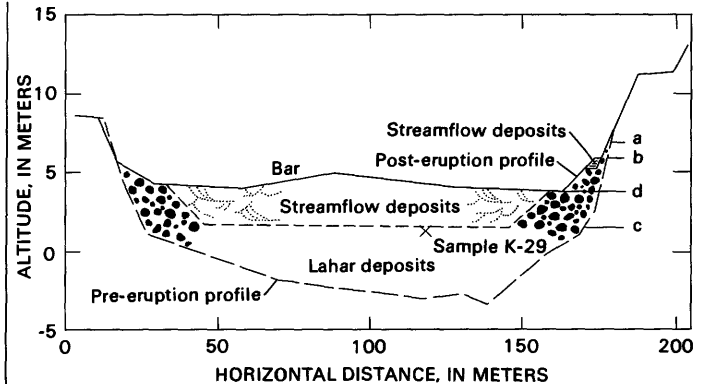


FIGURE 11.—Cross section showing deposits of the lahar originating in the North Fork Toutle River on May 18, 1980, and subsequent streamflow. Location is in the lower Cowlitz River near Rocky Point, 103 km downstream from the 1980 crater. Preeruption profile from Tudor Engineering; posteruption profile by U.S. Geological Survey. The stratigraphic position of a sample discussed in the text is projected to this section.

- a. Peak stage of lahar.
- b. Level representing the "runback" of debris flow that initially flowed upstream in the Cowlitz River above the confluence with the Toutle River during the rising stage, and then during recession reversed direction to flow back down the Cowlitz River.
- c. Level of lahar surface in center of channel when movement ceased (overriding streamflow continued).
- d. Level of post-lahar fill.

Deposits of streamflow that was either transitional with the receding lahar or followed the lahar and contained high concentrations of sediment derived from it, were inset against the lateral berms of the lahar throughout the lower Toutle and Cowlitz River system (fig. 11). Consequently these deposits were largely removed by lateral erosion during succeeding storms, a process that was accelerated by dredging but would have occurred naturally over a period of months. Although concentrations in the range of hyperconcentration were measured in streamflow after the North Fork lahar (initial measurement in fig. 2) and also after the South Fork lahar (streamflow 3 hours after the peak stage had a concentration of 1,160,000 mg/L), most of the resulting deposits were not like those of hyperconcentrated runout flows. Well-stratified sand, having distinctly better sorting than that of the runout deposits, composed most of the post-lahar streamflow deposits (table 4; fig. 10).

Figure 11 illustrates the geometry of the streamflow deposits relative to those of the North Fork lahar in the Cowlitz River. Level b represents a recessional stabilization of flow (not recorded by the sporadic stage measurements, fig. 2) during which as much as 1 m of well-laminated silt and fine sand was deposited. The level probably represents the "runback" of the debris flow that, during the rising stage, flowed upstream in

the Cowlitz River above its confluence with the Toutle River. Reversal of the flow and its addition to the recession stage temporarily stabilized flow at this level downstream. Charred wood fragments are abundant in the surficial part of the lahar at this level and in the sediment deposited from streamflow on the surface of the moving lahar. The debris flow flowing upstream during the nearly 2-hour rise (fig. 2) of the lahar would have ponded a significant volume of Cowlitz River streamflow that, as the debris flow reversed, would have been released to flow across the receding lahar. Velocity of the water surge may have exceeded that of the receding debris flow. Level d represents the surface of the main post-lahar streamflow deposit, which consists mainly of crossbedded sand. Level c was the surface of the lahar at the time movement ceased, as interpreted from the texture of a sample from the top of the lahar, which is discussed in the section on peak-flow deposits of the North Fork lahar.

None of the above types of streamflow deposits can be distinguished texturally as a useful facies model, although features such as clast angularity and charred wood can identify their association with a lahar. The characteristics are shown in table 4 and figure 10 to emphasize differences with the lahar-runout facies.

#### FACIES OF THE LARGEST LAHAR IN THE RIVER SYSTEM

The channel and flood-plain facies of the older lahars are closely similar to the corresponding facies of the 1980 flows. An exception is the first lahar of Pine Creek age (PC 1; Scott, in press), which was so large that the broad valley area along more than 10 km of the lower North Fork Toutle River was temporarily aggraded to a depth of 7–8 m in channels and 2.5 to 5.0 m on flood plains. The aggradation was caused by the channel constriction at the head of the gorge beginning just downstream from the Coal Bank Bridge. Similar valley-wide aggradation by the same flow occurred upstream of a constricting gorge near Tower (fig. 1).

Because the large lahar aggraded both the channel and flood-plain areas upstream from constrictions, the characteristic channel facies resulting from flow through and out of channels (leaving only residual bar deposits and a sole layer) did not develop at those locations. Channels filled, flow continued, but at least some of the channels remained filled as a result of the extensive aggradation. These paleochannel fills are thus a variant of the normal channel facies. Figure 12 illustrates the facies of the first and third Pine Creek lahars (PC 1 and PC 3) and the 1980 North Fork lahar. The similarity of the large channel fills to the typical channel facies is shown by extensive regions of clast support

in the older deposits and the unusually well-developed sole layer described here as the "ball-bearing bed." Exposures in other reaches, however, show the normal facies distinctions and some extremely coarse graded bars that can be correlated with flow PC 1.

#### SIZE DISTRIBUTIONS OF THE LAHARS

The most widely studied aspect of lahar texture is particle size distribution. It is therefore the best means of comparing the flows in the river system with those in other areas, but only if the comparison is with the same phase and facies. Applications of textural study include, for example, inferring the dynamic behavior or origin of an ancient flow from the known behavior and origin of a modern textural analog.

Lahar deposits containing pebble-size and finer sediment were analyzed by wet sieving of the sand-size and coarser parts of the sample and by pipet analysis of the silt- and clay-size fractions. Some samples were sieved both dry and wet and, except where organic material was a significant part of the sample, the results of the two methods were generally coincident within 1 percent. During 1980 and most of 1981, the 1980 lahar deposits remained moist; only in late summer of 1981 did drying begin. To minimize aggregation of fine particles, the samples were maintained in a moist state by sealing in plastic bags. A sample of the peak flow of the North Fork lahar, which contained an amount of silt and clay typical of that flow, was split and analyzed both with and without a chemical dispersing agent. The resulting analyses were identical, indicating both that no significant postdepositional or post-sampling aggregation had occurred, and also that the clay was deposited in an unaggregated state.

The graphic standard sorting measure of Folk (1966, 1980) is used to represent sorting, because of its near equivalence to the widely reported  $\sigma_\phi$  of Inman (1952) and because  $\phi_{16}$  and  $\phi_{84}$  can be measured or accurately extrapolated for size distributions analyzed with Wentworth class intervals (unit phi intervals). The inclusive graphic standard deviation was calculated for comparison whenever possible, but the value of  $\phi_{95}$  cannot be readily extrapolated for distributions in which much of the sediment is in the coarsest interval. The same comments apply to graphic skewness, which was used for the reported skewness values, and to the calculation of inclusive graphic skewness for comparison. The lahars are so poorly sorted that their particle size distribution commonly ranges over 12 to 14 classes, which are sufficient to define the size distributions accurately without the use of fractional class intervals.

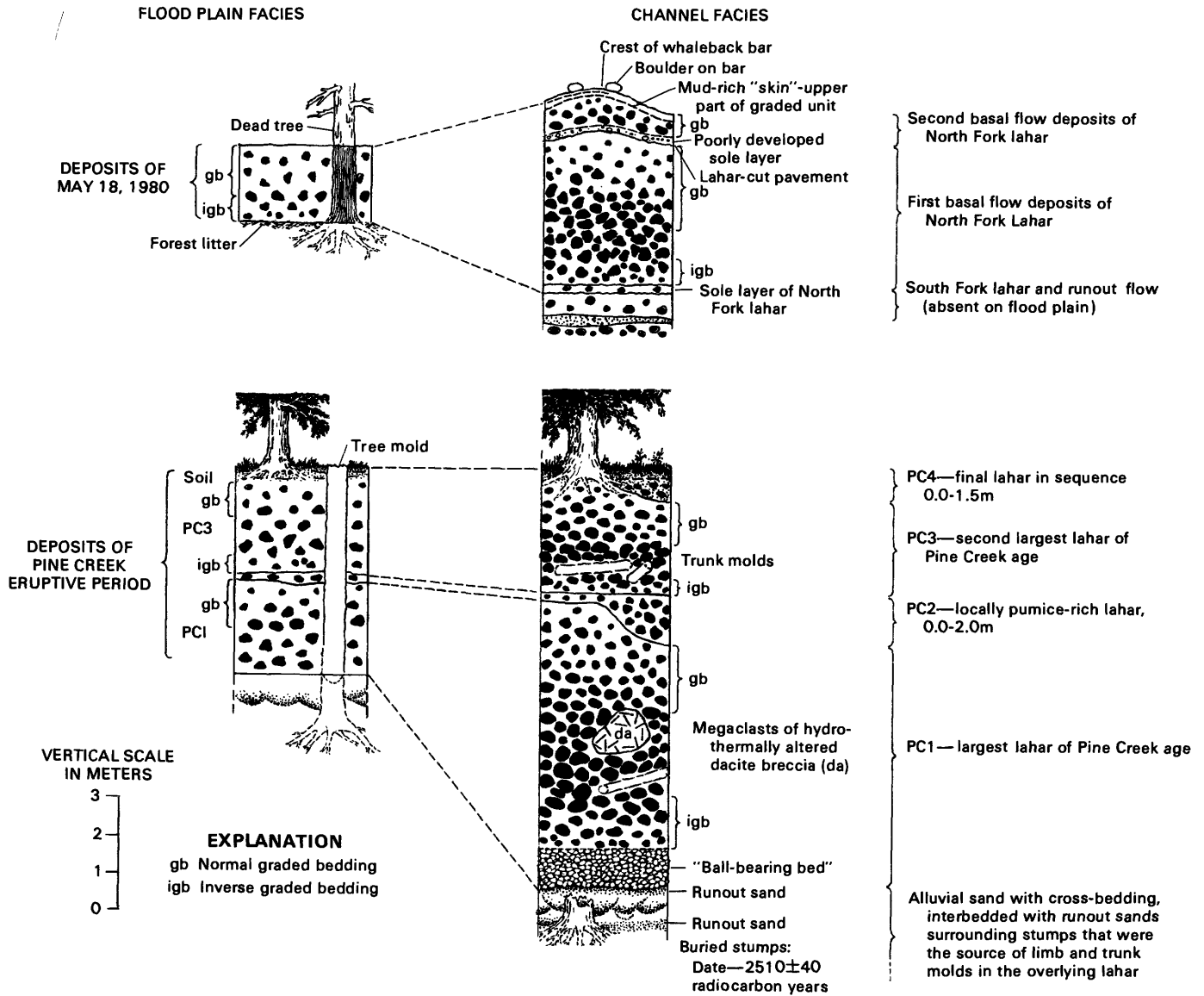


FIGURE 12.—Channel and flood-plain facies of the 1980 North Fork lahar at the Coal Bank Bridge, and of the lahars of Pine Creek age near the Green Mountain Mill, based on sections exposed between 1980 and 1983, 3.8 km upstream from confluence with the South Fork. Stratigraphy of associated deposits is also shown. Plotting of Pine Creek unit thicknesses as seen over the time interval of exposure leads to a total thickness greater than that present at any point and an apparent exaggeration of the paleochannel depth. The relative magnitude of the ancient and modern flows is not apparent because of the influence of differing valley width on deposit thickness.

Except for separate analyses of the matrix in coarse, clast-supported deposits, all the size distributions are from samples large enough to be representative of the specific deposit. The size distributions of deposits too coarse for laboratory analysis were measured in the field using grid sampling and the point-counting technique of Wolman (1954). Although this procedure yields frequency by number in a given class, the results are directly comparable with frequencies by weight as determined in normal laboratory analyses (Kellerhals

and Bray, 1971). A point count and a matrix analysis thus can be combined to obtain the total distribution of a very coarse deposit.<sup>3</sup>

<sup>3</sup>Procedure used for obtaining a complete cumulative curve for coarse samples: During the field point count, the frequency of particles larger than  $-1 \phi$  (2 mm) was recorded, and a grab sample of matrix was collected that needed only to be large enough to yield the accurate relative proportions of particles smaller than  $-1 \phi$ . Point-count frequencies were plotted first; then the remaining distribution in the classes smaller than  $-1 \phi$  was proportioned to accommodate the relative quantities determined from the sieve and pipet analyses. The assumption of near uniformity of matrix over the area of grid sampling is probably valid. (See subsequent discussion of critical diameter.)

**NORTH FORK LAHAR—PEAK-FLOW DEPOSITS OF THE FLOOD-PLAIN FACIES**

The bulk of the flood wave of the large North Fork lahar consisted of a mudflow whose deposits ranged in silt and clay content from 19 percent in upstream reaches to 28 percent in downstream reaches. Total sand, silt, and clay content meets the Varnes (1978) criteria for a mudflow and ranges from 62 percent on the surface of the debris avalanche to 88 percent in the Cowlitz River near its confluence with the Columbia River. Although many dispersed, mainly pebble-size clasts are clearly visible in the deposit, sand and silt are the dominant constituents. The deposits look muddy but are only slightly cohesive, as documented by a low clay content of 3–5 percent. Even this amount of clay is high in comparison with the content of nearly all other lahars in the Toutle River system.

The North Fork lahar did not transform to a lahar-runout flow, but it did undergo gradual, progressive textural changes downstream (fig. 13). These correspond in trend to the more rapid changes in other lahars, such as the South Fork and 1982 lahars, as they approached the transformation to lahar-runout flows. During the more-than-90-km course of the flow from its origin on the surface of the debris avalanche, mean grain size decreased from approximately 0.3  $\phi$  (0.81 mm) to 2.3  $\phi$  (0.21 mm). Correspondingly, sorting improved progressively from approximately 4.4 to 2.9  $\phi$ , a range typical of mudflow deposits reported in the literature. The other lahars in the river system transformed to runout flows as sorting reached values of 2.0  $\phi$  or less.

Skewness showed a consistent downstream trend from slight negative skewness (excess coarse material) to slight positive skewness (excess fine material). This change corresponds with the gradual downstream loss of bimodality in the distribution; the coarse mode drops out, as shown in the histograms in figure 14. Positive skewness and a unimodal size distribution in the flood-plain facies can thus be regarded as potential indicators of distance from source in lahars of this textural type.

Kurtosis showed no pronounced trends; values were in the range of 0.95 to 1.09, indicating general Gaussian normality of the size-distribution curve in terms of peakedness—the relative amount of sorting in the tails of the curve to that in the central part. A tendency toward slightly higher values of kurtosis downstream reflects the loss of the coarse peak in the bimodal distribution. The histograms in figure 14 illustrate this gradual downstream change.

The downstream textural change (fig. 13) is an example of the minimum amount of change expectable in older lahars in the river system; greater rates of change are expectable in flows with a lower clay content. The

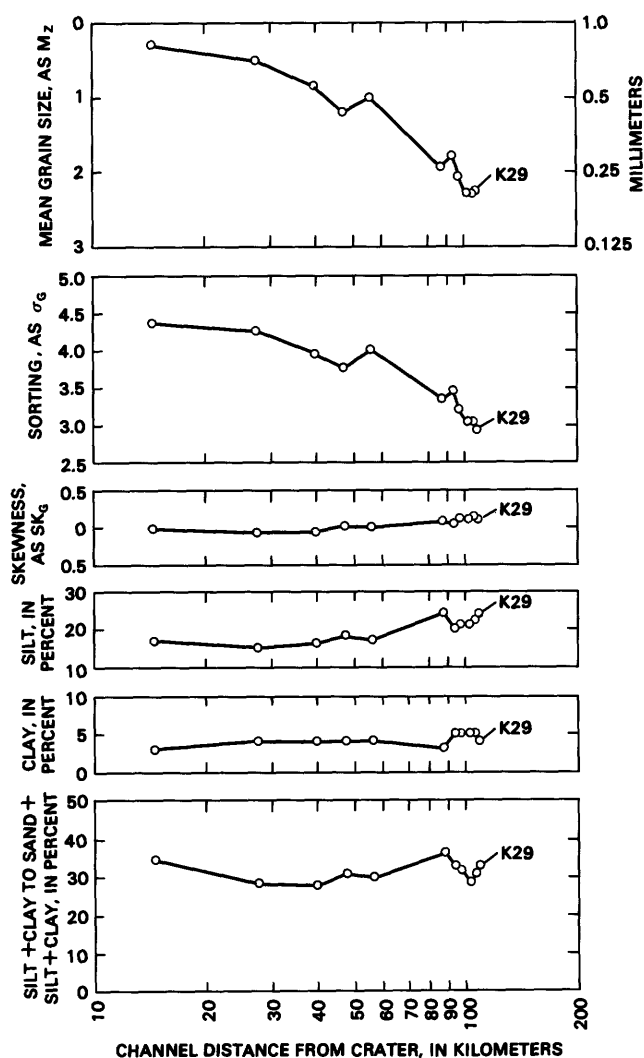


FIGURE 13.—Particle-size distribution characteristics of peak-flow deposits of the 1980 North Fork lahar: downstream changes in mean size (graphic mean,  $M_z$ ), sorting (graphic standard deviation,  $\sigma_g$ ), skewness (graphic mean,  $Sk_g$ ), percent silt, percent clay, and ratio (in percent) of silt-clay to sand-silt-clay. Sample K 29 is discussed in the text.

changes occurred at a relatively constant depth in the flow; samples were collected 1.0–1.5 m below peak stage. The three histograms inset in figure 14 illustrate the size distributions of deposits at varying levels of flow in a partly destroyed house on the flood plain. The samples represent three levels within a single, generally synchronous deposit rather than separate deposits formed successively during a rising stage or a recession sequence. They indicate that the coarser fractions are concentrated with depth to form the characteristic bimodal size distribution. Mean size changed from 2.18  $\phi$  (0.22 mm) at a depth of 0.1 m, to 2.00  $\phi$  (0.25 mm) at 1.9 m, and to 1.21  $\phi$  (0.44 mm) at 3.8 m. Concomitantly, sorting worsened with depth from 3.06  $\phi$  to 3.26  $\phi$

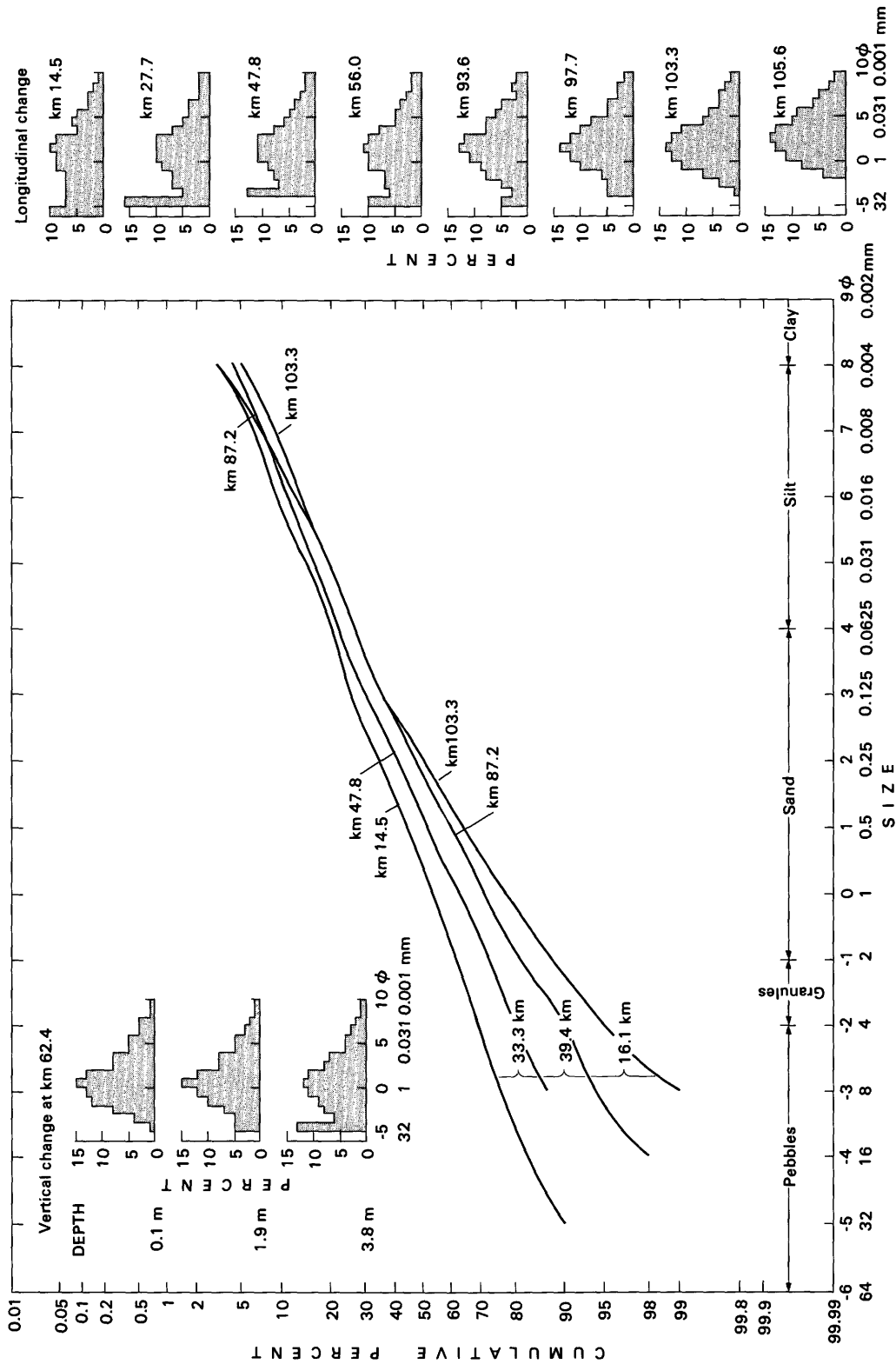


FIGURE 14.—Cumulative curves and histograms of particle sizes in the peak-flow deposits of the North Fork lahar. Phi classes 9 and 10 in the histograms include sediment finer than phi class 8 proportioned by projecting cumulative curves. Channel distance is in kilometers from the 1980 crater.

and to  $3.68 \phi$ . The changes in a vertical profile of flow are thus as pronounced as the changes over many tens of kilometers of flow at the same depth. The change in size distribution with distance between km 47.8 and km 105.6 (at a depth of 1.0–1.5 m) and the change with depth, between 3.8 and 0.1 m, at a point, are similar (fig. 14).

The histograms (fig. 14) show that both the vertical and longitudinal changes involve primarily the gravitational settling of sediment coarser than a critical diameter, which corresponds approximately to the upper boundary of the sand size range ( $-1 \phi$ ; 2 mm). This settling of gravel in a sandy matrix is reflected in well-developed coarse-tail grading in the upper portions of the flood-plain facies. The flood-plain facies of the older lahars commonly also show normal grading reflecting the same critical diameter. Crandell (1971, p. 6–7) likewise has documented coarse-tail grading that mainly reflects variation in the amount of sediment coarser than sand.

The successive cumulative curves also show the settling of the coarser fractions (fig. 14). The steepening slope of the successive curves reflects the gradual but continuous improvement in sorting as sediment sinks in the flow. The temporary loss of a coarse size fraction, such as the  $-4.0$  to  $-5.0 \phi$  (16–32 mm) class in the sample at km 47.8, reflects the randomness of sampling larger clasts that may be very widely dispersed in the flood-plain facies and may consist of low-density rock types.

The downstream size decline in the main part of the flow is thus almost entirely due to the debris flow equivalent of hydraulic or selective sorting—the cause of most downstream size decline in coarse fluvial sediment moved by a single catastrophic flood flow (Scott, 1967). The coarse material settled from the peak debris flow to incorporate in the basal flow and then was deposited in bars. Conversely, little eroded material was introduced to the peak flow from the basal flow, as indicated by the lahar bulking factors discussed in the section on clast roundness. Substantial volumes of eroded alluvium were introduced to the basal flow but were not further dispersed into the peak flow. Part of the longitudinal size decline in the basal flow was due to cataclasis, as discussed in the roundness section.

During dredging in the lower Cowlitz River near Kelso the contact between the mudflow deposits and the overlying streamflow deposits was temporarily exposed, and a sample (K 29) of the mudflow was obtained from the center of the channel (fig. 11). The texture is essentially the same as that of the peak-flow deposits along the channel boundary in the same reach, with

most size classes containing the same amount of sediment and no class differing by more than 2 percent by weight. This near identity in texture indicates that the mudflow in the center of the channel was part of the peak flood wave that continued for a short distance downstream during recession and was deposited at a level 3.6 m lower than the peak stage.

#### NORTH FORK LAHAR—BASAL-FLOW DEPOSITS OF THE CHANNEL FACIES

The bars in or adjacent to preexisting channels are coarser than the flood-plain deposits and commonly have a clast-supported framework. Where not clearly whaleback in shape, their geometry is nevertheless similar, with rounded forms predominating over flat-topped forms; they have formed generally on the downstream side of obstacles and in point-bar and backwater areas. Although the bars are highly variable in texture, both laterally and vertically, measurements at the coarsest part of each bar show that grain sizes do not decline between the debris avalanche and the vicinity of the confluence of the forks of the Toutle River. This finding concurs with similar observations by Gilkey (1983). In the main Toutle River below the gorge beginning at the Coal Bank Bridge the bar deposits were significantly finer than in upstream reaches and were not measured. Below the junction of the Toutle and Cowlitz Rivers the lahar was confined to the main river channel (fig. 11) and the basal deposits could not be observed except as dredge spoils.

Clasts in the size fraction of  $-10$  to  $-11 \phi$  (1024–2048 mm) were the coarsest observed. Mean size determined by field measurements at seven locations ranged between  $-3.1$  and  $-4.4 \phi$  (9–21 mm). Sorting ranged between 3.1 and 4.5  $\phi$ , and values for five of the seven samples were between 3.1 and 3.8  $\phi$ .

The upper 10 to 80 percent of each bar deposit, and of the analogous deposits in the stratigraphic record, is normally graded (fig. 15). The upward rate of size decline commonly increases sharply in the upper 0.2–0.5 m, culminating in a muddy surface layer in bars of the North Fork lahar. Bars of the South Fork lahar exhibit normal grading but do not have this surficial layer. Analysis of the layer near Kid Valley at a depth of 0.1 m reveals a silt and clay content of 15 percent, a mean size of  $0.01 \phi$  (1.0 mm), and sorting of 3.64  $\phi$ . By comparing a separate matrix analysis with a field measurement of the coarsest part of the same bar, the silt and clay content of the entire bar can be accurately estimated as 5 percent.



FIGURE 15.—Bar deposits of the North Fork lahar at the confluence of the forks of the Toutle River. The light-colored clast to the right of the shovel and the large clast to the immediate left of the shovel base consist of hydrothermally altered lithologies. The thickness of the section is 2.1 m. Note the high degree of rounding in several boulders of introduced stream alluvium.

#### NORTH FORK LAHAR—SOLE LAYER OF THE CHANNEL FACIES

Unlike the overlying clast-supported deposits of the channel facies, the coarse clasts in the sole layer are dispersed. Pebble-size clasts protrude from the eroding surfaces of the semiconsolidated matrix to give a characteristic “clast-studded” appearance (fig. 16).

Mean size in nine longitudinally spaced samples ranges between 1.4 and  $-2.1 \phi$  (0.38–4.4 mm); sorting from 3.2 to 4.3  $\phi$ . No significant downstream trend is present in either measure, as is the case for the overlying bar deposits. This lack of trend is in sharp contrast with the trends in the peak-flow deposits (fig. 13). No significant downstream change is evident in the total silt and clay (mud) content, which ranges from 11 to 21 percent, or in the clay content, which ranges from 2 to 5 percent. Compared with the peak-flow deposits at or near the same location, the sole layer is most commonly coarser but is generally similar in sorting. The difference

between the respective cumulative curves shown in figure 17 is typical.

The sole layer locally has crude stratification and color variations that correspond with variations in texture. In the lower of the two units forming the thick sole layer in figure 18, the central part has a mean size of  $-0.47 \phi$  (1.38 mm) and sorting of 4.29  $\phi$ ; color of the band is a pale bluish gray. The middle part of the overlying unit has a mean size of 0.05  $\phi$  (0.98 mm) and sorting of 3.22  $\phi$ ; color is a light grayish brown. Each unit of the sole layer at that point shows symmetrical grading—a normally graded upper part that is nearly a mirror image of the inversely graded bedding in the lower part.

All samples of the sole layer have a size distribution with at least two modal classes, and in all but one sample the coarsest mode is dominant (fig. 17). The coarse mode is mainly in the  $-3 \phi$  (8–16 mm) or  $-4 \phi$  (16–32 mm) size classes; the finer mode is mainly in the 3  $\phi$  (0.125–0.25 mm) or 2  $\phi$  (0.25–0.5 mm) intervals. Compared with the distributions of the peak flow shown in



FIGURE 16.—Channel facies of the North Fork lahar below Kid Valley. The resistant, light-colored sole layer overlies rounded pre-lahar alluvium and is overlain by darker, clast-supported bar deposits that are the fine-grained tapering edge of a whaleback bar to the left of the photograph. The sole layer averages 20 cm in thickness and surrounds protruding alluvial boulders at this locality.

figure 14, the variation from class to class is more irregular.

The histograms in figure 17 illustrate the typical "truncated" size distributions of the sole layer, in which the coarse tail is poorly developed and skewness is positive. Unlike the downstream trend toward positive skewness in the peak-flow deposits, skewness in the sole layer does not correlate with distance. The skewness of the size distributions shown as histograms in figure 17 ranges from  $-0.08$  to  $+0.84$ . Skewness of the sole layer size distribution shown as a cumulative curve is  $+0.10$ .

#### SOUTH FORK LAHAR—PEAK-FLOW DEPOSITS OF THE FLOOD-PLAIN FACIES

The peak flow of the South Fork lahar did not undergo the gradual changes described for the North Fork flow, because of the uniform confined, bedrock channel that conveyed the medial phase of the lahar at high velocities. Nevertheless, the basal flow did segregate

and form bars, including whalebacks near the downstream end of the medial phase. Textural change in the peak-flow deposits was largely concentrated in the proximal and distal phases of the lahar and in the rapid transition to lahar-runout flow at the end of the distal phase (fig. 19). In gross appearance the deposits of the peak flow of the lahars in each fork are very similar, however.

The South Fork peak-flow deposits were initially highly variable, inheriting the turbulent character of the deflating pyroclastic surge. As the water-mobilized phase dominated, the rate of change decreased. Throughout the medial phase the mean size ranged between  $0.7 \phi$  (0.61 mm) and  $1.7 \phi$  (0.31 mm) and sorting varied between 2.6 and 3.3  $\phi$ . The mean size is comparable to that of the North Fork lahar after a similar interval of flow, but the sorting is about 1.0  $\phi$  better. The better sorting is in part a function of a lower silt and clay content relative to the North Fork flow—11–20 percent silt and 2–3 percent clay in the South Fork

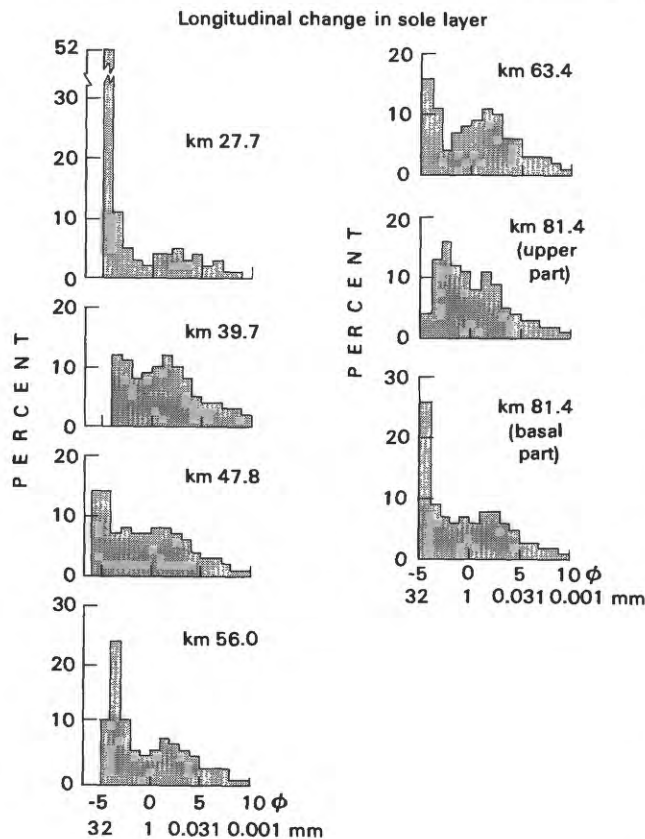
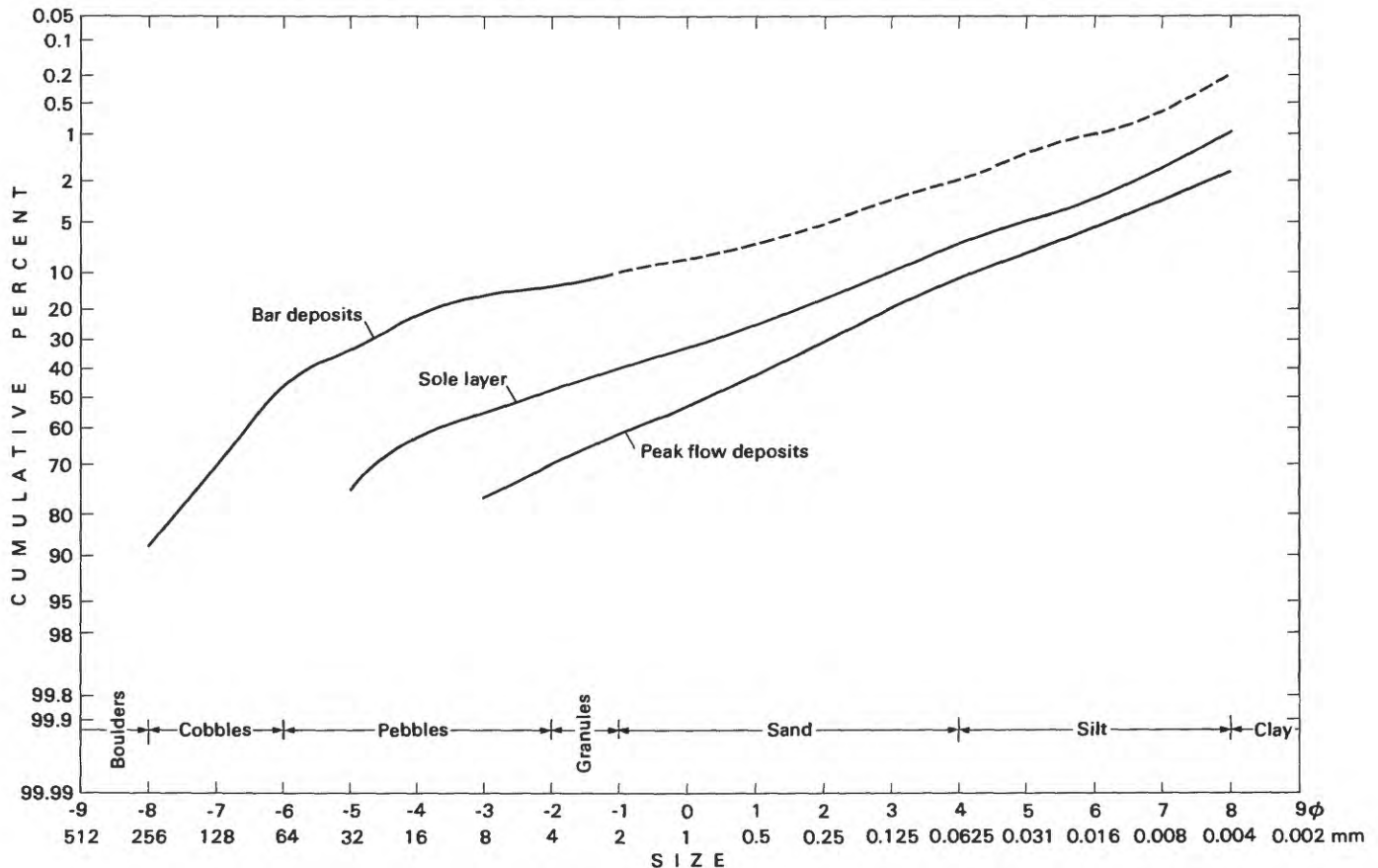


FIGURE 17.—Cumulative curves and histograms of particle sizes in the sole layer, bar, and peak-flow deposits of the North Fork lahar near Kid Valley. The size distribution of the bar deposits is based on field measurement of clasts larger than  $-1 \phi$  (2 mm) and a separate matrix analysis of smaller particles. The histograms illustrate downstream variation in the size distributions of the sole layer of the North Fork lahar.

versus 15–24 percent silt and 3–5 percent clay in the North Fork.

With the accelerated deposition caused by the entrance of flow into the expanding valley of the lower South Fork, mean size decreased and sorting improved significantly in the distal phase. Mean size dropped from approximately  $1.0 \phi$  (0.5 mm) to  $2.2 \phi$  (0.22 mm), and sorting approached  $2.0 \phi$ . Cumulative curves in figure 20 show these changes reflected in progressive loss of the pebble and sand size fractions. The continuation of this trend triggered the transformation to lahar-runout flow, seen in both the sequential cumulative curves and the histograms (fig. 20).

Skewness oscillated without a notable trend from small negative values to small positive values, in the range of  $-0.10$  to  $+0.36$  (fig. 19). Kurtosis also showed no trend, with values ranging from 0.93 to 1.25.

The consecutive histograms in figure 20 illustrate the overall textural change from deflating pyroclastic surge



FIGURE 18.—Sole layer of the North Fork lahar at the Highway 99 Bridge, showing the layer composed of two subunits. The top of the shovel handle marks the contact between the 52-cm-thick sole layer and the underlying runout deposits of the South Fork lahar. Shredded wood from the blast zone is concentrated at the base of the lahar-runout deposits, overlying well-stratified pre-lahar alluvium. Deposits overlying the sole layer have been eroded. (Side of bridge pier forms background at top.)

to lahar to lahar-runout flow. Coarse material that was locally introduced to the peak flow in upstream reaches subsequently settled out as flow competence lessened during the distal phase. A noteworthy characteristic of the entire flow is the consistency of the modal class in the  $2\phi$  (0.25–0.5 mm) interval. Only in downstream reaches does a shift to the  $3\phi$  (0.125–0.25 mm) class begin. Where the distribution is bimodal, the finer mode is represented by the  $2\phi$  class, even in the pyroclastic surge deposits of Sheep Canyon shown in the three inset histograms in figure 20.

#### SOUTH FORK LAHAR—AVALANCHE DEPOSITS OF DEFLATING PYROCLASTIC SURGE AND BASAL-FLOW DEPOSITS OF THE CHANNEL FACIES

The avalanche and bar deposits both represent basal segregations of coarse material, from the deflating pyroclastic surge for the avalanches, and from the downstream water-mobilized lahar, with additions from

eroded alluvium, for the bars. The avalanche deposits differ from the lahar bar deposits in having a rubbly character and a smaller amount of muddy matrix, in spite of similar mean size and sorting (fig. 21) as determined from pebble counts. The field relations of the two types of 1980 deposits show them to be distinct, separate types and not the result of a continuous basal zone of flow. Much larger older avalanches that may have been analogs of the 1980 avalanches did continue downstream as lahars.

The avalanche deposits show no obvious trends in grain size or sorting, in part because of the difficulty in correlating separate flow units; the bar deposits show a general downstream size decline and improvement in sorting (fig. 21). The avalanche deposits lack a well-developed muddy matrix and consequently show only moderately positive skewness, in the range of  $-0.09$  to  $+0.42$ . The bar deposits have a muddy matrix and show positive skewness; skewness of the bar deposits in figure 21 is in the range of  $+0.35$  to  $+0.55$ .

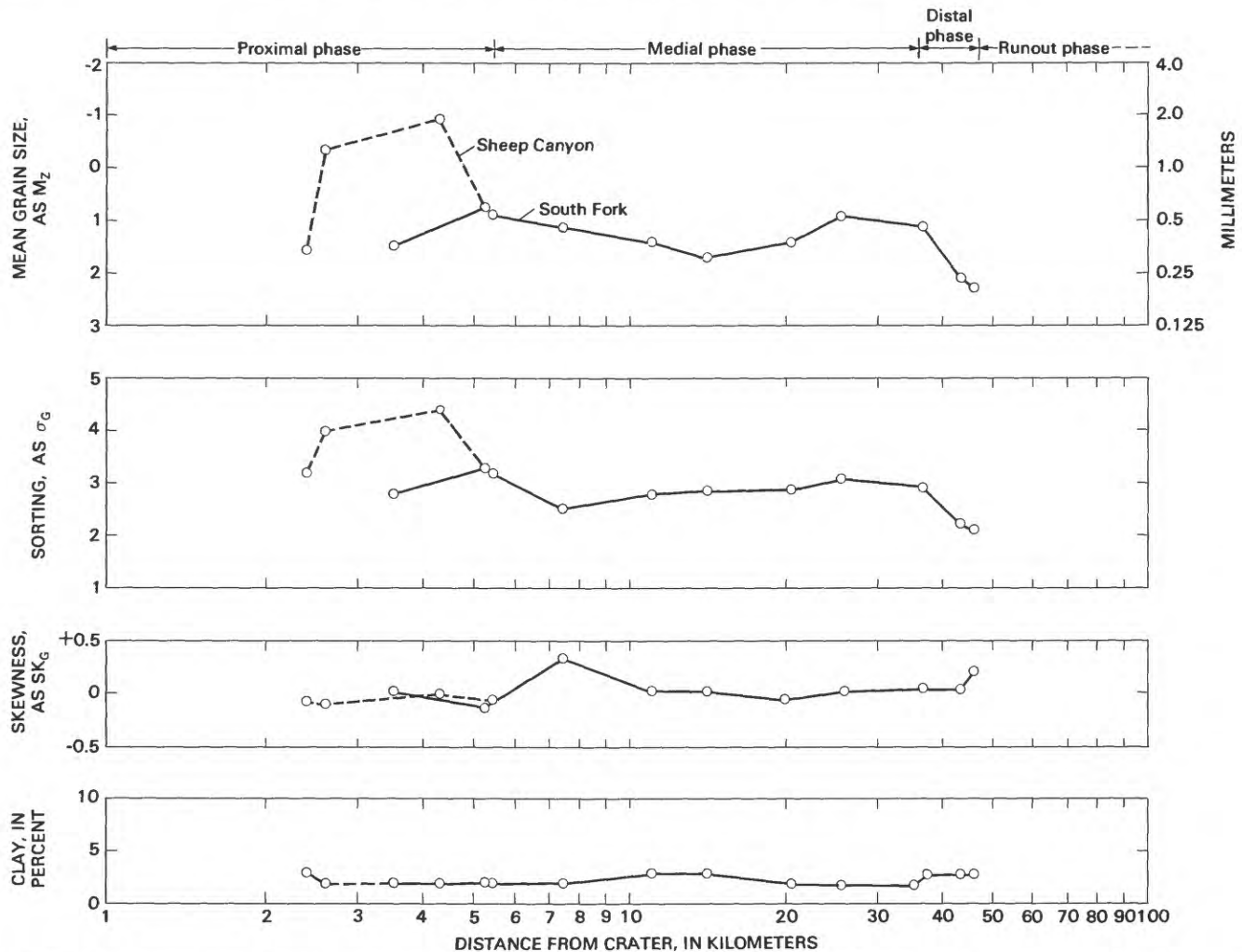


FIGURE 19.—Downstream changes in mean size (graphic mean,  $M_z$ ), sorting (graphic standard deviation,  $\sigma_G$ ), skewness (graphic skewness,  $Sk_G$ ), and percent clay in the peak-flow deposits of the 1980 South Fork lahar.

The lahar bulking factor discussed in the roundness section indicates that significant amounts of stream alluvium were eroded throughout the medial phase of the South Fork lahar. Incorporation of alluvium is also indicated by the local coarsening seen in the peak-flow deposits in the medial phase (fig. 20) and in bar deposits that are coarser than upstream avalanche deposits (fig. 21).

#### SOUTH FORK LAHAR—SOLE LAYER OF THE CHANNEL FACIES

The sole layer at the base of the South Fork lahar is closely similar to that of the North Fork lahar. It is a feature of the water-mobilized part of the flow; it was absent in the proximal phase and developed gradually over the initial 10 km of the medial phase. It was not observed as a discrete layer closer than about 12 km to the crater.

Mean size in seven longitudinally spaced samples ranges between 1.6 and  $-1.3 \phi$  (0.33–2.4 mm); sorting from 3.1 to 3.9  $\phi$ . These values are similar to those of the sole layer of the North Fork lahar, and likewise show no significant downstream trends. In terms of mean size, the sole layer is commonly coarser than the peak-flow deposits at the same point, as in most of the North Fork lahar deposits. The South Fork sole layer is, however, significantly more poorly sorted than the peak-flow deposits at the same point, by an average of nearly 1  $\phi$ .

All the South Fork sole-layer size distributions, like those of the North Fork, have at least two modes. The two dominant modes represent similar proportions of the sample; only in the farthest downstream sample does the coarse mode dominate, as is typical of the North Fork sole layer. (Compare fig. 17.) The modal classes of the South Fork sole layer are the same as

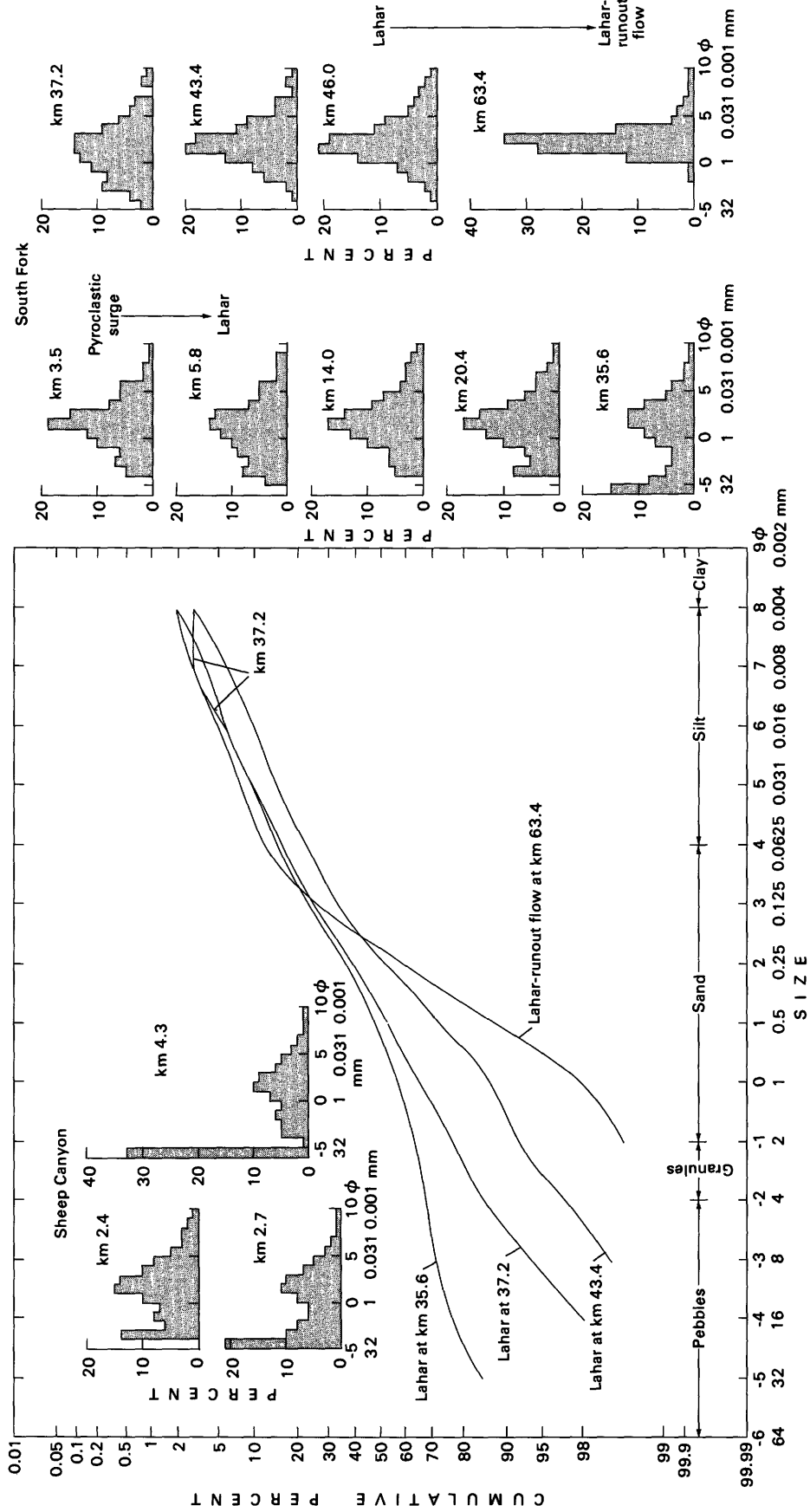


FIGURE 20.—Cumulative curves and histograms of particle sizes in the distal phase of the South Fork lahar and the lahar-runout flow derived from the lahar. Histograms show successive size distributions in the South Fork and Sheep Canyon.

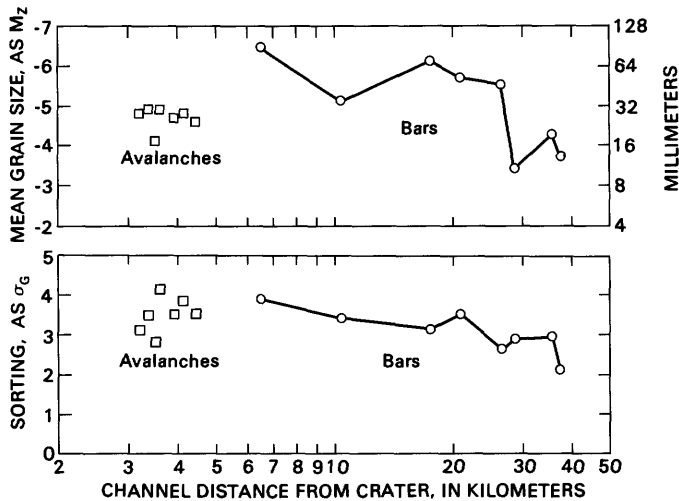


FIGURE 21.—Downstream changes in mean size (graphic mean,  $M_z$ ) and sorting (graphic standard deviation,  $\phi_G$ ) of the avalanche and bar deposits of the South Fork pyroclastic surge and lahar.

those typical of the distributions of the North Fork sole layer. The coarse mode is either the  $-3 \phi$  (8–16 mm) or  $-4 \phi$  (16–32 mm) class; the finer mode is either the  $3 \phi$  (0.125–0.25 mm) or  $2 \phi$  (0.25–0.5 mm) fraction. Skewness is in the neutral range of  $-0.22$  to  $+0.16$ , lacking the tendency toward positive values seen in the size distributions of the North Fork sole layer.

#### LAHARS OF PREVIOUS ERUPTIVE STAGES AND PERIODS

The stratigraphic record of older lahars (table 1) is dominated by the flood-plain facies. The size distributions (table 5) are similar to those of the 1980 flows in the dominance of sand and the relatively small amount of silt and clay, as compared with most mudflows in alpine and semiarid areas and with some large lahars such as the Osceola and Electron mudflows at Mount Rainier (Crandell, 1971, tables 2 and 10). The range in silt content is 3.3 to 15 percent; the range in clay content is 0.5 to 3.3 percent. Only three lahars, however, have a total silt and clay content of clearly more than 10 percent in the main body of the flow unit; the others exceed 10 percent only in the uppermost, muddier parts of some graded units.

A large older lahar that is exceptional in both silt and clay content is the lahar of Smith Creek age (unit 1 at Outlet Creek, unit 16 at the Coal Bank Bridge; Scott, in press). The unit contains 14.4 percent silt and 3.3 percent clay at Outlet Creek. This lahar is the only large flow that could be traced down the Toutle River and

that is texturally similar to the 1980 North Fork lahar. (A small lahar, also of Smith Creek age, has the same texture.) The similarity extends to the size, rounding, and proportion of coarse clasts. Like the 1980 North Fork flow, the large Smith Creek lahar does not show the rapid textural change associated with the transformation to runout flow.

The ratios and proportions of sand and finer sediment in older lahars (table 5) are quite consistent, whereas the proportions of gravel-size clasts differ greatly. The critical diameter separating these phases is, as in the 1980 lahars,  $-1 \phi$  (2 mm). The matrices in the clast-supported bar deposits and in flood-plain deposits with widely dispersed clasts are nearly identical.

The flood-plain facies of the older flows (table 5) are compared here to 1980 peak-flow deposits (figs. 13 and 19) collected from valley side slopes, not directly from the flood plain, because the modern flood-plain deposits were poorly exposed in the early days of this study. The validity of this comparison was investigated by comparing the valley-side deposits with the well-developed flood-plain facies of the 1980 flows once exposures became available. At six sites, three in each fork of the Toutle River, the amount of clay in the 1980 flood-plain deposits was slightly less than in the valley-side deposits. The difference, in each case a fraction of 1 percent in clay content, generally validates the comparisons of the two types of peak-flow samples. Relative to most of the older lahars, the 1980 North Fork flow is unusual in its content of fine sediment, and the 1980 South Fork flow has a content of fine sediment near the upper limit typical of the older flows.

#### LARGE LAHAR OF THE PINE CREEK ERUPTIVE PERIOD

This huge lahar (PC 1; Scott, in press) is composed mainly of rounded cobbles and pebbles in a silty sand matrix and contains from about 1 to less than 2 percent clay. Mean size of the channel facies shown in figure 20 is  $-3.70 \phi$  (12.8 mm), sorting is  $3.62 \phi$ , and skewness is  $+0.55$ . In the flood-plain facies at the same location, mean size is  $-0.25 \phi$  (1.2 mm), sorting is  $3.60 \phi$  and skewness is  $-0.25$ . The relations of the two facies of this flow are shown in figure 12.

#### “BALL-BEARING BED”

The layer of concentrated marble-size pebbles at the base of the first Pine Creek lahar (fig. 12) contains less than 1 percent clay. It is distinguished by a mode in either the  $-4$  to  $-5 \phi$  (16–32 mm) or  $-3$  to  $-4 \phi$  (8–16 mm) class; the coarser class is more common where the layer forms the base of the channel facies, and the finer class

TABLE 5.—*Textures of selected pre-1980 lahars and lahar-runout flows in the Toutle-Cowlitz River system*

[See Scott (in press) for stratigraphic sections at localities listed here. Analyses based on sieve analysis of sand and gravel and pipet analysis of silt and clay unless otherwise indicated. Leaders (—) indicate "not determined".]

Flow and locality	Unit <sup>1</sup>	Thickness of unit (m)	Sample position in unit	Mean size, M <sub>z</sub>		Sorting σ <sub>G</sub> (φ)	Skewness S <sub>KG</sub>	Content in pct			Silt+clay	
				φ	(mm)			Sand	Silt	Clay	Sand+silt +clay(pct)	Silt+clay (pct)
FLOWS OF PINE CREEK AGE												
Third lahar of Pine Creek age (PC 3):												
Green Mountain Mill (flood plain facies).	4	2.2	Middle	—	-0.31 (1.2)	3.10	-0.18	55.0	5.7	0.8	10.6	12.3
Outlet Creek	7	3.0	0.2 m above base	—	-2.49 (5.6)	3.33	+0.58	26.0	3.3	0.8	13.6	19.5
First lahar of Pine Creek age (PC 1):												
Green Mountain Mill:												
Flood plain facies	2	2.3	Middle	—	-0.25 (1.2)	3.60	-0.25	51.2	8.4	1.2	15.8	12.5
Channel facies <sup>2</sup>	4b	6.0	Basal 2.5 m	—	<sup>2</sup> -3.70 (13)	3.62	+0.55	17.0	4.4	0.6	22.7	12.0
"Ball-bearing bed"	4a	1.1	Middle	—	-1.92 (3.7)	2.67	+0.61	23.7	3.5	0.5	14.4	12.5
Outlet Creek	5b	4.8	0.4 m below top	—	-1.29 (2.4)	3.18	+0.67	29.8	7.7	1.8	24.2	18.9
			Coarse medial part	—	<sup>3</sup> -3.67 (13)	3.60	+0.55	---	---	---	---	---
			0.15 m above base	—	-0.75 (1.6)	3.97	-0.13	43.2	7.5	1.3	16.9	14.8
FLOWS OF SMITH CREEK AGE												
Runout flow of Smith Creek or Pine Creek age at Outlet Creek.	4b	0.5	Silt-rich upper part.	—	5.35 (0.024)	1.46	+0.08	16.2	76.0	7.8	0.8	9.3
	4a		0.2 m above base	—	2.10 (0.23)	1.60	+0.39	80.7	15.3	2.7	18.2	15.0
Lahar of probable Smith Creek age:												
Outlet Creek	1	>1.2	0.9 m below top	—	1.22 (0.42)	3.10	+0.11	58.2	14.4	3.3	23.3	18.6
Coal Bank Bridge	16	3.2	0.6 m above base	—	<sup>2</sup> -2.95 (7.6)	4.10	+0.25	52.1	6.9	0.9	13.0	11.5
Runout flow of Smith Creek age at Coal Bank Bridge.	15	1.0	Middle	—	1.13 (0.45)	1.51	+0.29	91.5	6.0	0.8	6.9	11.8
FLOWS OF SWIFT CREEK AGE												
Lahars of Swift Creek age at Coal Bank Bridge.	12	1.4	0.5 m above base	—	0.71 (0.60)	2.28	+0.17	62.6	9.7	0.9	14.5	8.5
	9	1.2	0.4 m above base	—	-1.85 (3.5)	3.00	+0.63	24.7	5.2	0.5	23.8	8.8
Rubby lahar of Swift Creek age at Coal Bank Bridge. <sup>2</sup>	8	1.0	0.3 m below top	—	<sup>2</sup> -1.06 (2.1)	4.38	+0.36	52.0	13.8	1.4	22.6	9.2
Lahar of probable Swift Creek age at Coal Bank Bridge (channel facies). <sup>3</sup>	1	>3.5	Upper half	—	<sup>3</sup> -3.64 (12)	4.20	+0.45	---	---	---	---	---

<sup>1</sup>As designated in Scott (in press).

<sup>2</sup>Combination of field pebble count of coarse fractions (>1 φ, 2 mm) and sieve and pipet analyses of finer fractions.

<sup>3</sup>Field pebble count.

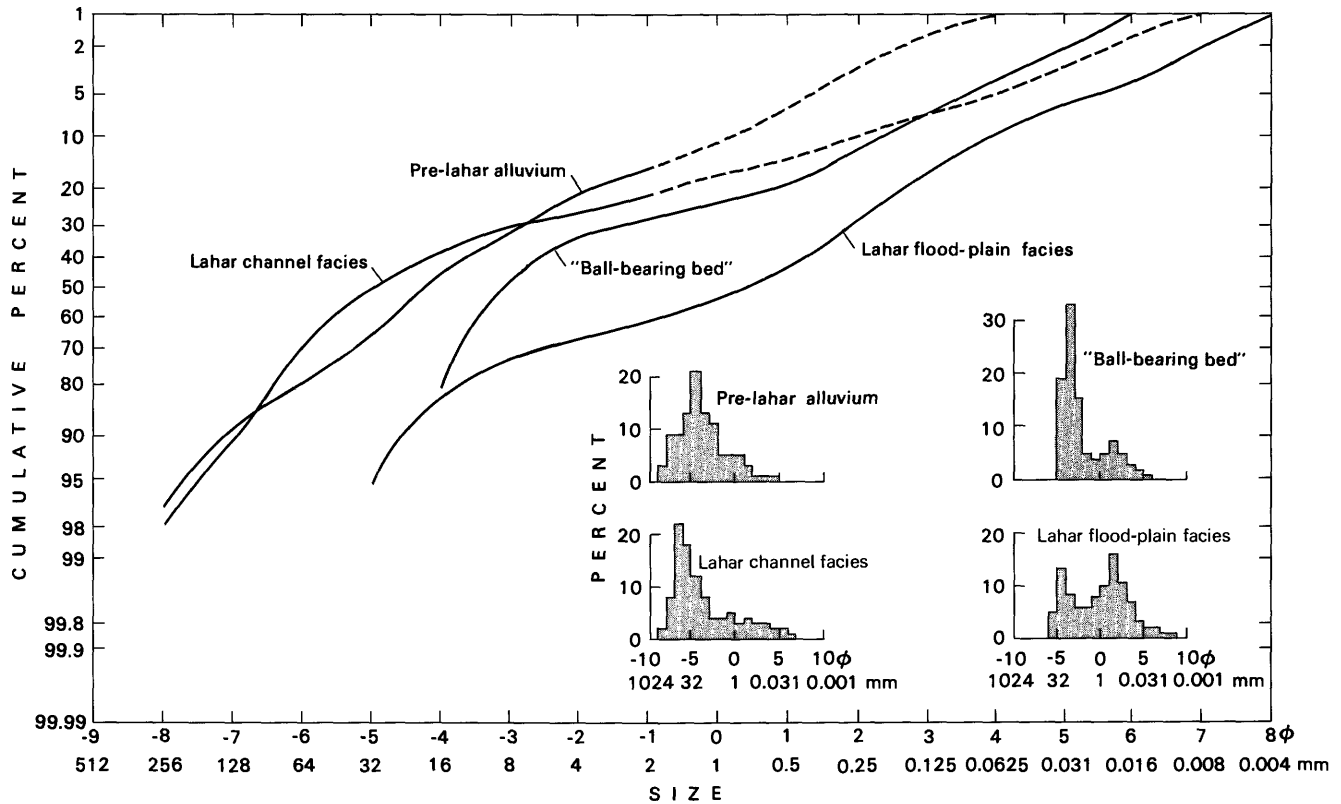


FIGURE 22.—Cumulative curves and histograms of particle sizes in the channel and flood-plain facies of the first lahar of Pine Creek age (PC 1), the “ball-bearing bed” at the base of that lahar, and alluvium in a megaclast (see fig. 24) included in that lahar. The size distributions of the lahar channel facies and the alluvium are based on field measurements of clasts larger than  $-1 \phi$  (2 mm) and separate matrix analyses of smaller particles. The megaclast is located near Pullen Creek; the lahar deposits are near the Green Mountain Mill.

is more common where the layer thins on valley side slopes. More than 50 percent (and as much as 67 percent) of the subunit is characteristically concentrated in one (the finer) or in both of these classes, which explains its striking appearance. The similarity of the layer to the sole layers of both main 1980 lahars in the watershed lies in the fact that the coarsest class present may also constitute the modal class and that the modal class is one of two classes forming the mode of the 1980 sole layers. The chief textural difference is that the clasts of the coarse mode in the “ball-bearing bed” are commonly in contact; whereas the coarse clasts of the sole layer of both 1980 lahars are dispersed.

The size distribution in figure 22 is from the locality illustrated in figure 23. Mean size is  $-1.92 \phi$  (3.7 mm), sorting is a surprisingly high  $2.67 \phi$ , reflecting the presence of a matrix like that of the rest of the unit, and skewness is  $+0.61$ . The cumulative curve of the “ball bearing bed” (fig. 22) and those of the 1980 sole layers (fig. 17) have similar shapes and similar relationships to the cumulative curves of the overlying channel facies.

The prevalence of broken and abraded clasts in the “ball-bearing bed” indicates an origin partly by crushing. The distributions do not conform to Rosin’s law, thereby suggesting that shear-induced sorting also played a major role in the unusual size distribution. The truncated, one-tailed distribution seen in the histogram in figure 20 is discussed in the section on boundary features.

#### ALLUVIUM—SOURCE OF SEDIMENT IN LAHARS OF THE PINE CREEK ERUPTIVE PERIOD

A megaclast incorporated in the first lahar of Pine Creek age near Pullen Creek contains five stratigraphic units of which the second (A in fig. 24) consists of coarse, undisturbed alluvium that was probably the source of most of the sediment in the lahar. The megaclast itself is rounded, and the roundness of the alluvium is compared with that of the clasts in the enclosing lahar in the section on roundness. The stratigraphy of the mass is discussed in the companion volume (Scott, in press).



FIGURE 23.—The “ball-bearing bed” at the base of the first lahar of Pine Creek age (PC 1). The bed is transitional to the overlying channel facies of the lahar at this locality, near the Green Mountain Mill. The flow line near the top of the shovel handle reflects peak 1980–81 streamflow in the adjacent channel.

The size distribution of the coarsest alluvium in the megaclast is generally similar to that of the sediment in the lahar (fig. 22). The alluvium became mobilized with the addition of only 4 percent silt and clay; the alluvium contains 1 percent silt and clay; the lahar channel facies contains 5 percent. The visual distinction resulting from the differing percentage of fine sediment is pronounced in the flood-plain facies but is not obvious in clast-supported parts of the channel facies.

#### CLAST ROUNDNESS AND THE LAHAR BULKING FACTOR

Particle roundness ( $r$ , the ratio of the average radius of curvature of particle edges to the radius of curvature of the largest inscribed sphere) is a useful means of distinguishing lahars from other gravel deposits.

Mullineaux and Crandell (1962) noted that the clasts in lahars of the Toutle River system are more angular than those in alluvium at a comparable distance from the volcano. Their figure 1, however, mainly compares originally rounded, broken clasts of stream alluvium bulked into lahar PC 3, with similarly rounded but unbroken clasts of stream alluvium. Abrasion processes in lahars normally are reduced through the partial cushioning of particle-to-particle contact by the viscous debris flow matrix; in the granular lahars of the Toutle-Cowlitz River system abrasion locally proceeded to the point of cataclasis.

Roundness varies significantly with size. Large particles become round with the least amount of transport; boulders can be abraded from angular ( $r < 0.15$ ) to subrounded ( $r = 0.25-0.40$ ) and even rounded ( $r > 0.40$ ) in less than 3 km of macroturbulent transport by a flood surge in a mountain stream (Scott, 1967). The same



FIGURE 24.—The large egg-shaped unit is a megaclast, 5×12 m, in the first lahar of Pine Creek age (PC 1). The mass protrudes about 1 m above the surrounding upper contact of the flow, which is overlain by 2 other lahars of Pine Creek age. The coarse, immediately overlying lahar (PC 3) is the second largest of the eruptive period. The depositional surface in the foreground is the lahar of March 19–20, 1982. The Pine Creek-age terrace surface is approximately 9–10 m above the flood-plain surface at this locality in the North Fork Toutle River just upstream from Pullen Creek. The stratigraphic units in the megaclast include alluvium (labeled A).

sizes and types of particles should be measured for a valid comparison. The pebble-size fractions of  $-3$  to  $-4 \phi$  (8–16 mm) and  $-4$  to  $-5 \phi$  (16–32 mm) were selected because those size classes are well represented in both the finer grained parts of the lahars, such as the peak-flow and sole-layer deposits, and the coarser grained bar deposits. Each of the reported roundness values is the mean of at least 50 measurements made by comparison with outlines of particles of known roundness.

Because scoriaceous particles round more rapidly than associated rock types, they were excluded from the analyses of the 1980 flows to make the values more comparable to those of the older flows. Scoriaceous andesite and basalt are present in the modern cone of Mount St. Helens, but are absent from rocks, and thus from lahars, of Pine Creek and pre-Pine Creek age. Pumice was also excluded. It is present in the 1980 North Fork lahar and the second South Fork lahar but is essentially absent

from the main South Fork lahar and from many of the older flows.

#### ROUNDNESS IN THE 1980 LAHARS

Clasts with a significant degree of angularity are typical of most of the 1980 lahar deposits. The exceptions are the basal-flow deposits of the channel facies of both the North Fork and South Fork lahars. They include clasts that are better rounded than those in the peak-flow deposits of the flood-plain facies. In the North Fork lahar near the confluence of the forks (fig. 25), the difference is between subangular pebbles in the flood-plain deposits and subrounded pebbles in the bars, based on the particles in the  $-5$  to  $-6 \phi$  (32–64 mm) range. The contrast is less pronounced in the finer sizes.

Particles with roundness greater than 0.25 are stream polished over at least part of their surfaces and represent

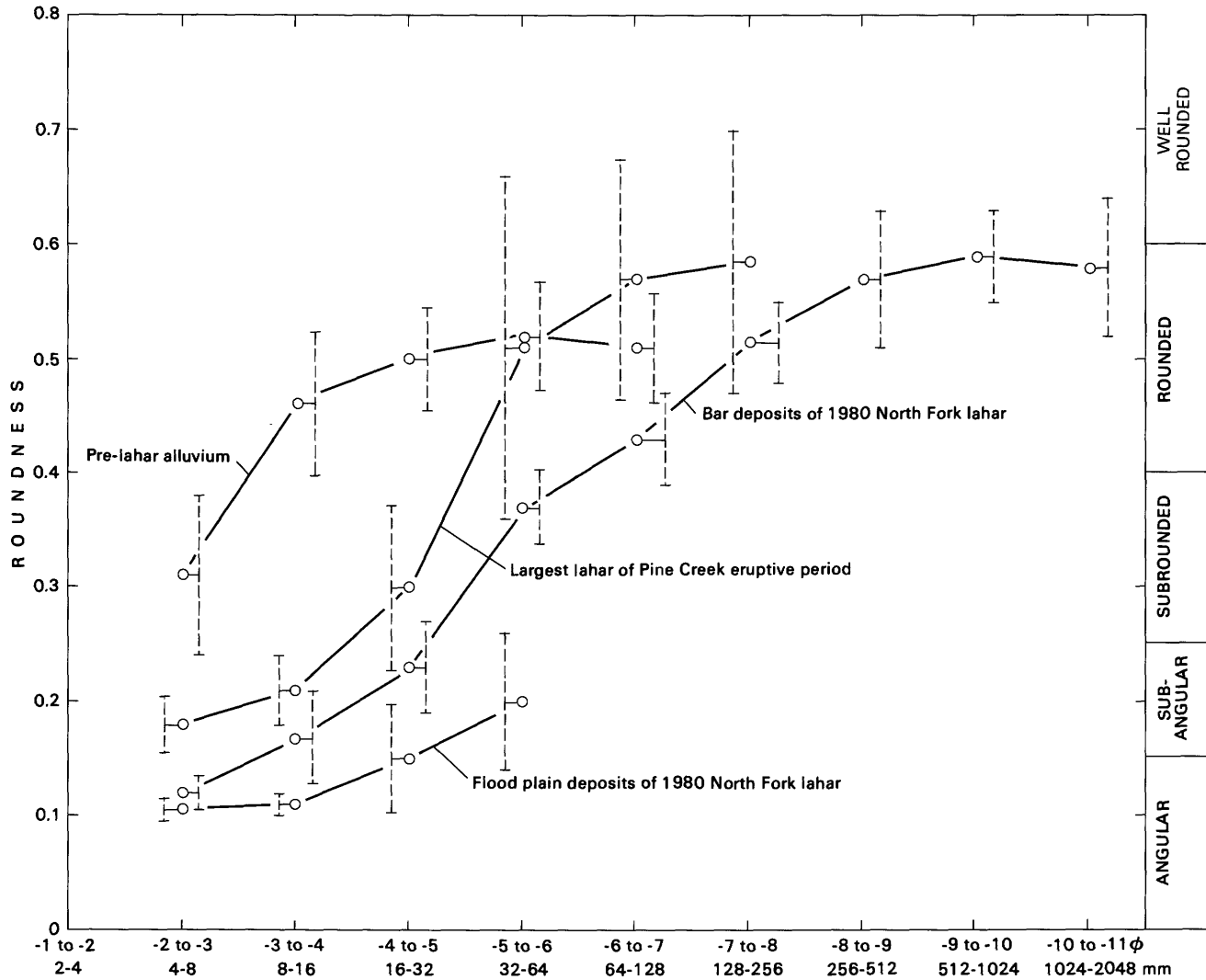


FIGURE 25.—Mean roundness in pebble, cobble, and boulder size classes of the first lahar of Pine Creek age (PC 1), in alluvium from a megaclast included in that lahar, and in bar and flood-plain deposits of the North Fork lahar. Lahar localities are near the confluence of the forks of the Toutle River; the megaclast is that shown in figure 24. Confidence limits are at the 95 percent level.

stream gravel bulked into the flow. The channel facies at the confluence of the forks (fig. 26E) contains 20 percent particles with roundness of 0.25 or more in the  $-3$  to  $-5 \phi$  (8–32 mm) range. Only 6 percent of the corresponding sizes in the flood-plain facies at that location are that rounded (fig. 26D). Such particles expectably increase downstream in each type of deposit but remain significantly more abundant in the bar deposits.

#### BULKING FACTORS OF THE 1980 LAHARS

The lahar bulking factor (LBF) is the proportion of sediment that can be shown to have been introduced by erosion during flow, as opposed to that present in a lahar at its point of origin. The LBF was determined

from roundness data as follows: All sediment in the  $-3$  to  $-5 \phi$  (8–32 mm) interval with roundness above 0.25 was assumed to have been derived from the stream channel. To this quantity were added (1) the obviously broken particles (with partial surfaces of stream rounding) in the 0.0–0.15 and 0.15–0.25 roundness categories and (2) some remaining clasts in those categories with surfaces produced entirely by cataclasis during flow—conservatively estimated as equal to the percentage of obviously broken alluvial clasts. Applying this reasoning to the North Fork lahar, LBF values are 48 percent for the channel deposits (fig. 26E) and 15 percent for the flood-plain deposits (fig. 26D). These values apply only to the  $-3$  to  $-5 \phi$  (8–32 mm) interval, representing the coarsest material that is common in the flood-plain

facies but an intermediate component of the channel facies. Based on roundness variation with size, an LBF of more than 48 percent would apply to the entire channel deposit, and a value of less than 15 percent would apply to the flood-plain facies.

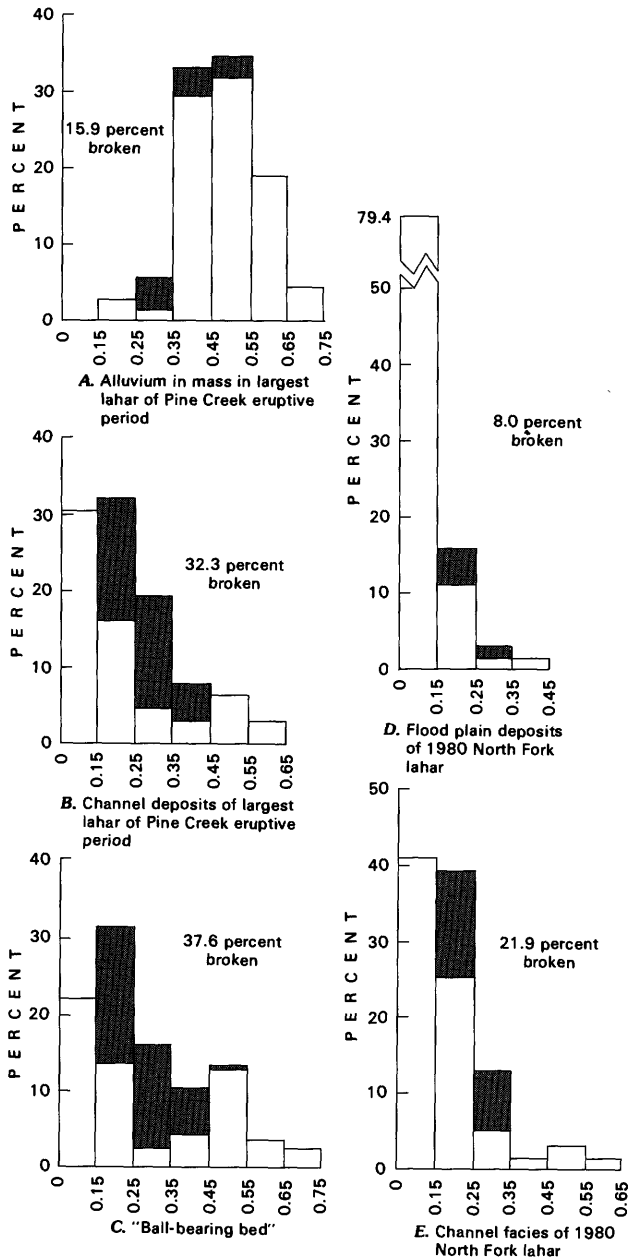


FIGURE 26.—Distribution of clast roundness in the -3 to -5  $\phi$  (8-32 mm) size interval. Locality A is at the confluence of the North Fork and Pullen Creek, B and C are near the Green Mountain Mill, and D and E are at the confluence of the forks of the Toutle River. The proportion of broken particles in each roundness class is shaded.

The flood-plain deposits of the South Fork lahar record a more rapid increase in roundness of the constituent particles than in the North Fork lahar (fig. 27). This difference indicates a greater LBF in the peak flow of the South Fork lahar, probably due to a less distinct segregation of the basal-flow and peak-flow divisions and a consequent greater mixing of eroded clasts throughout the South Fork flow, which had a greater velocity than the North Fork flow. In the North Fork lahar, moreover, the mud "skin" on the surfaces of the whaleback bars may have acted as a protective cohesive surface during recession flow. The lack of such a surface on bars of the South Fork lahar may have permitted erosion of early bar deposits, thus introducing a greater proportion of alluvial clasts into the peak flow.

ROUNDNESS IN THE PRE-1980 LAHARS

The two largest lahars of Pine Creek age (PC 1 and PC 3) contain pebbles and cobbles that are better rounded than clasts in the coarse mode of other pre-1980 lahars. The degree of roundness is striking but is somewhat less pronounced when the expectable variations in roundness with particle size are considered. Table 6 compares roundness in the two flows of Pine Creek age with roundness in flows of similar texture in

TABLE 6.—Clast roundness in pre-1980 lahars exposed near the confluence of the forks of the Toutle River

[Roundness=ratio of average radius of curvature of particle edges to radius of curvature of the largest inscribed sphere. Letters in parentheses denote locations of sections, as follows: a, Harry Gardner Park; b, Coal Bank Bridge; and c, Outlet Creek. Confidence limits are at 95 percent level]

Size class in $\phi$ (and mm)	Lahars of Pine Creek age		Lahars of Swift Creek and Smith Creek ages
	Largest flow (PC 1)	Second largest flow (PC 3)	
-6 to -7 (64-128)	0.61±.12 (a) .56±.12 (c)	Unit contains few cobbles.	0.33±.046 (b) .41±.062 (b)
-5 to -6 (32-64)	.51±.15 (a) .49±.13 (c)	0.52±.10 (c) .47±.069 (1)	.29±.042 (b) .33±.052 (b) .34±.050 (c)
-4 to -5 (16-32)	.30±.076 (a) .28±.074 (c)	.40±.054 (c)	.21±.035 (b) .25±.045 (b) .24±.041 (c) .23±.030 (1)
-3 to -4 (8-16)	.21±.034 (a) .17±.029 (c)	.19±.037 (c)	.14±.018 (b) .12±.015 (b) .15±.024 (c)
-2 to -3 (4-8)	.18±.025 (a) .12±.016 (c)	.13±.022 (c)	.12±.015 (b) .11±.013 (b) .12±.015 (c)

<sup>1</sup>Larger sample from locality c, above.

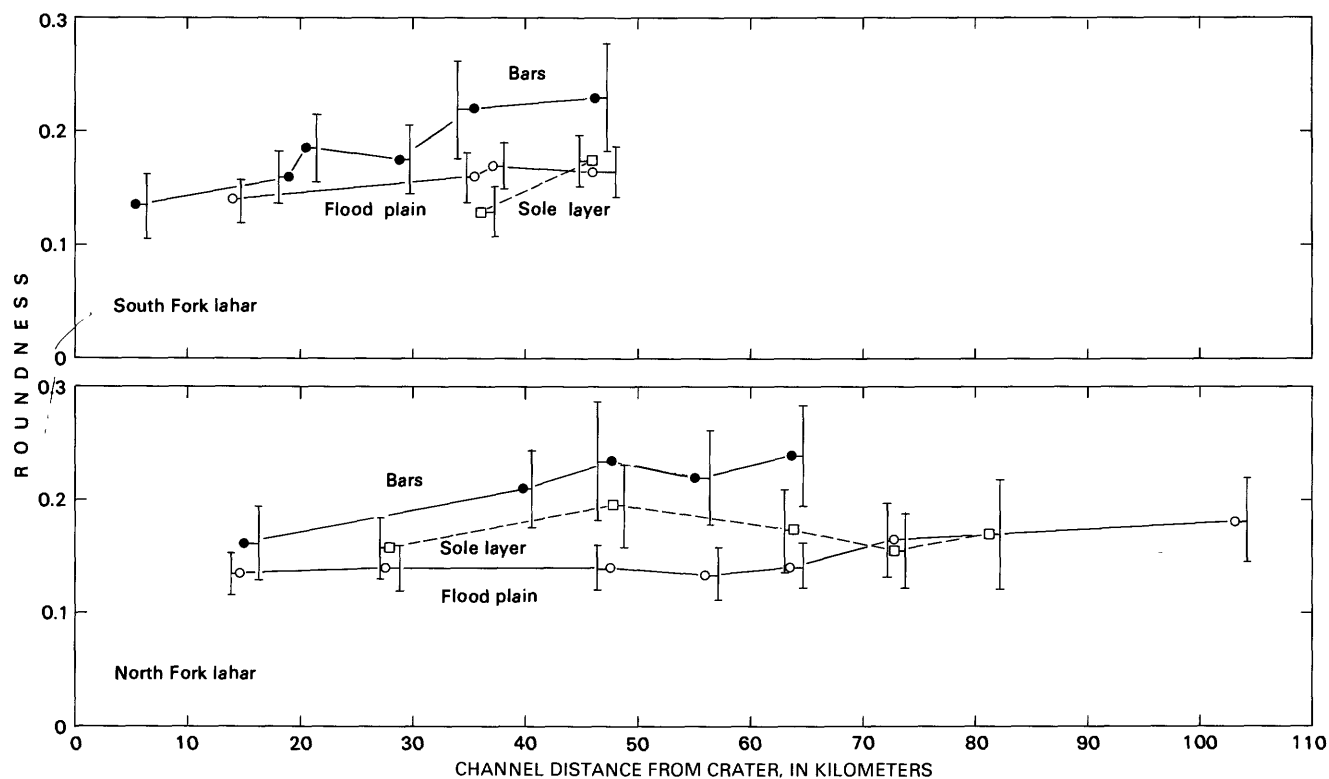


FIGURE 27.—Clast roundness in the  $-3$  to  $-5 \phi$  (8–32 mm) size interval of the sole layer, bar deposits, and flood-plain deposits of the 1980 North and South Fork lahars. Confidence limits are at the 95 percent level.

the Swift Creek eruptive stage and Smith Creek eruptive period. All the flows in these two intervals that have a cobble or coarse-pebble modal class are included. The coarser the size fraction that is compared, the more statistically valid are the roundness differences. The clasts in the first Pine Creek lahar (PC 1) are significantly better rounded than those in either the channel or flood-plain facies of the 1980 North Fork lahar (fig. 25).

#### BULKING FACTORS OF THE PRE-1980 LAHARS

Roundness data show that at least 69 percent of the  $-3$  to  $-5 \phi$  (8–32 mm) size range in the main body of the first lahar of Pine Creek age originated as eroded stream alluvium (fig. 26B). A similarly high degree of rounding is present in the “ball-bearing bed” (fig. 26C), but some of this rounding reflects grinding action during lahar transport. The resultant high LBF’s are minimum values; it is probable that many of the particles in the 0.0–0.15 roundness class were produced by the complete crushing of alluvial clasts during transport and thus that more than 90 percent of the sediment was added to the flow by erosion.

The dominance of introduced particles in the main body (channel facies) of the first Pine Creek lahar contrasts somewhat with the intermediate percentage of such particles in the bar deposits (channel facies) of the North Fork lahar, but a more apt comparison would be with the low proportion of stream alluvium in the North Fork flood-plain deposits, since they represent the main body of that flow. The huge older lahar is thus composed of sediment bulked into a flood surge from the stream channel, whereas the North Fork lahar consists mainly of sediment already in the lahar at its point of origin, or eroded from the debris avalanche surface by the lahar. Although LBF’s were not calculated for the second largest Pine Creek lahar (PC 3), the roundness values (table 6) indicate an alluvium content similar to that of the larger flow, as do qualitative observations of roundness in the other two flows in the series (PC 2 and PC 4).

A high LBF defined by rounding is not a feature of all older lahars formed by the bulking of eroded sediment in streamflow; it applies only to those in which the bulking occurred in a stream channel beyond the base of the volcano. Lahars transformed from streamflow on the slopes of the volcano or on the surface of a debris avalanche cannot be readily identified in this way.

### ROUNDNESS IN THE SOLE LAYERS

The coarse clasts dispersed in the sole layers of the 1980 lahars were a population of angular particles to which quantities of rounded particles were sporadically introduced from the stream channel. Mean roundness fluctuated downstream without an overall trend (fig. 27) as alluvial clasts were incorporated, broken, or dispersed upward in the flow. The particles in the sole layers of the 1980 lahars are more angular than those in the overlying bar deposits (fig. 27), reflecting the greater textural affinity of the sole layer to the peak-flow deposits than to the bar deposits.

The near-boundary concentration of shear during deposition of the sole layer is expressed by a higher percentage of broken clasts in the sole layer than in the peak-flow deposits. Such clasts typically have broken faces with roundness less than 0.15 but also have a part of the earlier unbroken surface, which has a roundness of 0.40 or better. Sole layers of both the North Fork and South Fork lahars contain 8–36 percent broken clasts in the  $-3$  to  $-5 \phi$  (8–32 mm) range, as compared to the flood-plain deposits which have a relatively uniform 0–9 percent broken particles in that size range. The bar deposits contain 5–25 percent broken clasts.

The “ball-bearing bed” at the base of the first lahar of Pine Creek age likewise contains a greater proportion of broken clasts than does the main part of the flow (fig. 26). The highest proportion of broken clasts in any size class of any lahar was observed in this unit (50 percent of the  $-4$  to  $-5 \phi$ , or 16–32 mm, class). This size class is commonly the modal class of the bed and is the class above which the coarse tail of the size distribution is truncated. The high percentage of broken clasts of this size suggests that destruction of larger clasts by cataclasis may explain the unusual size distribution.

### ABRASION AND CATACLASIS IN LAHARS

The roundness of lahar sediment is determined by the roundness of the original constituent particles, the bulking of rounded stream gravel, and two simultaneous processes within the flow that yield opposing results. These processes are intergranular abrasion—especially in the basal-flow carpet and in clast-supported sole layers like the “ball-bearing bed”—and the breakage of particles at and near the flow boundary. Shear stress is concentrated in a narrow vertical zone, in which the particles grind, rotate, or slide against each other rather than roll or saltate as in normal bed load.

The longitudinal trends in roundness show that values in the body of the lahar generally are more sensitive

to the introduction of alluvium than to the intralahar processes. Exclusive of the effect of particle introduction, the net effect of the debris flow process, in which dilatant fluid behavior is evident, may be to decrease roundness by intense cataclasis near the base of the flow. Roundness probably decreases in bedrock reaches where little bulking occurs, as the rounded clasts already in the flow are fractured and crushed.

A degree of rounding caused by abrasion and cataclasis was evident from roundness measurements, especially on particles from the “ball-bearing bed.” Hackly surfaces on some particles were formed both by abrasion and by the fracturing of angular corners, with the net result of increasing sphericity and thus, to some extent, of increasing roundness. In such cases, a roundness measurement became a judgment based on the scale of the observations—the crude overall rounding of the particle versus the hackly, smaller scale relief. The higher the magnification at which the particles were viewed, the more the angular surface relief influenced the roundness determinations. Intralahar abrasion was concomitant with continuing clast breakage. The “ball-bearing bed” recorded the extremes in both effects, and the uniformity and roundness of its clasts are partly due to abrasion and cataclasis during lahar transport. This applies particularly where the unit is best developed and exceeds 1 m in thickness. The effects of these processes combine with those of the shear-induced sorting that was the primary cause of the truncated size distribution and the concentration of marble-size clasts, as described in the section on boundary features.

The identification of lahars in stratigraphic sections away from the volcano was generally unequivocal, even if based only on the contrast in rounding with associated alluvial units. Cobble-size clasts in the lahars of Pine Creek age that consist mainly of eroded alluvium are as well rounded as those in alluvium (fig. 25), and those units could be misidentified at incomplete exposures. Clast support and poor grading in the lahar would add to the difficulty. However, a distinctive feature of the lahars, which is apparent in even a small sample, even for lahars formed mainly of stream alluvium, is the roundness variation with size; specifically, the relative angularity of the granules and the fine pebbles. Despite a high degree of roundness in coarser fractions (fig. 25), clasts in the finer pebble size classes are much more angular in the main bodies of the lahars formed from alluvium than in any fluvial deposit in the river system, including lahar-related streamflow deposits (table 4). A distinctive degree of angularity in that size range probably is produced in granular lahars by cataclasis even if the sediment is derived entirely from alluvium.

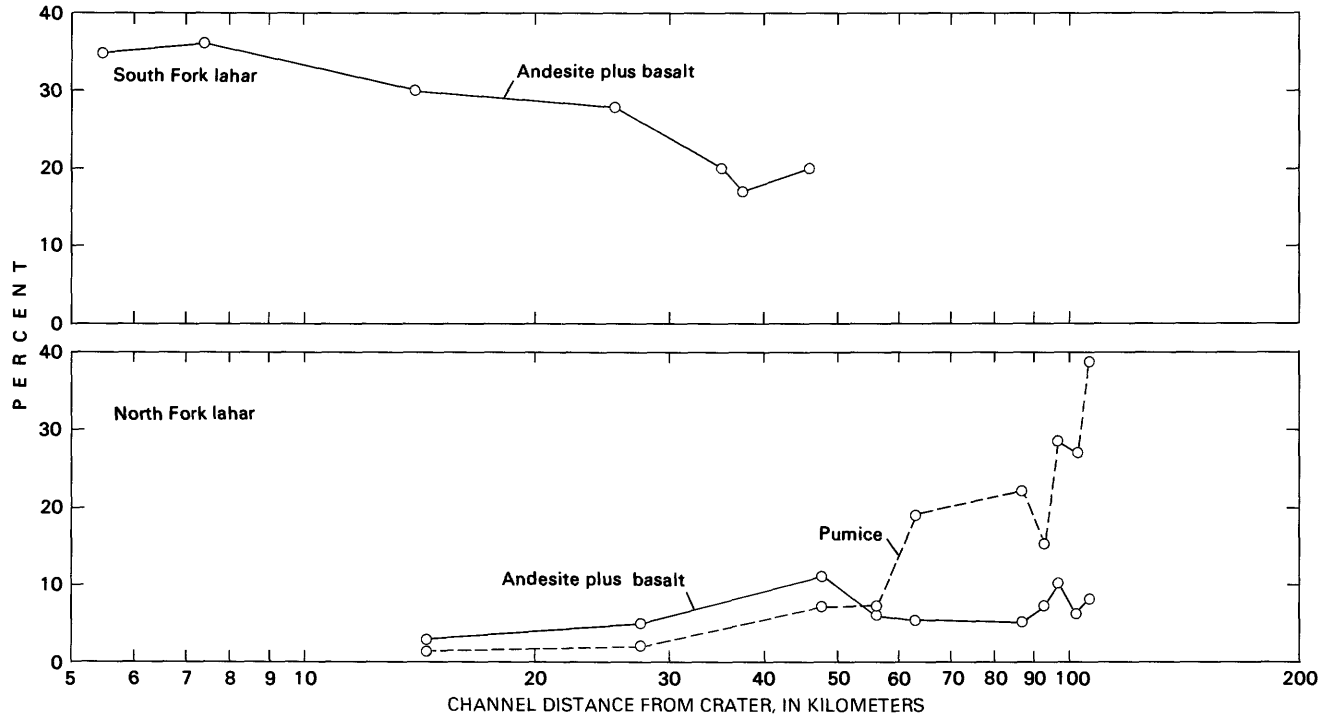


FIGURE 28.—Downstream variations in the combined percentage of pyroxene andesite and olivine basalt in the peak-flow deposits of the South Fork and North Fork lahars and in the percentage of pumice in the peak-flow deposits of the North Fork lahar.

## CLAST LITHOLOGY

The degree to which the 1980 lahars incorporated stream alluvium during flow also can be estimated from downstream changes in clast lithology. The construction of the modern cone of Mount St. Helens, which began about 2500 years ago, was marked mainly by a change from domes of hornblende-rich dacite composing the older volcanic center to cone-building lava flows of pyroxene andesite and olivine basalt (C. A. Hopson, Univ. California Santa Barbara, unpub. mapping, 1980; Crandell, 1987). Rock types abundant in the modern cone thus are absent from the lahars and alluvium of Pine Creek age and older. These older deposits were locally eroded by the 1980 lahars, thereby diluting the quantity of andesite and basalt in the 1980 flows by an amount proportional to the amount of erosion. Moreover, with the exception of some lahars of Castle Creek and Kalama age, the deposits of post-Pine Creek age in the river system away from the volcano also contain fewer rock types from the modern cone than were present in most of the 1980 lahars at their origin. Therefore, the erosion of these deposits also reduced the amount of andesite and basalt in the 1980 flows.

## PYROXENE ANDESITE AND OLIVINE BASALT

. Both dark rock types (andesite is more common) contrast with the fine-grained gray dacite composing the Kalama-age summit dome of the pre-1980 cone and with the porphyritic pink and gray hornblende-bearing dacites and andesites of the older volcanic center. The rock types are readily distinguished in the pebble size fractions (fig. 28). The trends indicate little bulking of the North Fork lahar but substantial bulking of the South Fork flow. Erosion that occurred during passage of the North Fork lahar was not enough to decrease the percentage of pyroxene andesite and olivine basalt significantly in the peak-flow deposits. The roundness data indicate that the North Fork basal flow eroded substantial sediment but that it was not dispersed into the peak flow in significant amounts. In contrast, the addition of sediment to the peak flow of the South fork lahar reduced the andesite-basalt percentage by approximately 42 percent (from 35 to 20 percent) between the base of the cone and the confluence of the forks. A similar trend in the peak-flow LBF is reflected in the roundness data.

Measurements of downstream change in composition and roundness by Gilkey (1983) showed no significant

trends in the South Fork bar deposits, possibly because the data were obtained from the entire bar deposit and thus may have been influenced by downstream change in particle size. Major (1984) distinguished significant compositional differences according to particle size in the 1980 lahars in watersheds south of Sheep Canyon. Data in figure 28 reflect the compositional changes in a constant, intermediate size range ( $-3$  to  $-5 \phi$ ; 8–32 mm), but these changes could be influenced by differential rates of clast breakage related to composition.

### PUMICE

Pumice content provides a logical means of identifying lahars formed in association with pumiceous pyroclastic flows. The main South Fork lahar originated with the initial explosion on May 18 and contains no pumice from the 1980 eruption. The second South Fork lahar was the result of interaction of pyroclastic flows with snow and glacial ice; it contained, before its erosion, 65 percent pumice by weight in the  $-3$  to  $-5 \phi$  (8–32 mm) interval at the base of the cone and more than 90 percent pumice in that size range at the confluence of the forks. The downstream increase in pumice reflects the progressive deposition of the normal-density constituents. More than 99 percent of the pumice in the flow at the base of the cone was from the 1980 eruption, as was 97 percent of the pumice in the flow downstream.

The North Fork lahar also formed after the Plinian eruptive phase began on May 18, but the areas of lahar formation on the debris avalanche were mainly outside those affected by the northeast-directed air fall. Of the small amount of pumice in the flow, more than 50 percent is of 1980 origin. The remainder was derived by erosion of older tephra units. The changes in pumice content of the peak-flow deposits are plotted in figure 28. The downstream increase can be ascribed to gradual upward flotation of the lighter particles. In a house inundated by the North Fork lahar near Tower, a sample 0.1 m below the peak stage contained 19 percent pumice, and samples 1.9 and 3.8 m below the peak stage contained negligible amounts.

### LOW-DENSITY ROCK TYPES FROM DOMES

Some dome rock types older than that forming the Kalama-age summit dome consist of dacite lava or breccia with a density sufficiently low for clasts to have been concentrated at the lahar surface. Boulders of dome rock as large as  $1.6 \times 0.8 \times 0.6$  m protruded from the berm surfaces of the North Fork lahar in the Cowlitz River channel. The most distinctive dome rock is that of the

cryptodome intruded in early 1980. The juvenile microvesicular dacite has a mean density of 1.66 (Hoblitt and others, 1981). It is present in all the lahars of May 18, including those formed outside the zone of the lateral blast, with the exception of the second South Fork lahar and its analogs in other watersheds. The distinctive bluish-gray, prismatic jointed rock type is obvious as cobbles and boulders on berm surfaces, even though it composes no more than 2 percent of the peak-flow deposits of both the North Fork and South Fork lahars.

The 1982 lahar contained a larger amount of modern dacite, which was mainly concentrated in the coarser pebble fractions. In the upper, debris flow portion of the transition facies above Kid Valley, the dacite locally composes 45 percent of the pebble size class. The dacite locally forms most of the clasts embedded in the surface of the flow deposit, as opposed to the pumice deposited on the surface by dilute recession flow. The dacite was derived from erosion of the 1980 lateral-blast deposits and of the 1982 dome; the pumice had been eroded from 1980–81 pyroclastic flow deposits.

### JUVENILE DACITE DERIVED FROM FACIES OF THE DEBRIS AVALANCHE

The color variations in subunits of the sole layer of the North Fork lahar (fig. 18) reflect materials derived from different parts of the debris avalanche. The initial slumping of material is believed by Harry Glicken (oral commun., 1985) to have occurred in an area of the avalanche in which a block facies is overlain by a matrix facies and, in turn, by a surficial unit consisting of as much as 5 m of lateral-blast deposits rich in juvenile dacite. In one of the first flights over the avalanche, Glicken observed lahars ponding (but not flowing downstream) in that area before noon on May 18, 1980. The bluish-gray color of the lower unit of the sole layer is derived from comminuted juvenile dacite mixed in that earliest part of the lahar. The subsequent and main source area of the lahar is interpreted by Glicken to have been a more distal part of the avalanche, which consisted of mixed block and matrix facies and no surficial blast deposits. The upper, brownish-gray unit of the downstream sole layer was accreted from the later portion of the lahar wave, derived from that source.

### ERODED SOIL

The finer grained parts of the main South Fork lahar have a more brownish cast than those of the North Fork

lahar. The runout deposits of the South Fork flow are also distinctively tan or light brown. The brown coloration is present in the proximal-phase slope deposits on the flanks of the volcano and thus may represent the scour of thin alpine soils by the macroturbulent pyroclastic surge. Soil was eroded locally along the course of the North Fork lahar, and clasts of soil were locally deposited on bar surfaces. The amount of included soil was, however, insufficient to color the main deposits of that flow.

## LAHAR BOUNDARY FEATURES

The amount of shear stress concentrated at or near the boundaries of the lahars appears to vary greatly. Surfaces underlying the flood-plain facies generally show little erosion; undisturbed forest litter is locally covered by the matrix-supported deposits. The channels that conveyed sustained flow show a highly variable amount of boundary shear. Locally the sole layer, which is a characteristic of the channel facies where it is best developed, rests on easily erodible sand; the sole layer of the North Fork lahar, for instance, locally overlies deposits of the South Fork lahar-runout flow (fig. 18), which were freshly deposited about nine hours before. Little erosion of the runout sand occurred. At other localities, however, boulders in the preexisting stream alluvium were truncated in place by the action of clasts in the overriding flow.

## LAHAR-ABRADED PAVEMENT

In places, dense volcanic boulders were cut at the flow boundary of the North Fork lahar, producing a surface similar to a glacial pavement cut in conglomerate. Although the surface was not grooved or polished, the surfaces of individual boulders were sharply truncated, apparently by grinding and impacts from boulders in the basal-flow carpet. A similar surface was formed between two pulses of the basal flow of the North Fork lahar at the confluence of the forks of the Toutle River (fig. 29). The lahar deposits in which that surface was formed are finer grained than the alluvium but contain some boulders, which were truncated like those locally forming most of the main flow boundary.

The lahar-abraded pavement and the sole layer were observed in close lateral association at the base of the bar deposits but were not seen stratigraphically superimposed. The pavement directly underlies lahar bar deposits without a sole layer, and at those points the

compaction that is characteristic of the sole layer has been imposed on the preexisting deposits. The deposits above and beneath the surface shown in figure 29 are texturally similar; the difference in erodibility, which allowed the deposits overlying the surface to be stripped away, is due to the compaction of the underlying deposits by the flow that formed the surface.

The lahar-abraded surface occurs only (1) where it is directly overlain by bar deposits that have a coarse mode in the boulder size range, or (2) at localities that are less than several hundred meters upstream from bars containing boulders. This correlation indicates that cutting occurred beneath the basal flow wherever intergranular stress was applied as a grinding action on the flow boundary. Pressure compacting the substrate was sufficient to hold boulders in the unconsolidated alluvium while they were being truncated.

The sheared surfaces at the base of the North Fork lahar were observed within 1 to 2 m of the altitude of the channel thalweg in reaches where the peak flow was in the range of 8 to 12 m in depth and the slope was 0.006. Where the surface was formed between two pulses of the basal flow of that lahar, maximum flow depth above the surface was only 3.5 m at a slope of 0.0045. The relatively low values of boundary shear at the more shallow depth indicate that the pavement cutting is not just a function of shear, but also is related to the coarseness of the basal sediment load under conditions of rapid energy loss. This is evident from the more common boundary condition (a sole layer overlying erodible sediment) where the calculated boundary shear was an order of magnitude higher than in some reaches having pavement. Where the sole layer was preserved, in channel reaches of approximately constant energy gradient, dispersive stress in the inversely graded boundary layer kept the coarse material away from the boundary.

As indicated by its spatial distribution, stratigraphy, and compaction, the sole layer generally was formed early in the flow and then was locally eroded by the pulses of basal flow that cut the pavements. That the concentration of shear and the degree of basal-flow clast interaction were extremely variable is also shown by the local inclusion of weak clasts near the boundary (fig. 15) and by the fact that, at most points, a substantial amount of flow traversed the surface of the accreted sole layer with little erosion.

Similar intense shear would have been focused on the spillways of any impoundment structures present in the drainage at the time of the eruption. Upstream energy losses in a filled debris basin (associated with expanding flow and reduced slope) would probably create basal flow with shear focused directly on the flow boundary



FIGURE 29.—Surface formed by compaction and truncation at the contact of two units of the bar deposits of the North Fork lahar. The overlying bar deposits have been removed by erosion. The shovel points in the direction of flow. Location is the confluence of the forks of the Toutle River.

by the interaction and settling of boulder-size clasts. The effects of the 1982 lahar on the spillway of the debris basin upstream from Camp Baker, constructed after the 1980 eruption, illustrate this point. That flow passed over several parts of the structure, where the shear associated with relatively shallow depths of flow, in the range of 1–3 m, was sufficient to abrade steel-reinforced, roller-compacted concrete and locally to remove emplaced boulder-size riprap. The exposed ends of reinforcing rods were sharpened to points analogous to those on the bayonet trees.

#### SOLE LAYER

The term “sole layer” is applied to the variety of texturally distinct basal subunits that are present in many of the modern and ancient lahars. The features can be subdivided into three general textural types, designated

according to the amount of near-boundary shear with which they were associated.

#### TYPE I—SANDY SOLE LAYERS LACKING DISPERSED COARSE CLASTS

Basal layers consisting mainly of sand are relatively common in flood-plain facies of the older lahars and are the product of relatively passive flow. They rarely show the compaction evident in the Type II sole layers. They also differ from Type II layers, in lacking dispersed coarse clasts and thus do not have a texture characteristic of the overlying lahar. The Type I layer and the overlying bed were parts of a single flow, however, as shown by the similarity in texture of the layer and the matrix of the overlying part of the lahar, and by the transition between the parts of the unit (unit 9 in fig. 30, for example).

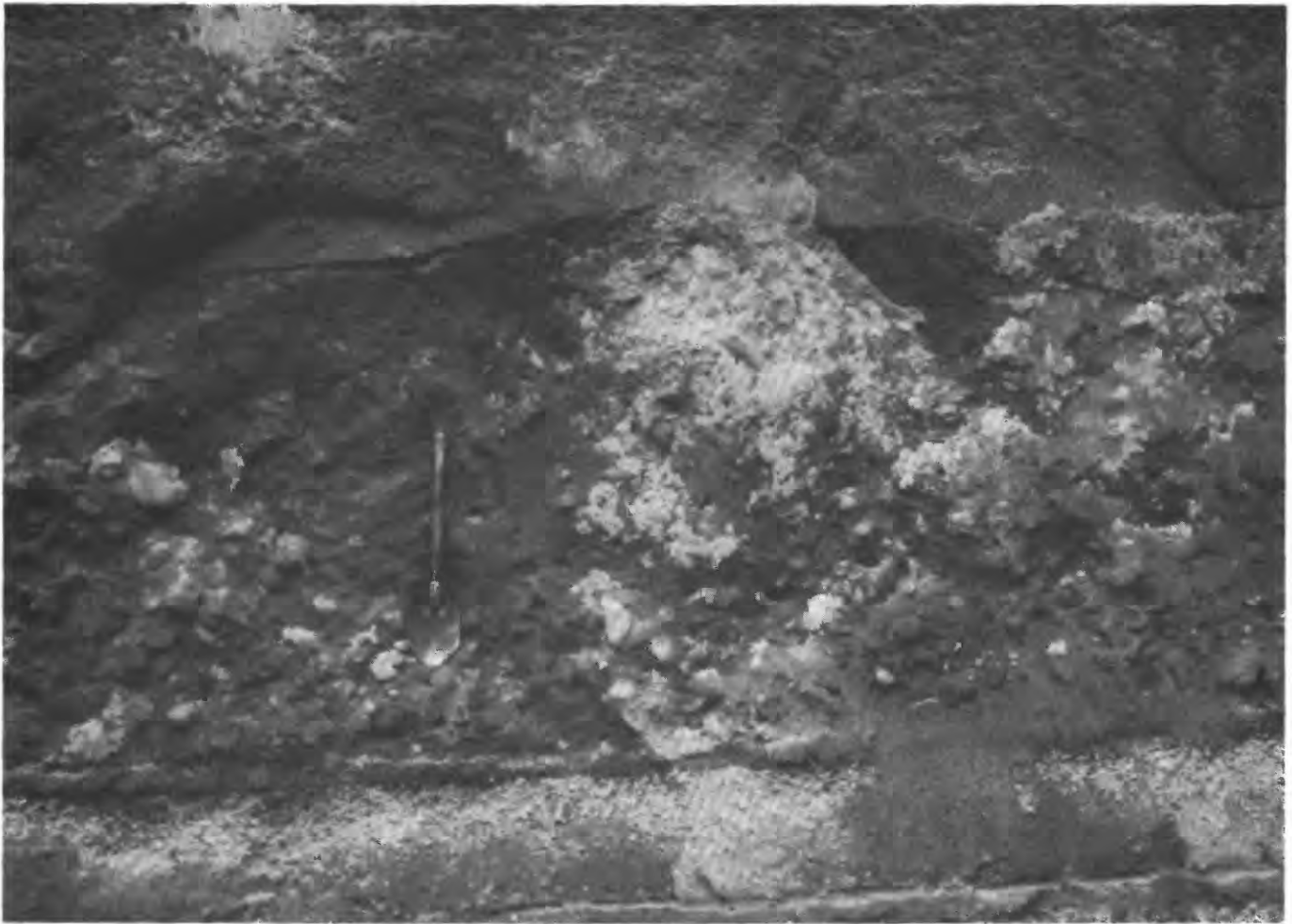


FIGURE 30.—Flood-plain facies of three older lahars, units 7, 8, and 9 of the Coal Bank Bridge section (Scott, in press). The lower half of the oldest unit is inversely graded. Only the basal 10–20 percent of the middle rubbly unit is inversely graded. The basal 15–20 cm of the overlying unit is a poorly developed Type I sole layer transitionally overlain by an inversely graded zone forming 0.2 m of the 1.2-m-thick bed. Total thickness exposed is 2.8 m.

The frequency of Type I layers in the pre-1980 lahars, and their minor part of the unit thickness (typically 10–20 percent), indicate that sole layers cannot all be explained as exact analogs of the basal, sandy parts of the transition facies. The analog explanation applies where the downstream thickening of the sole layer is progressive and the upper, debris flow part of the unit is replaced. A different explanation applies to many flows that have a Type I layer. Even where these flows encountered a large roughness element, the sole layer varies little in thickness. The sole layer was thus formed by a boundary effect within the flow rather than as the product of a distinct and rheologically different earlier part of the flow. Both explanations can thus fit this type of sole layer, but the evidence indicates that most Type I layers were created as boundary effects.

#### TYPE II—SOLE LAYERS WITH DISPERSED COARSE CLASTS

The best-developed sole layers of both the 1980 South Fork and North Fork lahars are Type II; they are finer grained, texturally more uniform, and strikingly more compacted than the generally coarser overlying bar deposits in the channel facies. As described in the section on texture, the layers commonly have bimodal size distributions and consist of silty sand containing dispersed pebbles that rarely exceed  $-5 \phi$  (32 mm). Textural affinity to the peak-flow deposits is greater than to the bar deposits that commonly overlie the layer; particle-size distributions are similar to those of the peak-flow deposits in the sand and finer grades, but show a greater development of the coarse mode in the  $-3$  and  $-4 \phi$  (8–16 and 16–32 mm) classes. The peak-flow

deposits show the progressive development of a coarse mode in the  $-3 \phi$  (8–16 mm) class with depth (fig. 14). The size distributions of the sole layer also are more likely to be truncated (no coarse tail) than those of the peak-flow deposits (compare figs. 14 and 17).

The freshly deposited sole layers of the 1980 channel facies, which tended to fracture like a partly consolidated rock, have locally resisted erosion (figs. 16 and 18). They were apparently consolidated by a simple physical process, and their cohesion cannot be attributed to clay content, which is no higher than in other lahar deposits, as shown by the relative amounts of clay in the sole layer and peak-flow deposits (compare figs. 14 and 17). The “clast-studded” appearance of the weathered surfaces of the layer reflects retention of the dispersed large clasts in the compacted matrix. The layers locally exhibit a primary foliation that is distinct from stratification and is developed parallel to the flow boundary. This fabric is particularly evident where the layer forms upward-tapering, cone-shaped pedestals around the bases of trees but is not common in the sole layers of older lahars.

The Type II layer ranges from 8 to 52 cm in thickness in the 1980 lahar deposits and commonly forms less than 10–15 percent of the thickness of a flow unit. Contact with overlying deposits is sharp in some places and gradational over several centimeters elsewhere. Various types of grading are present, but inverse grading, in at least the lower part of the layer, is most common. Where Type II layers are transitional to overlying bar deposits, inverse grading in the sole layer may continue into the overlying unit. Locally the sole layer is crudely stratified but shows little textural variation between strata. Symmetrically graded units of differing color (fig. 18) were seen only in the lower Toutle River. As discussed in the section on composition, there is convincing evidence for deposition of these subunits from different segments of the single lahar flood wave.

#### TYPE III—SOLE LAYERS OF CLAST-SUPPORTED GRAVEL; THE “BALL-BEARING BED”

The “ball-bearing bed” is an unusual sole layer at the base of the first lahar of Pine Creek age (PC 1). This remarkable concentration of fine pebbles in a silty sand matrix constitutes the basal 0.45 to 1.10 m of the total thickness (5.9 to 7.6 m) of the lahar channel facies or of channel fills (fig. 23). Pebbles in the  $-3 \phi$  (8–16 mm) and  $-4 \phi$  (16–32 mm) classes form the mainly clast-supported framework of the bed. This is in contrast with the Type II sole layers of the 1980 lahars, which have no intact framework, even though their modes are commonly in those same size classes.

Other features of the bed indicate that it is the sole layer of the huge overlying lahar: It is commonly present at the base of the channel facies (fig. 12) and is absent from the flood-plain facies, in which vertical tree molds define the flow as generally passive and of short duration. The upper contact of the bed is sharp in many places; elsewhere it is transitional over an interval that is commonly about 1 cm but locally greater.

A thinner, finer grained version of the “ball-bearing bed” that is less completely clast supported is common where the lahar deposits are on valley side slopes. At the locality shown in figure 31, the flow depth of the lahar approached 30 m on the flood-plain surface, and the equivalent of the “ball-bearing bed” is present within 5 m of the level of maximum stage on a reconstructed valley side slope of 8–10°. This relation shows that the bed was not the product of a separate flow, nor was it derived from an earlier part of the lahar that was subsequently overrun by the main flood wave. The bed would be present only at lower levels in either case. The presence of the unit on slopes and in channels, but not in association with passive deposition on flood plains, indicates that it is the product of boundary-related dynamics.

#### INVERSE GRADING

In their study of older lahars in the Toutle River system, Mullineaux and Crandell (1962) recognized normal grading as a useful criterion for recognizing a laharc debris flow beyond the base of the volcano. Inverse grading in the basal parts of the 1980, 1982, and older lahars (fig. 30) is as common. Although the inverse grading involves a smaller proportion of flow thickness (table 4), it is especially diagnostic because of its comparative rarity in deposits of other origins. Schmincke (1967) described inverse grading in lahars, and Fisher (1971) observed the feature in a variety of debris flow deposits. The following vertical sequence is variable but is clearly the typical pattern for lahars in the Toutle-Cowlitz River system, as well as those at most other Cascade Range volcanoes: (1) inverse grading beginning at the flow boundary or in or above a sole layer, (2) an ungraded or poorly graded central core (which may be absent), and (3) normal grading in the remaining upper part of the unit. The degree of grading development and the relative thicknesses of the sequential subdivisions vary between lahars.

Much of the normal grading and part of the inverse grading is coarse-tail grading, in which particles below a critical diameter are ungraded or very poorly graded. The obvious normal grading mainly involves sediment coarser than  $-1 \phi$  (2 mm). This is shown by the vertical



FIGURE 31.—Sole layer at the base of the first lahar of Pine Creek age on a valley side slope 310 m WNW. of right-bank abutment of the Kid Valley Bridge. The knife marks the top of the bed, which is 10–12 cm thick below 1.4 m of lahar deposits. This sequence correlates with that seen at the present channel thalweg in figure 23. Note the fluvial rounding of the clasts in the lahar.

changes in size distributions (fig. 14, insets) and by the longitudinal consistency in the relative proportion of silt and clay to sand, silt, and clay (fig. 13) as coarser sediment settled in the flow. Crandell (1971, table 2) describes normal grading that qualifies as coarse-tail grading in a group of lahars, including two in the Toutle River system, where the critical diameter is also  $-1 \phi$  (2 mm). The inverse grading, however, may be a function of overall size changes—distribution grading or shifting-mode grading—especially in the clast-supported deposits.

The basal 0 to 20 percent of bed thickness of the 1980 channel facies is commonly inversely graded (table 4), and the difference in mean size between the bottom and top of the zone is highly variable. From 15 to 50 percent of the flood-plain facies of the 1980 and older lahars is inversely graded, and the mean size difference between the lowest and coarsest parts of the bed is typically at least 2 phi classes. The size change in the inverse grading of both facies types is commonly an exponential

decrease as the boundary is approached. The same relation occurs in lahar deposits on steep valley side slopes and was seen in Type I and II sole layers preserved on vertical channel walls. Inverse grading thus is also, like most of the sole layers, the product of a boundary effect.

#### ORIGIN AND RELATIONS OF THE BOUNDARY FEATURES

Several partly related processes are recorded by the boundary features. They include (1) shear stress concentrated near the flow boundary and the consequent sorting and inverse grading produced by coarse particles preferentially moving up in the flow; (2) shear concentrated at the flow boundary at sites of rapid energy loss, where coarse clasts directly abrade channel alluvium rather than being supported away from the boundary by particle interactions; (3) the suppression of dilatancy so that frictional forces dominate and cataclasis occurs within the boundary layer of the flow; (4) variations in grading type and intensity due to migration of the boundary of the intralahar plug; and (5) accretionary smoothing of the boundary during the rise of the lahar wave. Also locally influencing the boundary features are alluvium bulked into the flow and water incorporated from streamflow overrun by the lahar. The latter process is discussed in the section on flow transformations; in the transition interval from lahar to lahar-runout flow it produces inverse grading and a basal layer locally like a Type II sole layer.

The boundary features record the degree to which shear was concentrated, sustained, and modified at the channel boundary. The following depositional sequence was observed in passing from areas where intense shear occurred near the channel thalweg to areas of passive deposition on the flood plain:

1. A lahar-abraded pavement overlain by clast-supported bar deposits with a mode in the boulder size range, which commonly have poorly developed basal inverse grading. The Type II sole layer is mainly absent, probably having been eroded.
2. A highly compacted Type II sole layer in sharp contact with overlying bar deposits that have basal inverse grading and a mode in the pebble or cobble range.
3. A less distinct, less compacted sole layer transitional to deposits that have basal inverse grading affecting as much as half the unit and a mode in the pebble range.
4. Sole layer absent; basal inverse grading.
5. Less pronounced inverse grading.

The close relation of the Type II sole layer to inverse grading is indicated by the distributions of both

features in a reach without a flood plain (fig. 32). Both are less well developed near the flow margin, though inverse grading is the more persistent. The thicknesses of both features vary with flow depth at this locality, where the deposits are intermediate between channel and flood-plain facies. The Type II sole layer in particular occurs where the channel was hydraulically smooth and boundary shear was maximal; it dies out laterally where the velocity distribution was disturbed by vegetation. Near the main channel, the sole layer laps up the bases of the remaining trees to form the pedestal bases studded with dispersed pebbles. The thickness of the pedestals shows that deposition was more rapid in the "dead" region of flow at the apex of the angle formed by the tree and ground. The pedestals are in turn continuous upward with the layers of mud coating the trunks. Both pedestals and coatings show the compaction and foliation characteristic of the sole layer.

The stratigraphic relations of the Type I and Type II sole layers show that the first are features of deposition on flood plains, the second of deposition in channels. The amount and duration of shear stress determined which type was formed. Nevertheless, the flood-plain facies of the 1980 North Fork and South

Fork lahars generally show only inverse grading, not a well-developed Type I sole layer. The flood-plain facies of lahar PC 1 also does not have a pronounced sole layer. Each of these flows was the first major flow of an eruptive period, and consequently the downstream flood plains were densely vegetated. Roughness was so extreme and flow consequently so passive that the Type I layer did not form. The flood-plain facies in each of these three cases includes a large volume of vegetation (removed by weathering from lahar PC 1). The Pine Creek-age lahars following PC 1 flowed across relatively smooth surfaces and developed Type I sole layers, especially in flows PC 3 and PC 4.

Pyroclastic flow units commonly have a fine-grained, inversely graded basal zone known as the basal layer (Walker, 1971; Sparks and others, 1973; and Sparks, 1976). As described by Sparks (1976), it is not a discrete layer and also differs from the sole layer in that the inverse grading is always transitional to the main body of the flow unit. The feature occurs irrespective of flow depth and channel side slope. Because pyroclastic flows represent partly fluidized debris flow (Sparks, 1976), the boundary forces producing both features are probably similar.

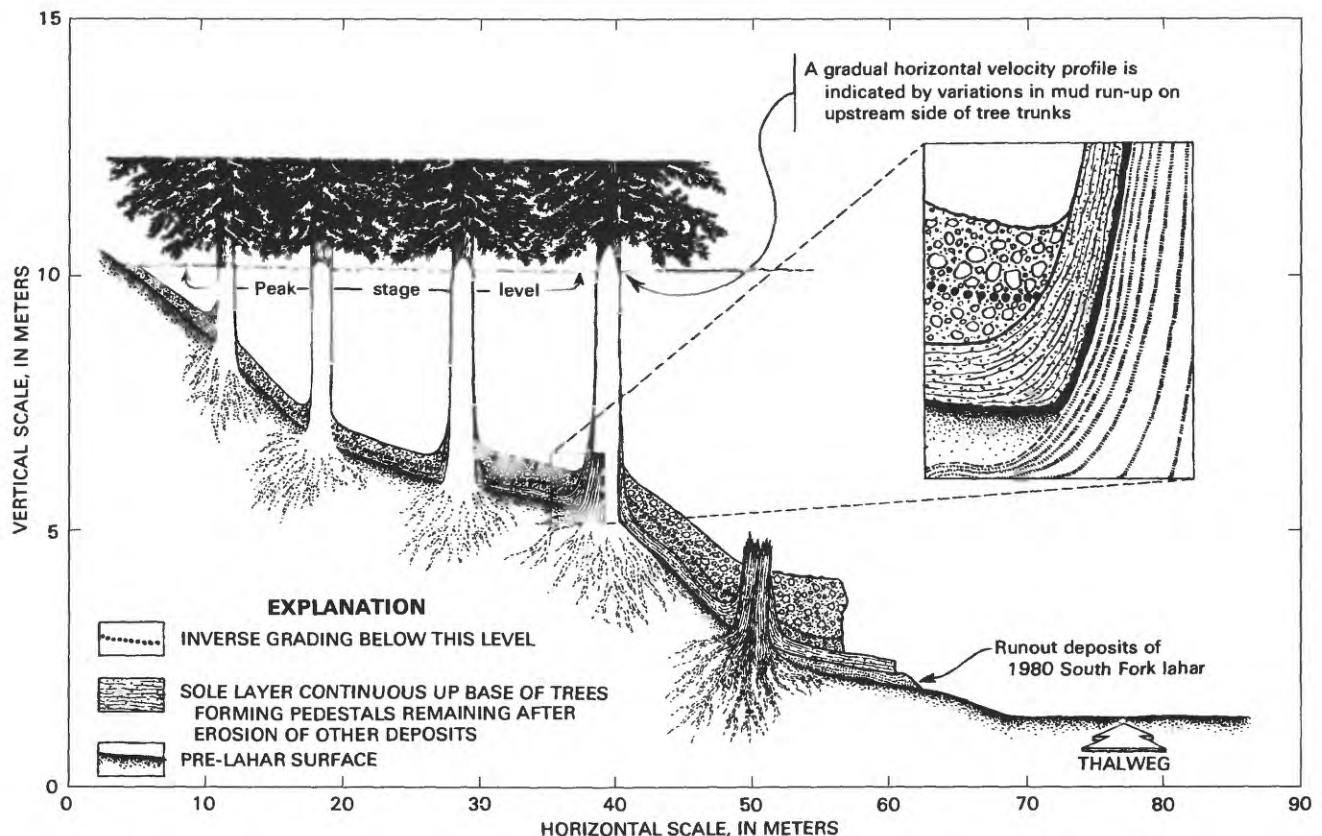


FIGURE 32.—Distribution of sole layer and inverse grading in the North Fork lahar shown in diagrammatic cross section on the left side of reach (viewed from upstream) near Tower Bridge.

The basal, finer grained parts of debris flow deposits—including both the discrete fine-grained zones like the sole layer and the inversely graded zones—have been subject to many interpretations. Naylor (1980) reviewed a group of hypotheses based on the premise that larger clasts tend to be concentrated upward within the flow. In explaining inverse grading he favored a reverse concept, based on the behavior of clays, in which the larger clasts are dropped out of the flow as a result of loss of strength of the clay matrix. This mechanism can be excluded as the origin of the sole layer or of the inverse grading in the 1980 lahars, both because of the relatively low clay content of those flows and because the hypothesis fails what Naylor describes as the critical test: the necessary coarse lag deposits, representing the material dropped from the flow, are absent. The bar deposits represent coarse material concentrated and deposited from the base of the flow, but they occur above, or have eroded, the sole layer, which clearly formed earlier in the lahar flood wave.

The Type I sole layers are close analogs of the basal zones of a series of Tertiary lahars described from central Washington by Schmincke (1967). The sole layers of those deposits are mainly composed of poorly graded sand, are less than 20 cm thick, and form the bases of lahars from 2 to 5 m thick. The lahars contain a non-graded, clast-supported central zone of coarser sediment that, like the basal zone, has less than 10 percent silt and clay. Schmincke was essentially correct in describing the basal zones as a type of inverse grading possibly related to shear distribution in the granular flows.

In commenting on the basal zones of Schmincke, Crandell (1971) noted that beds of sand underlie many lahars but that most he observed were part of underlying fluvial sequences rather than of the lahar. The observation raises the possibility that sole layers consist mainly of sandy alluvium from the channel that was incorporated into the lahar. The lack of textural correlation of the Type II sole layer with easily erodible underlying sediment is illustrated both in figure 16, which shows the North Fork sole layer overlying coarse stream alluvium, and figure 18, which shows it overlying runout sand from the South Fork lahar. The relation shown in figure 18 prevailed continuously downstream from the confluence of the forks of the Toutle River. Even the large change in boundary sediment—from coarse alluvium to fine sand—induced no corresponding changes in the texture of the sole layer (fig. 17); its texture remained related to that of the peak-flow deposits of the lahar. The same textural comparison applies to localities where the base of the “ball-bearing bed” is visible; that Type III sole layer also overlies texturally dissimilar fluvial and runout sand and gravel as well as soils and clay-rich beds.

The features of the Type II sole layer that are relevant to its origin are summarized in table 7. Where well developed, the layer reflects an interval of accretion from a probably inversely graded boundary layer during rising and peak flow. Once deposited, the layer was subject to intense compaction in channels but generally was not eroded, except locally by the coarse basal-flow carpet, because of its function in hydraulically

TABLE 7.—*Characteristics of the sole layers of the 1980 North Fork and South Fork lahars*

Characteristics	Interpretation
Sole layer overlain by bars with crests locally extending to within 1.7 m of peak flow stage. Texture of sole layer resembles that of peak flow deposits more than that of overlying bars.	Sole layer formed before or during flow peak; bar deposition was most rapid during earliest part of recession stage.
Sole layer locally compacted and semiconsolidated, though overlying deposits in sharp contact are not. Sole layer has primary foliation; overlying deposits do not.	Sole layer underwent intense shear during significant time interval between its deposition and that of the overlying deposits.
Color banding and stratification present locally in North Fork sole layer.	Sole layer was locally accretionary over a significant time interval. Color differences record flow from different facies of 1980 debris avalanche.
Development of sole layer is proportional to flow depth and lack of roughness elements.	Development of sole layer was related to intensity of boundary shear.
Sole layer better developed in broadly peaked North Fork lahar than in smaller South Fork lahar, even where depth and slope were similar.	Thickness and compaction of sole layer were in part a function of flow duration.
Sole-layer size distributions lack coarse tails, are characteristically bimodal, and have dominant, narrow coarse mode in -3 or -4 $\phi$ (8-16 or 16-32 mm) classes, regardless of coarseness of overlying sediment.	Size distribution was truncated at coarse end; coarser clasts moved away from flow boundary.
Character of sole layer not affected by the highly variable deposits that form the flow boundary.	Sole layer resulted mainly from intraflow processes, rather than the introduction of eroded sediment.

smoothing the flow boundary. The primary foliation seen in the 1980 sole layers, best developed in finer grained, relatively clay-rich equivalents such as the pedestal deposits around trees, is probably similar to the foliation induced by experimental shearing and compaction of the matrices of clay-rich debris flows. The degree of compaction corresponds with flow depth and thus with the amount of boundary shear.

The locally sharp upper contact of the sole layer represents an interruption in the processes that otherwise might form only an inversely graded basal zone, like that of pyroclastic flow deposits. That interruption is the interval of increased pressure and sustained shear that compacts the layer and produces the foliation. The sharpness of the contact correlates with the amount of compaction. The hiatus represents the passage of the flood peak and transport of the pulses of basal flow, the deposition of which initiates the formation of the whale-back bars.

The inverse grading is primarily the result of coarse clasts moving away from the boundary during flow as a result of particle-to-particle interaction. The effect is clearly seen at steep or vertical flow boundaries. This clast movement is also indicated by the positioning, in lahar PC 1, of clasts eroded from the bedrock gorge below the Coal Bank Bridge. The lahar eroded boulders of pre-Mount St. Helens volcanic rocks that are not a significant part of the flow deposits upstream from the gorge. In the first lahar exposures at the distal end of the gorge, the locally derived boulders are present only in the coarsest medial part of the flow unit. They moved several meters from the flow boundary to associate with clasts of similar size near the center of the flow, in an obviously brief interval of transport. The usual hypothesis of a lack of particle interactions in debris flows is based on the assumption of clast dispersal in a clay-rich matrix with a consequent lack of clast collisions. The relatively granular character of the Toutle River lahars evident in their particle-supported silty sand matrices, compared to some other debris flows with a higher clay content, is a logical explanation of behavioral differences involving more intense particle interaction.

The inverse grading is most readily explained by dilatant flow behavior in the sense of Bagnold (see Denlinger and others, 1984). The mechanism of kinetic sieving (Middleton, 1970), whereby small grains pass downward through the interstices of larger particles during dilation, may explain part of the inverse grading in clast-supported units such as the bar deposits. The process has been shown to be effective in experimentally produced shear zones in clast-supported materials (Mandl and others, 1977).

The textures of the Type II and Type III sole layers also show a response conforming to the behavior of a dilatant fluid (with coarse clasts preferentially moved

away from the boundary by particle interactions, and consequent truncation of the size distributions). The coarse mode of both types is remarkably consistent in the  $-3 \phi$  (8–16 mm) and  $-4 \phi$  (16–32 mm) fractions, and larger clasts are almost entirely absent. More than half of the "ball-bearing bed" is concentrated in those classes (fig. 22), suggesting that the mainly clast-supported unit represents the extreme product of shear-induced sorting. The high percentage of broken clasts in the unit (fig. 26) and a degree of rounding by cataclasis indicate that the response to shear stress of clast movement was replaced by one of abrasion and breakage. This response probably changed after clast support and the accompanying truncation of the size distribution in the boundary layer were achieved. In experimental shearing of granular material, total shear stress can be separated into (1) that acting to dilate the shear zone and (2) frictional stress acting to dissipate energy by intergranular friction and grain breakage (Mandl and others, 1977). Suppression of dilatancy and consequent grain cataclasis occurs with increased normal load. The flow producing the "ball-bearing bed" was the fastest and deepest flow in the system and also had a clay content as low as any flow, ancient or modern. This combination of characteristics yields the greatest intergranular stresses as well as the greatest potential for suppressed dilatancy and consequent grain cataclasis.

Some of the variation in shear concentration recorded by the boundary features is probably explained by fluctuations in the internal boundary between the rigid core (or "plug") of the lahar and the zone of laminar flow around its edges. The intraflow boundary forms at the level at which internal shear stress exceeds yield strength (see Johnson, 1970, 1979) and will occur in either plastico-viscous or dilatant fluid behavior. The boundary migrates continuously during flow due to changes in slope and roughness (Hampton, 1975). The frozen flow lines preserved in the deposits of anastomosing tributary flows of the North Fork lahar on the debris avalanche (fig. 33) and in logged valley flats (Lipman and Mullineaux, 1981, photograph on p. 460) indicate plug flow like that of both experimental (Johnson and Hampton, 1969, fig. 3.9) and natural debris flows (Johnson, 1970, fig. 14.9). After the lahar entered a single confined channel downstream, shear was more widely distributed in the horizontal plane. Figure 32 illustrates a gradual horizontal velocity profile shown by runup heights on trees. The distribution of shear in the 1980 lahars on forested flood plains and in confined channels was apparently distorted by vegetation and bedrock roughness elements.

The lahar-abraded pavement occurs at locations where changes in depth and velocity would have caused the plug boundary to approach the flow boundary,



FIGURE 33.—Lateral margin of lahar deposit on the surface of the debris avalanche near Elk Rock. Flow lines asymptotically approach parallelism with flow margin near backpack and are transverse to flow throughout most of the central area of plug flow. Flow is toward left foreground. Earlier position of flow margin preserved as an island in right foreground.

thereby concentrating the shear. The variation in thickness of either the inversely graded basal part or the coarse central part of a typical lahar unit may be a function of the amount of plug boundary migration. Hampton (1975) noted that the migration would produce a grain size variation but did not describe the variation. Although the plug is rigid with respect to flow behavior, large clasts are free to settle within the plug, concentrating progressively with depth. (See vertical changes in size distributions in figure 14.) The typical upper zone of normal, mainly coarse-tail grading is ascribed to this settling.

## FLOW TRANSFORMATIONS

The following sections describe the main types of flow transformation that have recurred in the river system: the formative transformations, from pyroclastic surge, avalanche, and flood surge to debris flow, and the distal transformation from debris flow to hyperconcentrated streamflow.

### PYROCLASTIC SURGE AND AVALANCHE TO DEBRIS FLOW

Evidence that the 1980 South Fork lahar began as a highly inflated pyroclastic surge includes (1) a rapid

decline in discharge at the base of the cone, (2) deposits in the same interval that record the hydraulically continuous transformation from a highly dispersed, air- and gas-mobilized state to a water-mobilized state, (3) photographs documenting this change in flow behavior, and (4) the effects of the flow on overrun vegetation and bedrock roughness elements. Because of the originally continuous exposures of the flow deposits, the evidence for the 1980 transformation is unequivocal. The same transformation probably also produced lahars from pyroclastic surges in pre-1980 eruptive periods; the conditions that provided the water content of the 1980 surge—cone saturation and snow and ice cover—would have been present at the time of any similar catastrophic ejection of material.

The solids dispersed in the inflated flow ejected into the South Fork watershed were mainly accessory lithic material from the modern cone. They formed a thin, uniform, noncohesive coating—locally more like a “dusting”—on valley side slopes at flow depths of over 100 m. On the middle and lower slopes of the cone the deposits are associated with only small amounts of erosion. Dynamically consistent peak-flow marks document the continuity of this inflated flow as it moved downslope to continue as a lahar with water as the continuous phase. The deflation is reflected by the rapid decrease in flow velocity and discharge (fig. 34). The collapse of the flow reflects the loss of ingested air and

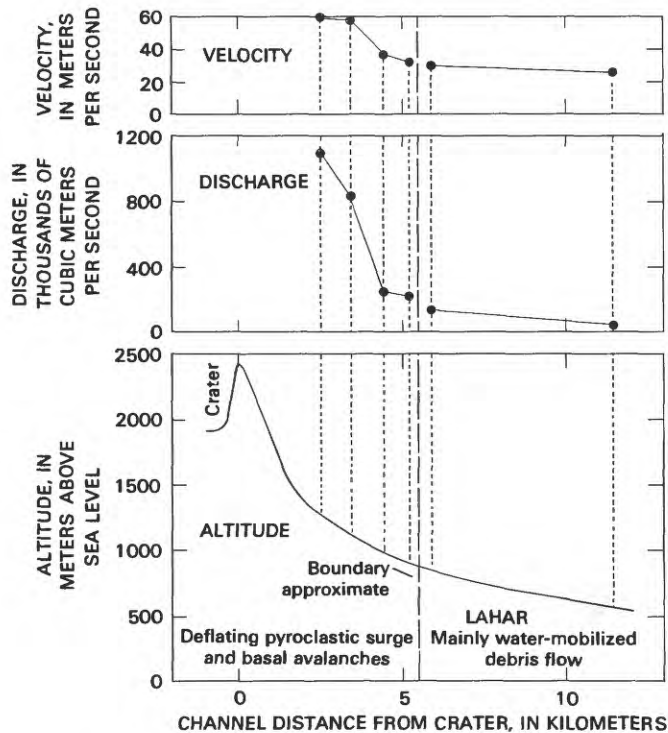


FIGURE 34.—Discharge and velocity of the pyroclastic surge and main lahar in the South Fork Toutle River on May 18, 1980. The measurements upstream of km 5.5 apply to the pyroclastic surge after its channelization in canyons cut into the slopes of the cone.

probably the condensation of steam, as well as the expectable attenuation of the sharply peaked flow wave. Only a small proportion of the total flow volume was lost through deposition from basal avalanches. The avalanches were coarse material that concentrated at the base of the surge and moved as segregated, rubbly flows.

The pyroclastic surge deposits consist of both the thin deposits extending high on valley side slopes, and the rubbly berms of the basal avalanches low in the channel. The transition to the downstream, water-mobilized lahar is shown in figures 6 and 34 at the approximate point where debris flow berms (distinguished by a muddy matrix and surfaces with water-deposited sediment and buoyed low-density clasts) completely replace both types of surge deposits. Much of the deflation had already occurred upstream from that point, however, as seen in the drop in discharge (fig. 34). Downstream from the transition, the limits of the peak-flow lahar deposits, rather than the limits of the slope deposits of the pyroclastic surge, define the peak stage.

Stratigraphic relations show that the inflated flow that transformed into the South Fork lahar was closely related to the directed volcanic blast that devastated the 600-km<sup>2</sup> area north of the mountain. That

phenomenon is variously described as a lateral blast (Hoblitt and others, 1981), a pyroclastic surge (Moore and Sisson, 1981), a pyroclastic density flow (Waite, 1982), or a high-velocity ash flow (Walker, 1983). Locally that flow swirled across the northern drainage divide of the South Fork at velocities probably near those of the main part of the flow, estimated by Rice and Watson (1981) at 150–250 m/s. The resulting deposits—layer A1 of the blast deposits (Waite, 1981)—mainly underlie, or were eroded by, those of the slower South Fork flow, which moved at about 60 m/s in the areas reached by the blast (fig. 34). Layer A1 locally overlies the deposits of the South Fork flow, however. Aerial photographs (fig. 5) show a distinct (at this scale) contact between the two flows and thus indicate a definite (but probably small) time interval between the main part of each. Although air-fall layer A3 of the blast deposits was poorly developed on the southwest side of the volcano and was rapidly eroded, it was observed on top of the South Fork lahar deposits beyond the base of the cone (R. J. Janda, oral commun., 1982). That relation establishes deposition of the lahar within approximately 15 minutes of the 0832 eruption. The actual time difference was much less, as shown by the relationship of the deposits to layer A1.

Ground photographs (fig. 35; and fig. 24 of Foxworthy and Hill, 1982) show that the South Fork inflated flow was created by the first and largest of the explosive events recognized by Moore and Rice (1981) and by Rice and Watson (1981). The resulting cloud circled the mountain outside the blast zone. The photographs show only the surficial cloud rising above the main body of the surge; the deposits and the effects on vegetation record the passage of the main part of the flow at depth.

That the basal avalanches settled from the surge and continued to flow in channels (fig. 7) is indicated by the stratigraphic relations and the geometry of the deposits. Moreover, the lack of pumice in these deposits verifies their origin before the second South Fork lahar in the afternoon of May 18. Sorting of the avalanche deposits is poor, from 2.8 to 4.2  $\phi$  (fig. 19), and mean size is in the coarse pebble and cobble ranges. Unlike the basal bar deposits of the downstream lahar, the basal avalanche deposits contain little fine material; in a relatively muddy sample, total silt and clay content is less than 4 percent. The basal avalanches were clearly subordinate in flow volume to the main part of the surge that yielded the downstream lahar (fig. 7). As revealed by the relative heights of the avalanche berms and the peak-flow stage, the flow depth of the avalanches was 2 to 10 percent of the flow depth of the surge. The segregation of the avalanches from the deflated part of the surge and the subsequent segregation of the bar deposits from the deflated, water-mobilized lahar are



FIGURE 35.—The leading edge of the pyroclastic surge descending the southwest flank of Mount St. Helens, 2 min, 20–25 s after the beginning of the 0832 P.d.t. eruption of May 18, 1980. The watershed of the South Fork Toutle River and tributary Sheep Canyon forms the left (west) margin of the volcano. Note the lighter colored layer that is best developed in the headwaters of the South Fork. The faint cloud above the west flank of the volcano is an atmospheric effect of the eruption. Photograph by Harold Fosterman. Time of photograph estimated by S. D. Malone (Univ. Washington, written commun., 1984).

analogous in sequence to the initial segregation and subsequent re-segregation of block and ash flows from a primary and evolved secondary ash cloud surge as described by Fisher and Heiken (1982).

The thin deposits coating valley side slopes high above the berms of the basal avalanches have a geometry and texture showing that the upper, non-avalanche part of the surge was air and gas mobilized. Although the boundaries of both the pyroclastic surge and the downstream lahar appear sharp in figure 5, the surge boundary was not obvious in the field once the deposits had dried. The thin (several centimeters or less), uniformly distributed surge deposits feathered to a peak-flow level that was indistinct over a distance of several tens of centimeters, in contrast to the precisely defined peak-flow mark of the downstream lahar. The slope deposits are indistinctly stratified and are variable but mainly noncohesive mixtures of silty sand with scattered small pebbles. (Sediment size terms are applied to the surge ejecta for comparison with the downstream lahar.) Sorting in the slope deposits is equivalent to or poorer than that of the avalanches and ranges between 2.8 and 4.4  $\phi$  (fig. 21), but the mean size is distinctly finer, in the sand size range. The similar sorting in a much finer deposit mainly reflects the

relative lack of fine sediment in the rubbly avalanche deposits. Although the silt and clay content of the slope deposits is between 13 and 22 percent—nearly the same as in the downstream lahar—the vegetation overrun by the surge lacked significant mud coatings. Laminated, surficially vesicle-rich coatings as much as several centimeters in thickness were characteristic of vegetation inundated by the medial and distal phases of the lahar (fig. 6). The coatings reflect the progressively greater duration of the lahar flood wave as it moved downstream; they thin again throughout the increasingly dilute distal phase.

South of Sheep Canyon, on the southwest flank, the distinction between slope and basal avalanche deposits was not observed. There, Major (1984) described mainly coarse rubbly lahars that originated as catastrophically ejected avalanches high on the mountain. Those flows did not transform from a highly dispersed state and did not extend significantly beyond the base of the cone.

The dynamics of the highly dispersed surge, which deflated downstream to form the lahar, are revealed by the effects on vegetation. The upstream surfaces of trees that remained standing were shredded as if hit by grape shot, a coarser version of the sandblast effects

of a base surge described by Moore (1967). Angular pebbles penetrated the shredded surfaces like projectiles. Variation in the depth of trunk abrasion indicates that part of the coarser gravel fraction—other than that in the basal avalanches—moved in traction and that the maximum flux of particles was from 0.5 to 2.0 m above the flow boundary. Pebble-size gravel of normal-density rock types was supported by turbulence at the peak flow levels, and many small conifers were stripped only of their bark and needles by a sandblast effect that left small branches and twigs intact. This was in striking contrast to the “bayonet” trees, whose trunks were sharpened to a point by the downstream lahar. Locally the surge appeared to have jetted past rather than flowed around bedrock projections, as inferred from patterns of stripped vegetation.

The deposits and vegetation effects show that at depth, as the cloudlike leading edge seen in the photographs (fig. 35, for example) passed, the surge was settling and deflating. The bulk of the flow was rapidly channelized and behaved as a dense fluid without the ability of the more energetic, northward-directed blast to move across large topographic obstacles. The highly dispersed fine material seen in the ground photos continued to boil above the deflating surge like an ash cloud. The probably steam-rich cloud within the surge (fig. 35) did not yield significant deposits, nor did it obscure the peak-flow marks of the main, deflating body of the surge.

The flow dynamics, peak-flow marks, and sedimentology clearly define a single major flow that transformed downstream. Alternative hypotheses involve separate events, such as a hot pyroclastic surge closely followed by a meltwater flood that bulked with sediment to form the downstream lahar. A flood hypothesis cannot explain, by melting of ice and snow in a few seconds, an instantaneous peak water discharge that is even a small fraction of the measured value for the surge of 1,100,000 m<sup>3</sup>/s (fig. 34). The peak-flow marks clearly reflect a canyon-filling discharge. Flow volume near the base of the cone is estimated at 13,000,000 m<sup>3</sup> by Fairchild and Wigmosta (1983), and this volume would have passed in just a few seconds at the stated discharge rate. Moreover, the passage of a flood would have caused profound erosion and sediment transport on the middle and lower slopes, and these effects have not been observed.

#### TEMPERATURE OF THE PYROCLASTIC SURGE

The juvenile dacite from the 1980 cryptodome is present in the surge deposits in small amounts, generally less than 2 percent in the South Fork and less than 1

percent in Sheep Canyon. However, this and other low-density rock types are locally abundant on the surfaces of the lahar berms. The deposits of the lateral blast contain about 50 percent juvenile dacite (Hoblitt and others, 1981; Moore and Sisson, 1981; and Waitt, 1981), and the greatest amounts correlate with the areas of highest temperatures evident from wood charring (Moore and Sisson, 1981). Although most dacite blocks were broken during transport, some in the pyroclastic surge deposits and in the downstream lahar have prismatic cooling joints. Prismatic jointing can be evidence that the deposit was emplaced while hot if confirmed by consistent directions of thermoremanent magnetism (Crandell, 1980). Although thermoremanent magnetism was not measured, the occurrence of the jointed dacite blocks adjacent to uncharred wood shows that emplacement temperatures of both the surge and lahar deposits were not high.

A seared (but not burnt) zone near tree line on the side of the cone (Major, 1984) establishes that the temperature of the cloudlike leading edge of the flow was relatively low at that point. Even lightly charred vegetation was not seen in place below that point on the middle slopes of the cone. A small amount of macerated and charred vegetation is present in the main deposits of the surge but may have been derived from erosion of deposits of the much hotter lateral blast. Similar fragments are extremely rare at the timberline outside the blast zone.

The original temperature of the surge entering the South Fork and Sheep Canyon must have been lower than the initial temperature of the lateral blast, which was estimated as 327 °C (Davis and Graeber, 1980). Less juvenile dacite, more of the surficial parts of the cone, and a greater proportion of snow and ice were incorporated in the material ejected into those watersheds than into the blast zone. A ground observer 4 km from the base of the cone described the immediate lahar deposits as resembling warm concrete (Rosenbaum and Waitt, 1981). The appearance of fir needles remaining on trees generally suggested temperatures less intense than in the marginal seared zone of the lateral blast; needles used as thermometers at two locations in the seared zone indicated temperatures of 50 and 250 °C (Winner and Casadevall, 1981). Blistered and peeled vegetation at the tree line was observed by Major (1984) in a zone extending around the southwest flank of the volcano from Sheep Canyon and, by the same analogy, suggested temperatures in the 50–250 °C range.

The lack of muddy tree coatings from a pyroclastic surge was interpreted as evidence of temperatures over 100 °C by Moore (1967), in contrast to the cooler base surges. The lack of significant coatings from the South Fork pyroclastic surge, however, can also be ascribed

to the brief duration of the surge and to its dispersed state and coarser sediment, even if wet.

Evidence of a wet condition, and therefore of an emplacement temperature less than 100 °C, is the dark color and distinct definition of the pyroclastic surge deposits shown in figure 5, as contrasted with their light color and indistinct definition after drying. The wet lahar deposits downstream showed an identical color change; the initially dry deposits of the lateral blast in the watershed did not.

#### ORIGIN OF WATER IN THE LAHAR

The initial and probably main source of the water that mobilized the collapsed flow was water and steam that were derived from the preexisting rocks of the volcano and were initially mixed in the main body of the surge. The upper part of the mountain was apparently near or at saturation at the time of the eruption (Moore and Sisson, 1981; Voight and others, 1981), and elevated pore pressures from an artesian system may have contributed to the slope failure that initiated the debris avalanche (Voight and others, 1983). Subsurface water or derived steam would have been mixed throughout the surge. The largest lahars at Mount Rainier were derived from transformations of huge sector-collapse avalanches, and some of these were not associated with known volcanism, indicating that mainly interstitial water mobilized the material.

Additional moisture was derived from ice and snow incorporated in the surge. About half the combined volume of the Toutle and Talus Glaciers was removed on May 18, a total of 7 million m<sup>3</sup> (Brugman and Meier, 1981). Assuming (1) the estimated volume of the South Fork lahar of 13 million m<sup>3</sup> at a point just downstream from the point where deflation was complete and (2) the volume proportion of solids typical of debris flow (Sharp and Nobles, 1953; Pierson, 1980; 1985) of 0.60–0.78, a minimum of 3.25 million m<sup>3</sup> of water could have mobilized the flow. Half of the lost glacial ice, if incorporated in the pyroclastic surge, would have been sufficient to mobilize the deflated flow. Such incorporation is unlikely, however. Part of the ice and the associated snowpack was scoured by the surge entering the South Fork and Sheep Canyon; a majority of it—probably a large majority—was melted by the heat from tephra and numerous pyroclastic flows later on May 18 to form streamflow and the second lahar. The dynamics of the surge on the lower slopes suggest that the few seconds of scour and melting at the base of the surge would have yielded a basal concentration of ice fragments and water or steam that may not have mixed throughout the entire depth of the surge. Only

negligible parts of the Toutle and Talus Glaciers extended above the present crater rim and thus were explosively incorporated directly in the surge.

Most of the watersheds outside the zone of the lateral blast yielded lahars formed from catastrophically ejected material on May 18 (Major, 1984; Pierson, 1985). Those on the southwest flank of the volcano formed in a quadrant with little glacier ice, leading Major (1984) also to favor water of geothermal origin as the primary source. Streamflow is an additional source of incorporated water, but the volume in channels on the steep sides of the volcano in the early morning of May 18 would have been negligible relative to that of the lahars.

#### COMPARISON WITH OTHER PYROCLASTIC SURGE AND FLOW DEPOSITS

Pyroclastic surges differ from pyroclastic flows in being less dense, less continuous, and less likely to approximate steady-state conditions (Wohletz and Sheridan, 1979). They are turbulent, low-concentration gas-solid dispersions (Sheridan, 1979; Wright and others, 1980; Malin and Sheridan, 1982; Walker, 1983; and Fisher and Schmincke, 1984). Types include the ground surge (Sparks and Walker, 1973), the deposits of which underlie those of an associated pyroclastic flow; the base surge described by Moore (1967) and Waters and Fisher (1971) as the low-temperature density flow sweeping outward from the base of a weak phreatomagmatic eruption column; and the ash cloud surge formed by separation of fine material from the surface of a moving pyroclastic flow (Fisher, 1979).

The South Fork pyroclastic surge has in common with base surges a low temperature and an initially ring-shaped leading edge (fig. 35; see also fig. 4 in Waters and Fisher, 1971). The body of the South Fork pyroclastic surge that transformed to a lahar was clearly not a base surge, however. The slope deposits are significantly different from described base-surge deposits, and the differences suggest why no base surge has been observed to transform to a lahar. The better sorting and particularly the crossbedding of base surge deposits indicate a relatively low sediment concentration and suggest that those surges, upon deflation and collapse in their wet distal phases, lacked both the fine-grained matrix and the water content necessary to continue flow as a lahar. The South Fork pyroclastic surge at depth had a much higher sediment concentration. The derivation of lahars from a variety of upstream pyroclastic flows and surges in other eruptions is reported by, among others, Moore and Melson (1969), Neall (1976b), and Rose and others (1977). The direct

transformation of an inflated flow to a nonpumiceous lahar has not been documented previously, however. Sheridan and Wohletz (1981) consider the possibility of direct transformation and describe how either a lahar or a water flood may arise—indirectly—from the wet distal stage of water-pyroclastic interaction in a cooling ash cloud model.

The initial steam-rich phase of the pyroclastic surge in the main canyon of the South Fork was both over-run and followed by a colder and wetter part of the surge flow wave. No evidence of the early phase as a distinct ground surge deposit, the basal unit in a pyroclastic surge model applied to Bandelier and other Plinian deposits by Fisher (1979), was observed beneath the avalanche deposits. The lack of ground surge deposits may be due to the low height of the eruption column, as proposed by Fisher and others (1980) for Mount Pelée. Much of the material in the South Fork surge was probably ejected with a distinct lateral component.

The proximal flow characteristics are those of a pyroclastic surge. The deposits, however, have some of the characteristics of deposits of pyroclastic flows: heterogeneity, variability in sorting and grain size, and occurrence in thin deposits mantling steep slopes. They differ from most previously described surge deposits, including ash clouds or ash cloud surges (Crandell and Mullineaux, 1973; Crandell, 1987; and Fisher, 1979), because they are coarser and only indistinctly bedded. In these respects, however, they are similar to the ash cloud deposits at Mount Pelée described by Fisher and Heiken (1982). Sorting of the slope deposits is poorer than that of most surge deposits of equivalent mean size. (Compare Fisher and Waters, 1969, table 1; Waters and Fisher, 1971, table 1; Sparks, 1976, fig. 12; Wohletz and Sheridan, 1979, table 2; and Sheridan and Wohletz, 1983, fig. 3.) The crossbedding typical of nearly all previously described surge deposits (Wohletz and Sheridan, 1979), including a unit of the 1980 lateral blast deposits (Waitt, 1981), is absent from the 1980 South Fork surge deposits.

The basal avalanches are interpreted to have formed by gravity segregation like the block and ash flows at the base of the ash cloud surge at Mount Pelée (Fisher and Heiken, 1982). They are similar to some deposits described as lithic pyroclastic flows, such as parts of the Pine Creek volcanic assemblage on the south side of Mount St. Helens (Crandell and Mullineaux, 1973)—units not known to be associated with a pyroclastic surge other than an ash cloud. Lithic pyroclastic flows generally were emplaced at higher temperatures than the avalanches, as a result of their formation by dome collapse or explosion.

#### COMPARISON WITH KALAMA- AND POST-KALAMA-AGE DEPOSITS

The avalanche deposits are also similar to parts of a Kalama- and post-Kalama-age sequence of rubbly avalanches and lahars in the South Fork channel in a reach extending from the base of the cone to more than 12 km from the crater (dating and stratigraphy in Scott, in press). The sequence includes an avalanche and lahar associated with a pyroclastic surge deposit that is strikingly similar to the deposit of the 1980 lateral blast.

The effects of the mainly Kalama-age flows on vegetation were similar to those of the 1980 flow. The upstream sides of a few exhumed standing trees near the center of the largest flow show shredding and high-velocity rock impacts like those of the overrun modern trees. Evidence of temperatures high enough to singe wood is mainly lacking, but trees extending into the surge were charred on their upstream sides, like many of the trees exposed to the 1980 lateral blast. The depth of charring on trunks increased with distance into the flow. Fine twigs were preserved on smaller trees overrun by other flows, near the point where the 1980 surge had collapsed into a lahar and had begun to form the "bayonet" trees characteristic of the water-mobilized flow. This evidence, combined with the essential textural identity of the modern, Kalama-age, and post-Kalama-age avalanche and lahar deposits, suggests that the older flows also formed by the deflation of pyroclastic surges and by continuation of the basal avalanches.

The continuing flow of the avalanches, the erosion of soil, and the addition of water contributed to the downstream evolution of debris flows with muddy matrices. The Kalama- and post-Kalama-age avalanches were much larger than those in 1980 and probably constituted a greater proportion of the catastrophically ejected mass. Lahars forming directly from the smaller 1980 avalanches were not significant. In 1980, transformation of the upper, more dispersed part of the surge (but not the initial cloudlike phase) produced the main South Fork lahar. In the history of the volcano, many types of catastrophic-ejection behavior probably have occurred, from nearly pure pyroclastic surge, as in the South Fork in 1980, to explosively initiated avalanches with little or no associated surge. Lahars may have originated from any combination of these.

The direct transformation of a lithic pyroclastic surge or flow to a lahar is probably not unique to the 1980 eruption at Mount St. Helens. The conditions existing at the time of the 1980 explosive eruption, including saturation of the cone, would have yielded water- or steam-rich proximal surges, flows, and avalanches with any comparable previous eruption. Even avalanches not

associated with volcanism could have transformed to lahars under these conditions. Saturation conditions also probably exist presently at other Cascade Range volcanoes (Janda, 1981). The evolution of lahars at Mount Rainier from huge avalanches, some of which were probably not associated with volcanism, confirms the importance of that lahar-forming mechanism.

### FLOOD SURGE TO DEBRIS FLOW

The most common way lahars have formed and probably will continue to form during the modern eruptive period is by transformation of flood surges. The flood surges have been produced by the interaction of heat and pyroclasts with snowpack and, less importantly, glacial ice. Meltwater discharge from the major explosive eruption of May 18, 1980, produced the flood surge that transformed into the second lahar in the South Fork Toutle River. Surges also resulted from subsequent dome-building events in 1982–1984. In addition, part of the 1980 North Fork lahar may have been formed by transformation of spring discharge on the surface of the debris avalanche.

The bulking of flood surges with sediment occurs rapidly on steep and commonly denuded volcanic slopes underlain by fragmental pyroclastic debris. Even small discharges pass through the range of hyperconcentrated flow and transform to debris flow in such a setting. An example of rapid bulking is the small flood surge released on the surface of the debris avalanche in August 1980. The peak sediment concentration observed in this flow at Kid Valley was 568,000 mg/L at a discharge of only 50 m<sup>3</sup>/s (Dinehart and others, 1981), but it had probably debulked continuously below the end of the debris avalanche. On the avalanche surface, the small flow may have traveled briefly as a debris flow. The deposits were rapidly eroded and were not observed.

The snowmelt surge producing the 1982 lahar was amplified by brief impoundment and subsequent lake breaching in the crater (Waite and others, 1983). The much larger Pine Creek-age lahars formed from flood surges originating entirely as lake breakouts. The evidence that their formative surges were derived from ancestral Spirit Lake includes a comparison of the amount of water required to produce at least the largest of the flows (PC 1), with the amount likely from other sources (Scott, in press). Mapping of the area inundated by that huge flow (Scott and Janda, 1982) established that the transformation to debris flow was not complete until the surge had traveled 20 km from the northern base of the mountain. Harrys Ridge is the site of the 1980 blockage and possibly also of the ancient blockages. The characteristic peak-flow deposits of the lahar

appear gradually over a channel interval of several kilometers near the downstream end of the broad valley from which the alluvium was eroded to form the lahar. The transformation to debris flow in a valley beyond the base of the volcano was more gradual than with smaller flows, because of the vast amount of alluvium required.

A large debris flow (but one smaller than PC 1) was formed by bulking of a lake-breakout flood surge in the Bol'shaya Almatinka River in Russia in 1977 (Yesenov and Degovets, 1979). That flow began as a relatively small surge (maximum discharge of 210 m<sup>3</sup>/s) from breakout of a moraine-impounded lake. The flood surge transformed to a debris flow immediately by bulking, and the flow continued to enlarge by mobilization of channel alluvium and contributions from slope failures, evolving into a succession of waves. Although the dynamics of flow at the peak were similar to those of the PC 1 lahar, the continuing large expansion of discharge and volume are not seen in the behavior of the lahar at Mount St. Helens. The progressive attenuation of the lahar peak, once bulking was complete, is well documented by the mapping of the inundation area (peak stage) of flow PC 1 (Scott and Janda, 1982).

The probable volume of alluvium bulked into the PC 1 lahar does not require unrealistic amounts of upstream erosion. The area of pre-1980 flood plain in the channel interval between Spirit Lake and a point near Camp Baker is 31.6 km<sup>2</sup>. A minimum of 0.03 km<sup>3</sup> of uneroded PC 1 deposits remain in the river system, a volume derived from 1 m of net, flood-plain-wide erosion. The total volume of the flow can only be crudely estimated. Based on the assumption that the flood wave was sharply peaked, a total volume of the lahar flood wave of about 1 km<sup>3</sup> is possible. With adjustments for water content and for sediment derived from the blockage deposits, flood-plain-wide erosion of 10–20 m could have produced the flow. Erosion of 10–15 m was recorded during passage of the Russian debris flow cited above. Alluvial megaclasts in the PC 1 deposit document at least 5 m of erosion at a point.

### DEBRIS FLOW TO HYPERCONCENTRATED STREAMFLOW

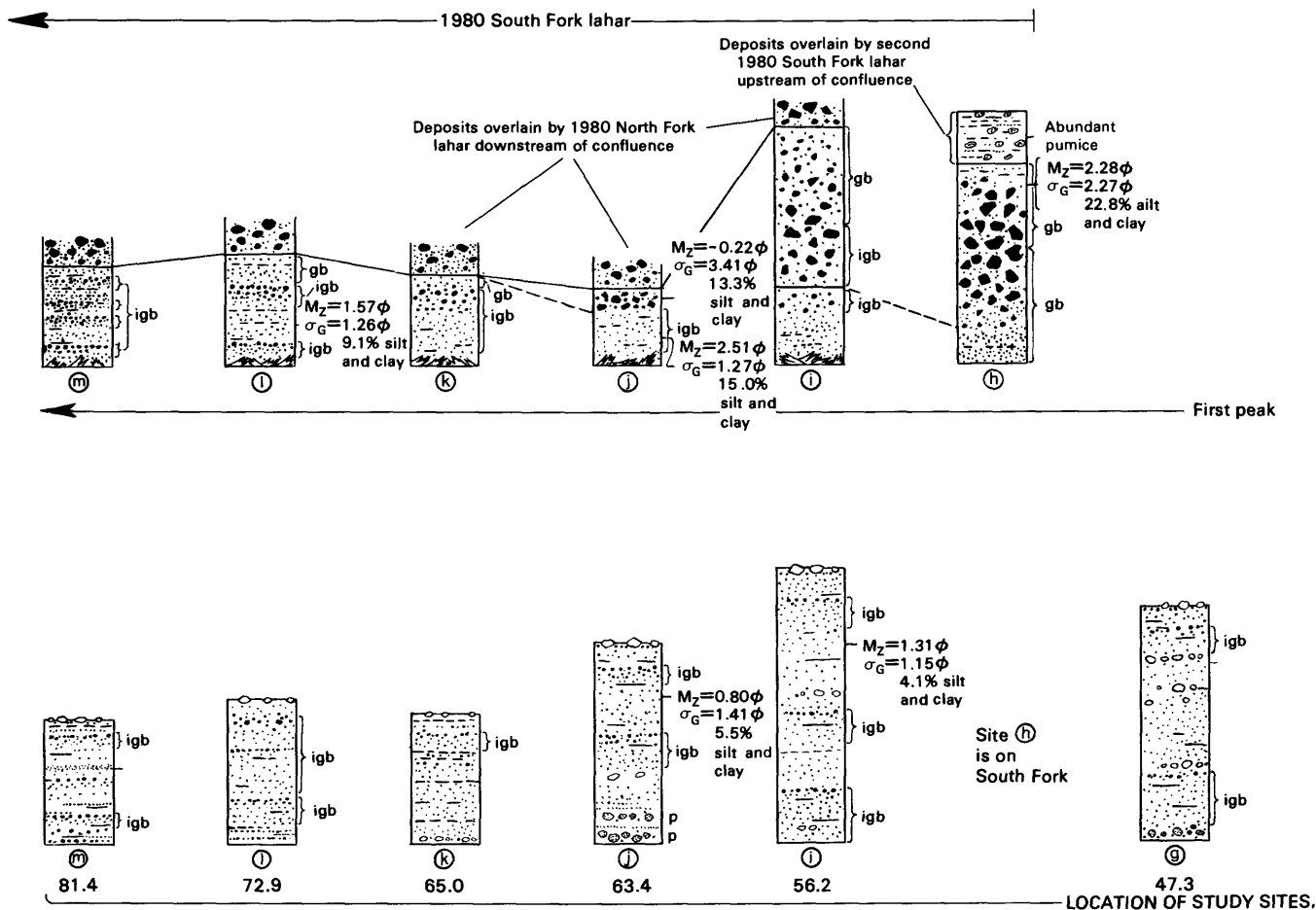
#### EVIDENCE FOR TRANSFORMATION

The evidence for the evolutionary transformation from lahars to hyperconcentrated lahar-runout flows comes from the vertical and longitudinal changes in texture and structure in the flow units. The transition facies—a vertical sequence of hyperconcentrated flow deposits overlain by debris flow deposits (fig. 10)—is

characteristic of a 19-km interval of the first peak of the 1982 lahar, and less than a 9-km interval of the second peak (fig. 36). Upstream from these intervals each flow unit consists mainly of debris flow deposits; downstream from these intervals, the units are composed of hyperconcentrated flow deposits. The same textural sequence occurs throughout a 9-km interval of the 1980 South Fork lahar and runout flow (fig. 36), but the changes could not be observed as continuously because of the thick overlying deposits of the North Fork lahar. Deposits of the 1982 lahar and its runout

flow were observed continuously from the end of debris avalanche to the Toutle-Cowlitz River confluence within days of their emplacement.

The transition facies occurs in the deposits of flows large enough to have inundated flood plains in previous eruptive periods, so it is not just the product of flow confined to channels. I have also seen it in association with relatively granular lahars at several other Cascade Range volcanoes. It may be evidence of a general mode of behavior of lahars with small amounts of cohesive sediment and particle-supported matrices.



EXPLANATION

- |  |  |            |                                      |
|--|--|------------|--------------------------------------|
|  | UNSTRATIFIED DEPOSITS WITH DISPERSED PEBBLE- AND COBBLE-SIZE CLASTS  | gb         | NORMAL GRADED BEDDING                |
|  | MASSIVE AND CRUDELY STRATIFIED DEPOSITS WITHOUT DISPERSED COARSE CLASTS  | igb        | INVERSE GRADED BEDDING               |
|  | BOUNDARY BETWEEN THE ABOVE TYPES OF DEPOSITS   | p          | HIGH PUMICE CONTENT                  |
|  | CLASTS OF LOW-DENSITY LITHOLOGIES—Pumice, juvenile microvesicular dacite (1980), and older hydrothermally altered dacite | $M_z$      | GRAPHIC MEAN SIZE                    |
|  | CLASTS OF NORMAL-DENSITY LITHOLOGIES—Dacite, andesite, basalt, etc.  | $\sigma_G$ | GRAPHIC STANDARD DEVIATION (SORTING) |

If the deposits of the transition intervals of the modern (fig. 36) and ancient flows were exposed continuously, they would look generally like the diagram of figure 37. The overlying debris flow deposits thin

progressively and disappear at the point that flow transformation was complete. The vertical contact between the two deposit types in each flow unit is transitional. The rate of transformation depends on the volume of

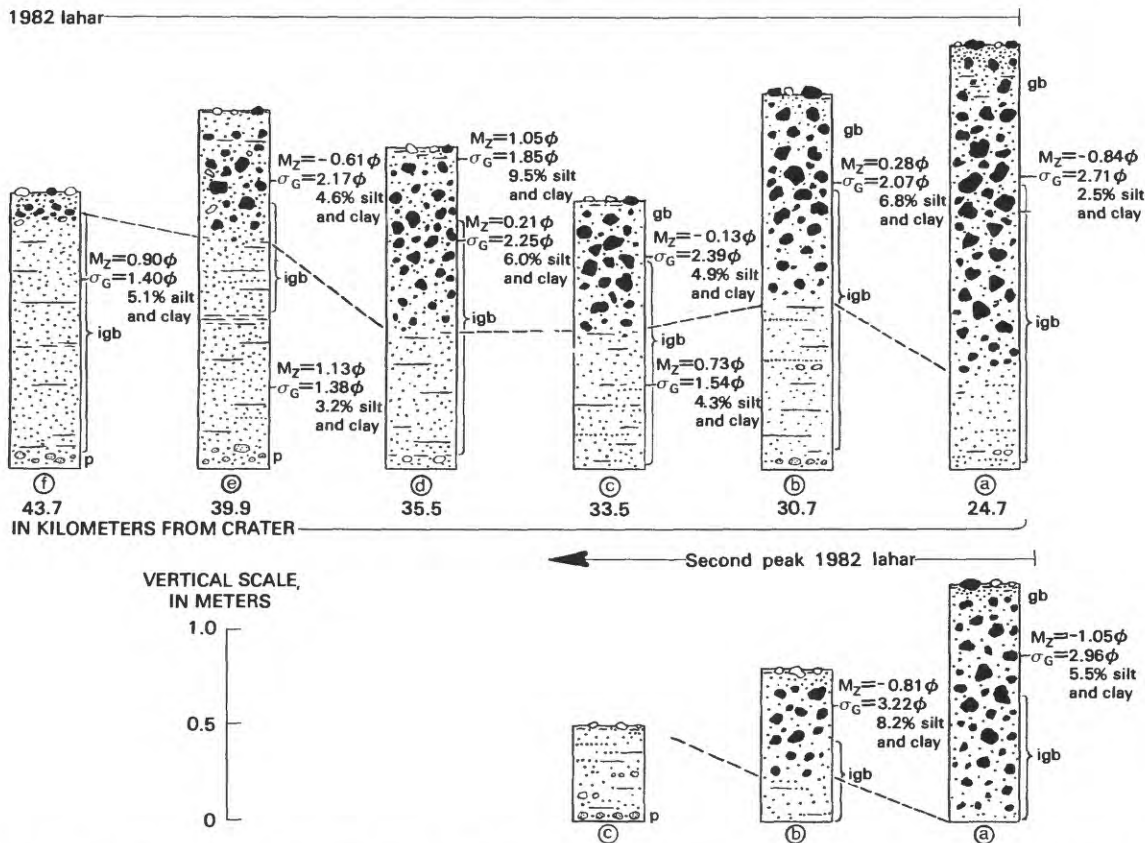
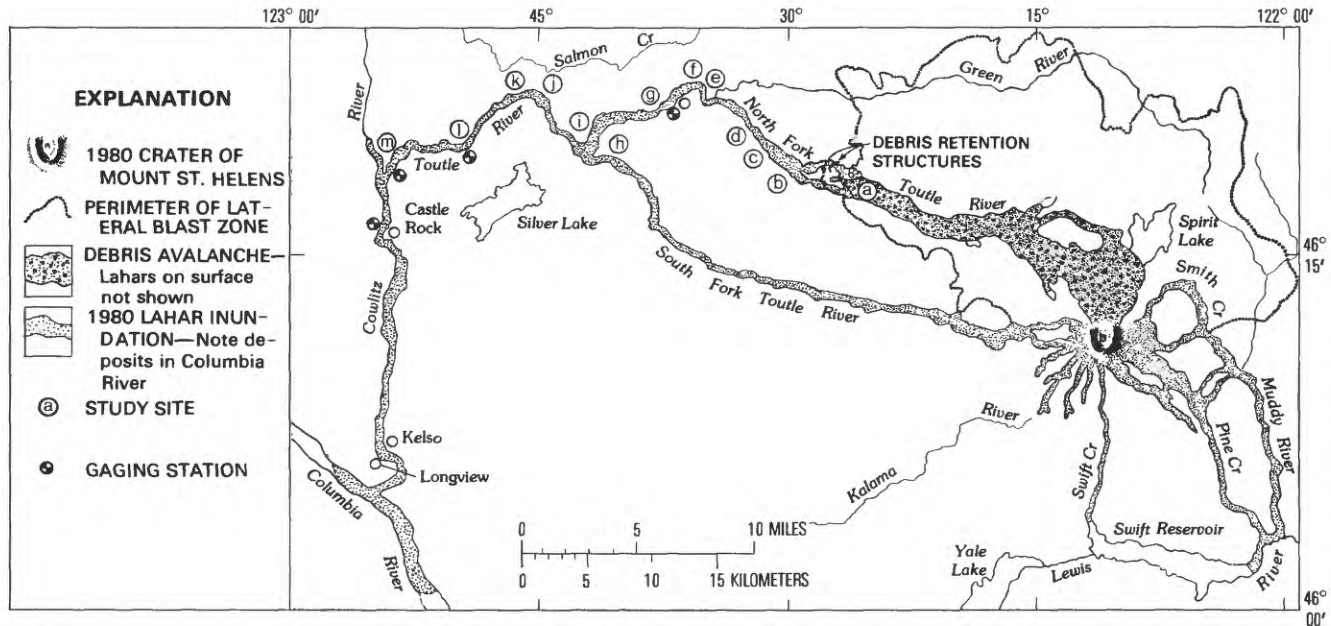


FIGURE 36.—Depositional units of the 1980 South Fork lahar, the 1982 lahar, and the runout flows evolved from those lahars. Variable thicknesses of the units reflect local changes in flow depth due to channel configuration, as well as downstream changes in discharge.

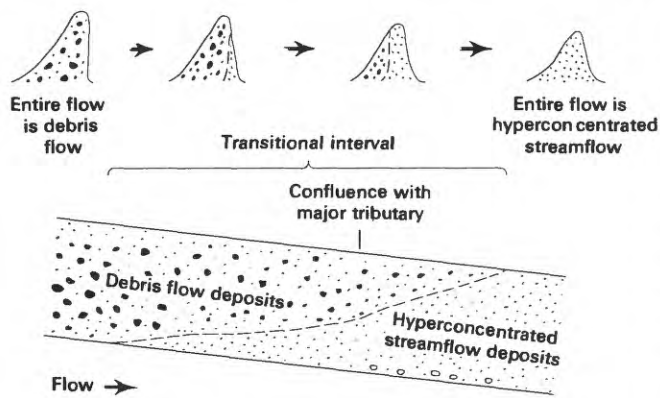


FIGURE 37.—Downstream change in texture resulting from transformation of debris flow to hyperconcentrated streamflow. Acceleration of the change occurs at the confluence with large tributaries, reflecting an increased volume of water to dilute the debris flow. Diagrammatic hydrographs show accompanying changes in character of the flow wave.

overrun streamflow in the channel, as shown by the increased rate of replacement of debris flow deposits by hyperconcentrated flow deposits at and downstream from major tributaries. The final part of the change in the 1980 South Fork lahar to its runout phase occurred in response to mixing with North Fork streamflow in the reach downstream from the confluence of the forks. Similarly, the final part of the conversion of the 1982 lahar to runout flow began with the addition of Green River streamflow (at km 39.7 in fig. 36). Both the 1980 and 1982 runout flows transformed to normal streamflow upon mixing with the Cowlitz River flow.

#### CHARACTERISTICS OF DEPOSITS OF HYPERCONCENTRATED LAHAR-RUNOUT FLOWS

The lahar-runout flow deposits are distinct from both the lahar deposits, which occur upstream, and the



FIGURE 38.—Deposits of the main peak of the 1982 runout flow at Kid Valley, near the downstream end of the transition interval. Note cobbles partly of low-density lithologies protruding from the flow surface. Point C is the level of maximum clast size at the top of the inversely graded part of the flow unit. Thickness of the deposits (overlying alluvium) is 1.4 m.

deposits of normal streamflow farther downstream. As a group, the following characteristics define lahar-runout flow deposits and can be used to identify that type of flow in the stratigraphic record where the complete transition from a lahar is not visible (tables 1 and 5). These characteristics apply to the hyperconcentrated runout deposits in the transition interval, where they form the basal part of the flow units, as well as downstream where they form the entire unit.

LACK OF STRATIFICATION IN PARTICLE- AND CLAST-SUPPORTED DEPOSITS

The most obvious characteristics of lahar-runout deposits are their generally massive or crudely stratified nature (fig. 36) and their particle- or clast-supported texture. Except for their massive appearance, both the modern and ancient depositional units, which range up to 2.5 m thick, might be mistaken for units of normal fluvial sand. Throughout the river system the latter show either crossbedding or well-developed planar stratification. The poor or nonexistent stratification in the runout deposits reflects the rapid and generally uninterrupted deposition from the runout flood waves.

The degree to which stratification may be developed depends on channel geometry. The deposits near the main channel thalweg, preserved by overlying lahar deposits (1980 runout flow) or observed before erosion (1982 runout flows), are more likely to be more completely massive. The 1982 runout flow eroded many spoil piles, triggering periodic fluxes of introduced sediment that locally created stratification downstream from and on the same side of the channel as the source. Stratification thus appeared slightly better developed in lateral and backwater areas of both the 1980 and 1982 flows. A thin (<1 cm), silt-rich stratum locally occurred near the middle of the 1982 runout-flow units.

INVERSE GRADING

The dominant feature of the 1980 and 1982 transition units is inverse grading in the basal part of each depositional unit (which is different in origin from the inverse grading in the lahars). It commonly extends continuously from near the base of the deposit in the portion representing the earlier, hyperconcentrated part of the flow wave, to the level of maximum clast size in the upper, debris flow portion of the bed (figs. 36, 38, and 39). The level of maximum clast size rises progressively downstream (fig. 37) as the debris flow subunit becomes thinner. The grading is interrupted locally by finer grained intervals or discontinuities, especially near lateral channel boundaries, but the continuous upward

increase in particle size is the more general case (figs. 39 and 40). After the complete transition to hyperconcentrated flow downstream, inverse grading is present but may be most pronounced in subunits (fig. 36). Generally, inverse grading disappears downstream. In the most distal runout-flow deposits a small degree of overall normal grading may even be present.

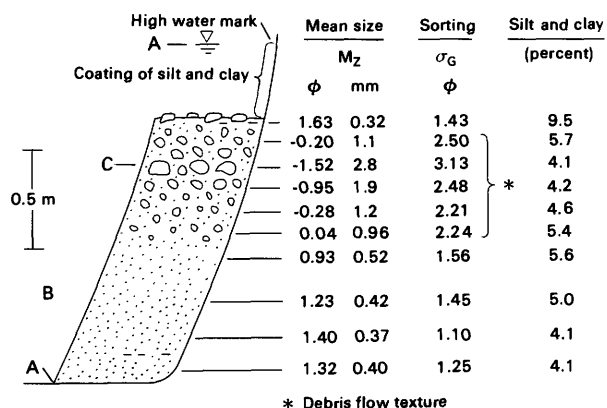


FIGURE 39.—Textural change in the transition facies of the 1982 lahar, 0.4 km upstream from Kid Valley (at locality shown in fig. 38). Points labeled A represent the flow boundary and the stage at the time of peak discharge, B represents the inversely graded central part of the unit, and C is the level of maximum clast size.

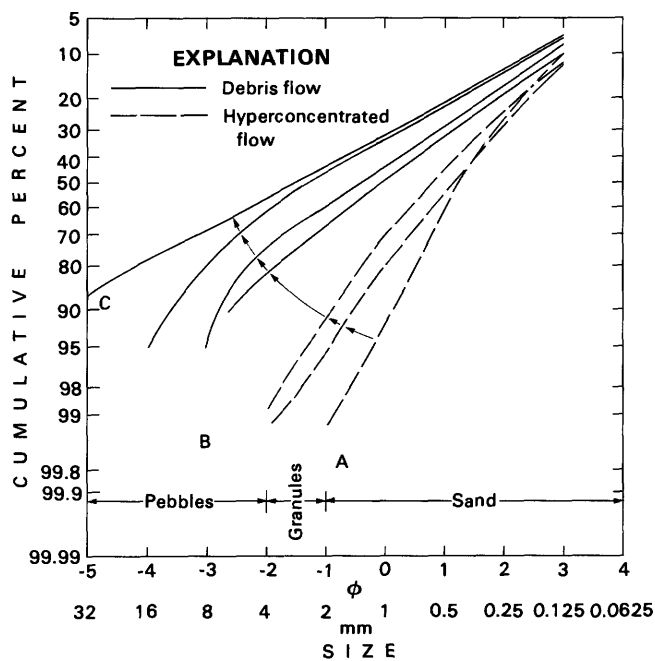


FIGURE 40.—Cumulative curves of particle sizes in the inversely graded part of the transition facies unit shown in figure 39. Arrows point stratigraphically upward in unit and indicate the progressive changes in flow deposits at a point. Points A, B, and C are shown in figure 39.

## COARSE-TAIL GRADING OF LOW-DENSITY CLASTS

Low-density lithic and organic fragments are expectable in the upper parts and on the surfaces of lahars and lahar-runout deposits. The concentration of wood fragments at the base of the 1980 runout flow units and of pumice near the base of some 1982 and pre-1980 units reflects the extremely rapid deposition from a hyperconcentrated flood surge. The front of the 1980 runout flow wave was marked by a moving mass of logs. This churning framework could have caused extreme but transitory turbulence producing the mainly framework-supported deposit of wood fragments that was buried by subsequent rapid deposition that approached mass emplacement in character. Many of the wood fragments are rounded, and the matrix is sand like that of the overlying deposit, as is the matrix in the units where pumice is concentrated at the base. The resulting grading is coarse-tail grading in which the coarse part of the distribution consists of low-density particles that in normal flows would be buoyed to the surface. This type of grading is attributed primarily to local extreme turbulence at the flow front, unlike the inverse grading in the transition interval that relates to the transformation of debris flow to runout flow. Intense turbulence is characteristic of the fronts of large, high-velocity debris flows in Yunnan Province, China (Hua Guo-xiang, Chengdu Univ. of Science and Technology, oral commun., 1985).

CONCENTRATION OF LOW-DENSITY CLASTS  
NEAR LATERAL BOUNDARIES

Pumice and wood fragments concentrated near the sides of the channel or on the inundated flood plain are distinctive of the modern runout flows and some of their ancient analogs. Where pumice is present in any runout flow unit, it is abundant near lateral flow boundaries, where it may occur in stringers that thicken toward the banks or valley side slopes. It accumulated in backwater areas where it then was incorporated in the deposit by rapid deposition from hyperconcentrated flow.

## SORTING

The most definitive characteristic of hyperconcentrated runout-flow deposits is sorting in a range intermediate between that of debris flow deposits and most normal streamflow deposits. The 1982 debris flow deposits—both upstream from the transition (fig. 36 and curve *a*, fig. 41) and in the upper parts of the flow units in the transition interval (fig. 36 and curve *b*, fig.

41)—have values of sorting that approach 1.8–2.0  $\phi$  as an approximate lower value. Although the deposits have low values of total silt and clay (typically 4–10 percent), relative to the 1980 lahars, the degree of clast dispersal is characteristic of debris flow, albeit toward the low-strength and noncohesive end of the spectrum. Similarly, the sorting of the distal 1980 South Fork flow declines (improves) downstream to at least 2.2  $\phi$  (fig. 20). The 1980 and 1982 hyperconcentrated flow deposits in the transition facies (fig. 36 and curve *c*, fig. 41) and downstream from the transition interval (fig. 36 and curve *d*, fig. 41) have values of sorting in the range of 1.1–1.6  $\phi$ . This improvement in sorting is reflected in grain and clast support, greater presence of void space, and lack of dispersed coarse clasts.

Judging by the dispersion of sediment sizes, the difference between hyperconcentrated runout-flow deposits and normal streamflow deposits is more subtle than the difference between debris flow and runout-flow deposits. Nevertheless, the difference is apparent where the deposits are juxtaposed as, for example, where the 1982 runout flow deposits were emplaced in bars and berms in contact with normal streamflow deposits of similar mean size. Like the 1981 and 1982 streamflow deposits illustrated in figure 41, most fluvial sand has sorting in the range of 0.5–0.8  $\phi$  (Friedman, 1962). However, the sorting of some, mainly fine-grained streamflow deposits in the river system overlaps the 1.1–1.6  $\phi$  range characteristic of the runout deposits. Runout deposits can be distinguished from streamflow deposits in the river system if they have sorting in the 1.1–1.6  $\phi$  range, have a mean size greater than approximately 2.5  $\phi$  (0.17 mm), and occur in units that have the other characteristics described here.

## TRANSITIONAL CUMULATIVE CURVES

The progressive steepening of the cumulative grain-size curves representing a distal lahar and the runout flow derived from it (figs. 40 and 41) is similar to the pattern of vertical changes observed in the depositional unit of a subaqueous sediment gravity flow (Visher, 1969, fig. 20A). That pattern records the progressively more dilute nature of a single flow, both laterally and vertically. The curves representing the successive, longitudinal parts of flows in the river system likewise appear to record gradual, evolutionary change. A reverse pattern of sequential changes is seen in ascending a vertical section of the inversely graded part of the transition facies (figs. 39 and 40) for reasons described in the following section on sediment transport.

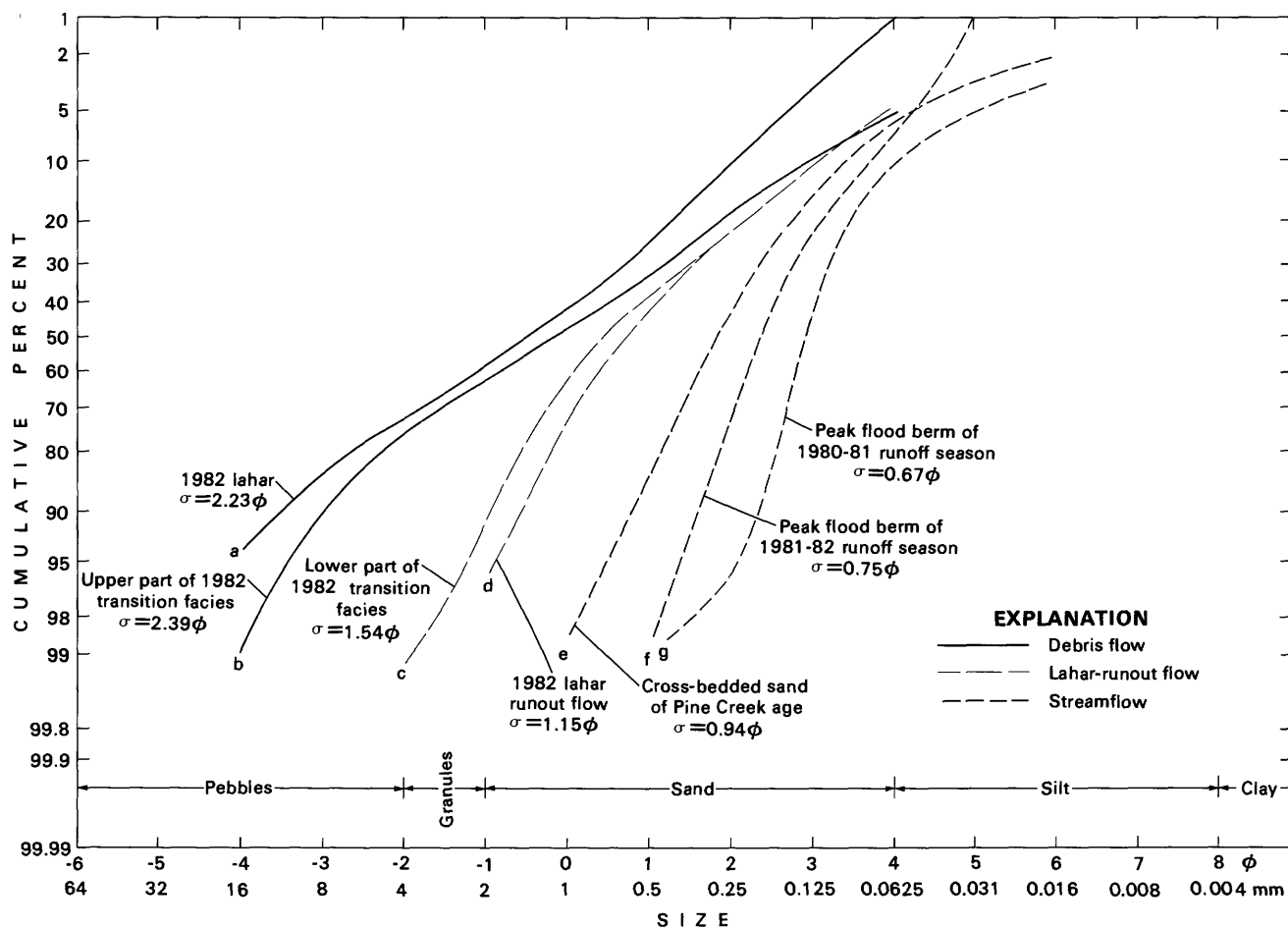


FIGURE 41.—Cumulative curves of particle sizes in representative samples of the 1982 lahar and lahar-runout flow deposits, compared with those of modern and ancient streamflow deposits. Localities: a, 1.5 km upstream from the North Fork debris basin; b and c, St. Helens (community); d, Coal Bank Bridge; e, Green Mountain Mill; f and g, near the confluence of the forks of the Toutle River.

#### LACK OF COARSE INFLECTION POINT IN CUMULATIVE CURVES

The cumulative grain-size curves of 18 samples of the runout deposits lack a coarse inflection point, illustrating the generally positive skewness of the distributions. The S-shape of curve *g* in figure 41, which shows both a coarse and a fine inflection, is typical of most fluvial deposits. The inflections are commonly interpreted to be the result of subpopulations of grains moved by different transport mechanisms, with the coarser inflection believed to be the point at which most coarser sediment—that represented by the part of the curve with lower slope—forms a subpopulation moved by rolling or sliding (see review by Visser, 1969) or traction, equivalent to bed load (Middleton, 1976; Bridge, 1981). The lack of this subpopulation in the runout deposits implies that the coarser sediment was not transported in a mode separate from that moving the remainder of the deposit.

#### SEDIMENT TRANSPORT IN THE LAHAR-RUNOUT FLOW OF MARCH 19-20, 1982, AND CORRELATION WITH DEPOSIT CHARACTERISTICS

Direct measurements of sediment concentrations in a lahar-runout flow, downstream from the transition interval, were obtained around midnight on March 19-20, 1982, by U.S. Geological Survey personnel at the three gaging stations shown on the Toutle River in figure 36. Samples were collected from the upper parts of the flow with heavily weighted open-mouthed bottles (mouth diameter 36 mm) lowered into the center of the channel from bridges and cableways. Consequently they do not represent integrated samples of the complete depth of flow. The concentration data indicate the same generally uninterrupted wave of sediment recorded in the deposits.

The most complete record of the 1982 runout flow, collected at Tower Road (fig. 42), shows that sediment concentrations characteristic of hyperconcentrated flow

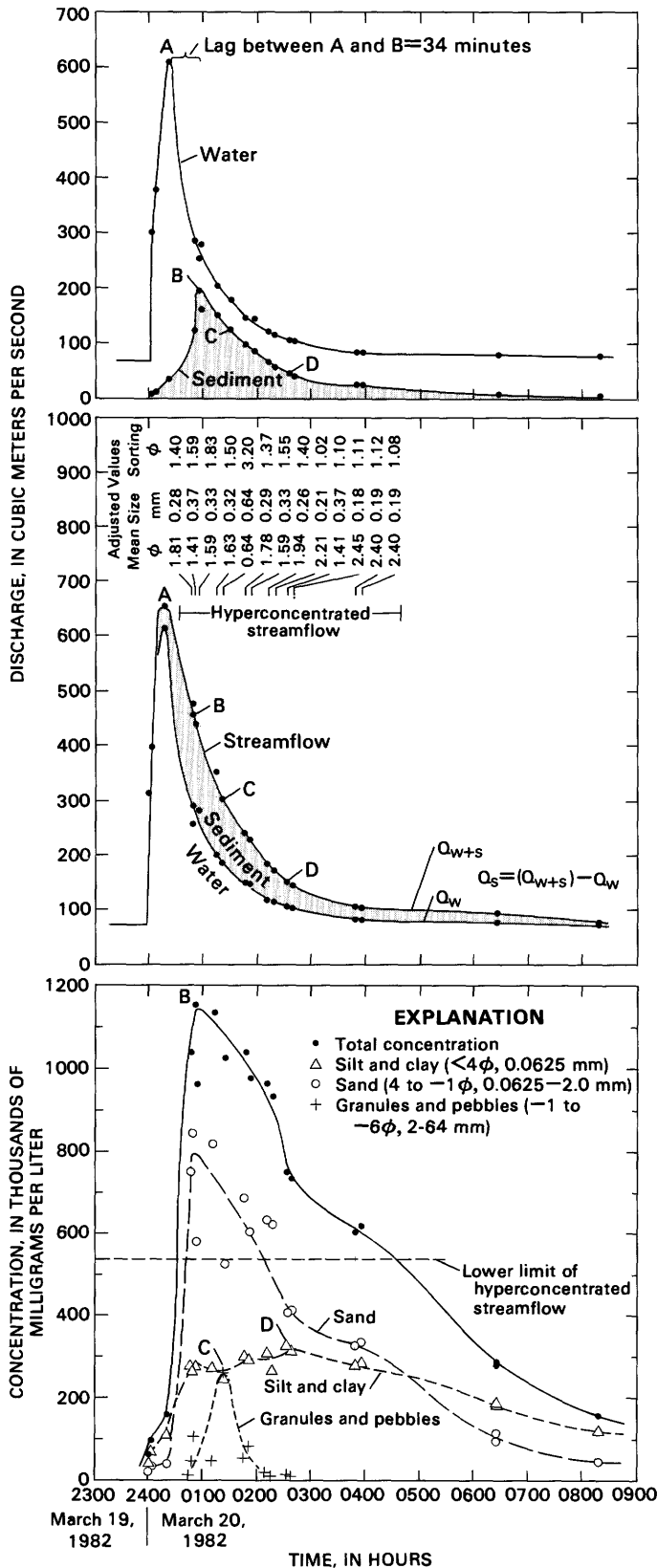


FIGURE 42.—Discharge and sediment concentration of the 1982 runout flow at Tower Road.

(530,000–1,590,000 mg/L) were reached after peak discharge and then continued throughout much of the recession. As at the upstream station at Kid Valley, concentrations at Tower Road approached or exceeded 1,000,000 mg/L for at least an hour. Only slightly lower concentrations were present for a similar duration at the downstream station at Highway 99, 1.6 km above the confluence with the Cowlitz River. Peak discharge declined from 960 m<sup>3</sup>/s at Kid Valley, to 650 m<sup>3</sup>/s at Tower Road, and to 450 m<sup>3</sup>/s at Highway 99 (Pierson and Scott, 1985). Dilution of the runout flow to normal streamflow by mixing with Cowlitz River water is shown by the data from the Castle Rock gaging station, 3.9 km below the confluence, where the river stage rose only 0.3 m and the maximum concentration was only 158,000 mg/L.

The runout flood wave at Tower Road consisted of water during the rise and of water and sediment during the recession (fig. 42). At the peak streamflow discharge (point A on fig. 42), 94 percent of the flow volume was water. At the time of maximum sediment discharge (point B), 34 minutes into the recession, 44 percent of the flow volume (67 percent by weight) consisted of sediment. The conversion to a clear-water equivalent for the peak streamflow discharge thus is minor (a reduction of 6 percent), yet a corresponding correction of the total runout flow volume, reflected by the shaded area under the streamflow hydrograph in figure 42, is substantial (a reduction of 39 percent).

The common relation in a flood wave is for peak sediment discharge to precede the streamflow peak and for the resulting deposits to be normally graded. After flow competence has peaked and bar deposition has begun, both the concentration and the size of the suspended sediment in the flow typically decline. Rates of bed load discharge normally also fall throughout flow recession. Yet, in the 1982 lahar-runout flow and in some normal flood flows in the Toutle-Cowlitz system, concentration initially increased as streamflow declined (fig. 42). This lagging concentration peak, its high level, and the coarseness of sediment in the runout flows cause the dominant grading to be inverse. Other instances in which peak sediment discharge lags behind the flow peak may result from the contribution of sediment from a downstream subwatershed during flow recession or from a long travel time during which wave celerity exceeds mean water velocity. A long lag in the concentration peak generally reflects a significant fine-material load (Heidel, 1956).

The sediment transport curve of the 1982 runout flow (fig. 43) is a hysteresis loop reversed from the normal direction. (Compare Leopold and others, 1964, fig. 7-15, for instance.) Sediment load (discharge by weight) on the “falling” limb of the hydrograph is more than an

order of magnitude greater than that at the same height on the "rising" limb. This dramatic increase in sediment concentration, discharge, and size (fig. 42) as streamflow discharge initially falls illustrates the dynamics that produce the inverse grading. The lag between peak discharge and peak concentration was 34 minutes at Tower Road and increased downstream, to 50 minutes at Highway 99 and to 1 hour at Castle Rock on the Cowlitz River. The lag intervals are approximate in that the sediment sampling was periodic.

The variations in the proportions of water and sediment and in sediment size in the runout flood wave correlate with the texture of the lateral berms. The correlation is shown by comparing sediment transport in the lahar-runout flow at Tower Road (fig. 42) and the textural sequence in the transition facies near Kid Valley (fig. 39). Deposit grading and geometry are similar at Tower Road and Kid Valley; the deposits at Tower Road, however, are downstream from the transition interval and do not record the transition from debris flow to lahar-runout flow. Although only the flow recession was sampled at Kid Valley, beginning about 90 minutes after the streamflow peak, the complete pattern of transport there was probably similar to that at Tower Road, but with a shorter lag period. Extrapolating from the lag at downstream stations to the point of no lag (the upstream end of the transition interval) shows the lag at Kid Valley was approximately 15 minutes.

Deposition can be assumed to have begun after peak streamflow discharge (point A in figs. 39 and 42). Maximum scour depth normally coincides with peak streamflow discharge and, given the low proportion of sediment in the peak runout flow, almost certainly did in this case. During recession, however, the higher sediment content increased the density of the flow and partially offset the effect of falling depth on boundary shear. Nevertheless, the point of maximum sediment concentration and sediment discharge (synchronous in this case; point B) was probably near the point of most rapid deposition. It probably corresponds approximately with the middle of the inversely graded part of the unit (figs. 39 and 42). Continuing the correlation, the coarsest upper part of the inversely graded berm deposits corresponds with the maximum flux of gravel (point C in figs. 39 and 42). The uppermost, normally graded part of the berms correlates with the initial part of the subsequent decline in both sediment and water discharge and the accompanying fining of sediment. As recession continued, deposits formed earlier during the flow were incised, and the concentration of silt and clay peaked (point D in fig. 42).

Thus the peak flow preceded the deposition of the berm surface; the surface formed well into flow

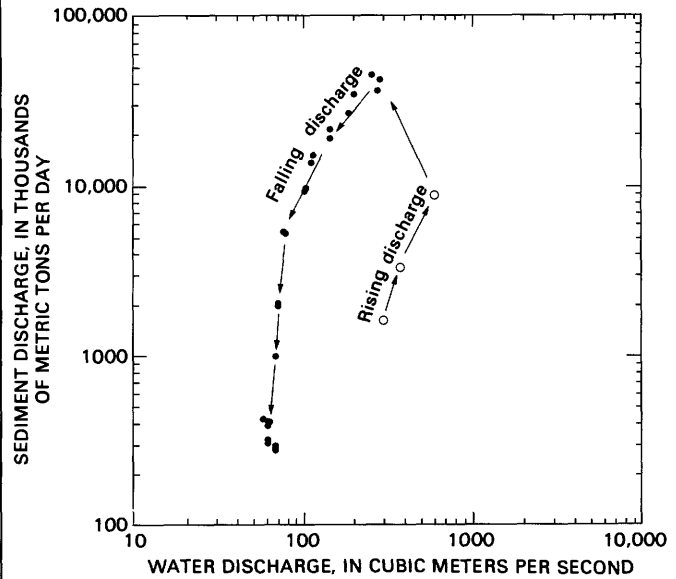


FIGURE 43.—Sediment transport curve of the lahar-runout flow of March 19-20, 1982, at Tower Road. Water discharge was calculated by subtracting sediment discharge from the streamflow discharge.

recession. This conclusion is supported by the character of the thin, fine-grained coating of the peak-flow boundary (fig. 39), which evidences the dilute streamflow at peak streamflow discharge rather than the sediment-charged flow during berm emplacement. The streamflow hydrographs (such as fig. 42) show that the coating must have come from the peak and could not have come from a dilute water flow overriding or following a sediment gravity flow, as I had proposed earlier for flows in steep, semiarid watershed (Scott, 1971). The berm surface probably formed when the entire channel was filled with deposits and flowing sediment to the level of that surface or to a dynamically related level.

The variation in concentrations of various size fractions (fig. 42) shows that the sediment component of the flow at Tower Road was virtually a wave of sand. At the peak concentration (point B), 73 percent of the sediment was sand. Only then did larger clasts appear in the flow, reaching a peak (point C) that lagged the peak concentration by approximately another half hour. The further lag of the peak in silt and clay content (point D) can be ascribed in part to volumetric displacement of the fine-material load by coarser sediment earlier in the flow and in part to the addition during recession of fine sediment draining from incised, earlier deposits. It may also reflect the downstream effect of a second, lower peak in the flow, which was recorded by upstream deposits (fig. 36) but did not extend to Tower Road, based on the gage height record,

eyewitnesses, and the deposits. The general case, as in this instance, is for the fine-material load in hyperconcentrated flows in the river system to be highly persistent (Dinehart, 1983).

#### EFFECT OF POSTDEPOSITIONAL DRAINAGE ON DEPOSIT TEXTURE

During the field study of the 1982 deposits, large areas of both the runout and transition facies were as firm as sand on a beach; only local areas of the upper debris flow deposits of the transition facies retained pore fluid and remained quick. Observers of the 1982 runout flow (R. L. Dinehart, written commun., 1982) noted that the deposits were firm when they first appeared above the receding flow. The firm deposits were located near berm cutbanks; the quick deposits remained only locally in subordinate backwater areas away from channels and in which water was replenished from local runoff. The firmness therefore was largely the result of interstitial drainage in hydraulic continuity with the recession flow. As the upper, debris flow parts of the transition units also drained, they probably lost some fines that were retained in most of the upstream, more poorly sorted distal debris flow deposits. (See Pierson and Scott, 1985.) Subsequent observations showed both types of transition-facies deposits to function as permeable aquifers. The amount of silt and clay remaining in the transition debris flow deposits was similar to the low values in the runout deposits, but more variable (fig. 36). Drainage from the debris flow parts of the transition facies was facilitated by the inversely graded transition from the underlying runout sand.

At time of deposition the interstitial space in the rapidly deposited, framework-supported units was filled by fluid with high concentrations (but probably not hyperconcentrations) of silt and clay, much of which probably drained as the flow receded. If a similar proportion of fine sediment is subtracted from the concentrations measured in the flow, the adjusted distribution statistics closely resemble those of the deposited sediment. The sediment in the flow samples with concentrations over 1,000,000 mg/L consisted of 28–31 percent silt and clay at Kid Valley (4 samples) and 23–29 percent silt and clay at Tower Road (5 samples). These values are higher than the general range of 4–6 percent (one fine-grained sample has 9.4 percent silt and clay at Highway 99) in the deposits (fig. 36). By assuming the loss of all but 5 percent of the silt and clay from the sediment in the flow samples, the sorting is reduced from more than  $2.0 \phi$  in cases where the distribution was not skewed by a single large clast, to the 1.1–1.6  $\phi$  interval that is characteristic of the modern and

ancient runout deposits (fig. 42, table 8). Some fine sediment was, of course, regained by the flow directly from the accreting flow boundary, but a significant part would have been incorporated in the deposit and then would have accompanied the draining interstitial fluid.

#### ORIGIN AND EVOLUTION OF LAHAR-RUNOUT FLOWS

The transformation of a lahar to a lahar-runout flow involved the fluid component of the flow separating from and outrunning the sediment in a manner more complex than normal, progressive deposition as flow competency fell. The downstream increase in lag time between the streamflow and concentration peaks illustrates the continuous separation of the two phases once transformation began. The lag developed because the close juxtaposition of particles in the hyperconcentrated flow inhibited the ability of the fluid to move the sediment at the same speed.

The transition facies (fig. 10) indicates that the transformation was triggered by the mixing of the leading part of the lahar with streamflow in the channel. Successive parts of the debris flow wave continued for progressively greater distances in the transition interval (fig. 34) before increased water content caused a significant decline in yield strength and conversion to hyperconcentrated streamflow. The debris flow flood wave was transformed progressively from leading edge to tail. Thus were formed the inversely graded units consisting of downstream-thinning debris flow deposits overlying downstream-thickening hyperconcentrated flow deposits.

An expected mode of formation of the runout flows, given the common behavior of debris flows in alpine and semiarid settings (Costa, 1984), was for the debris-flow front to stop and be overrun by the more fluid recession flow. However, the progressive changes in the transition facies, as well as the systematic change in texture of the distal lahar flow, establish the direct evolution of one flow type from the other. The evolution is facilitated by the miscibility of the grain- and clast-supported lahars with streamflow, which results from their low clay content and consequent low cohesiveness. The large majority of lahars in the river system have such characteristics, as a result of their formative flow transformations from flood and pyroclastic surges. The formation of lahar-runout flows was facilitated by the occurrence of lahars in channels with substantial streamflow volumes. Based on the large size of some of the lahars transformed this way, however, the process can require only a relatively small volume of water. The older overbank runout flows show that, once the transformation began, textural change continued with little additional water.

TABLE 8.—Measured peak sediment concentration and adjusted mean size and sorting values for the lahar-runout flow of March 19–20, 1982, at Kid Valley and Highway 99

[Mean size and sorting adjusted as described in text. Values at Tower Road are shown in figure 42]

Time on 20 March	Sediment concentration (mg/L)	Silt and clay (percent)	Sand (percent)	Granules and pebbles (percent)	Adjusted mean size, $M_z$		Adjusted sorting, $\sigma_G$ ( $\phi$ )
					$\phi$	(mm)	
Kid Valley gaging station <sup>1</sup>							
0001	1,140,000	28	69	3	1.77	(0.29)	1.46
0003	1,150,000	29	69	2	1.69	(0.31)	1.52
0010	1,160,000	29	69	2	1.78	(0.29)	1.51
0015	1,090,000	31	67	2	1.86	(0.27)	1.44
Highway 99 gaging station <sup>2</sup>							
0135	882,000	30	69	1	1.97	(0.25)	1.31
0150	834,000	39	60	1	2.30	(0.20)	1.22
0158	968,000	31	68	1	1.96	(0.26)	1.32
0220	977,000	32	67	1	2.02	(0.25)	1.32
0225	929,000	35	64	1	2.10	(0.23)	1.29

<sup>1</sup>Kid Valley peak discharge = 960 m<sup>3</sup>/s at 2230 hours, 19 March.<sup>2</sup>Highway 99 peak discharge = 450 m<sup>3</sup>/s at 0030 hours, 20 March.

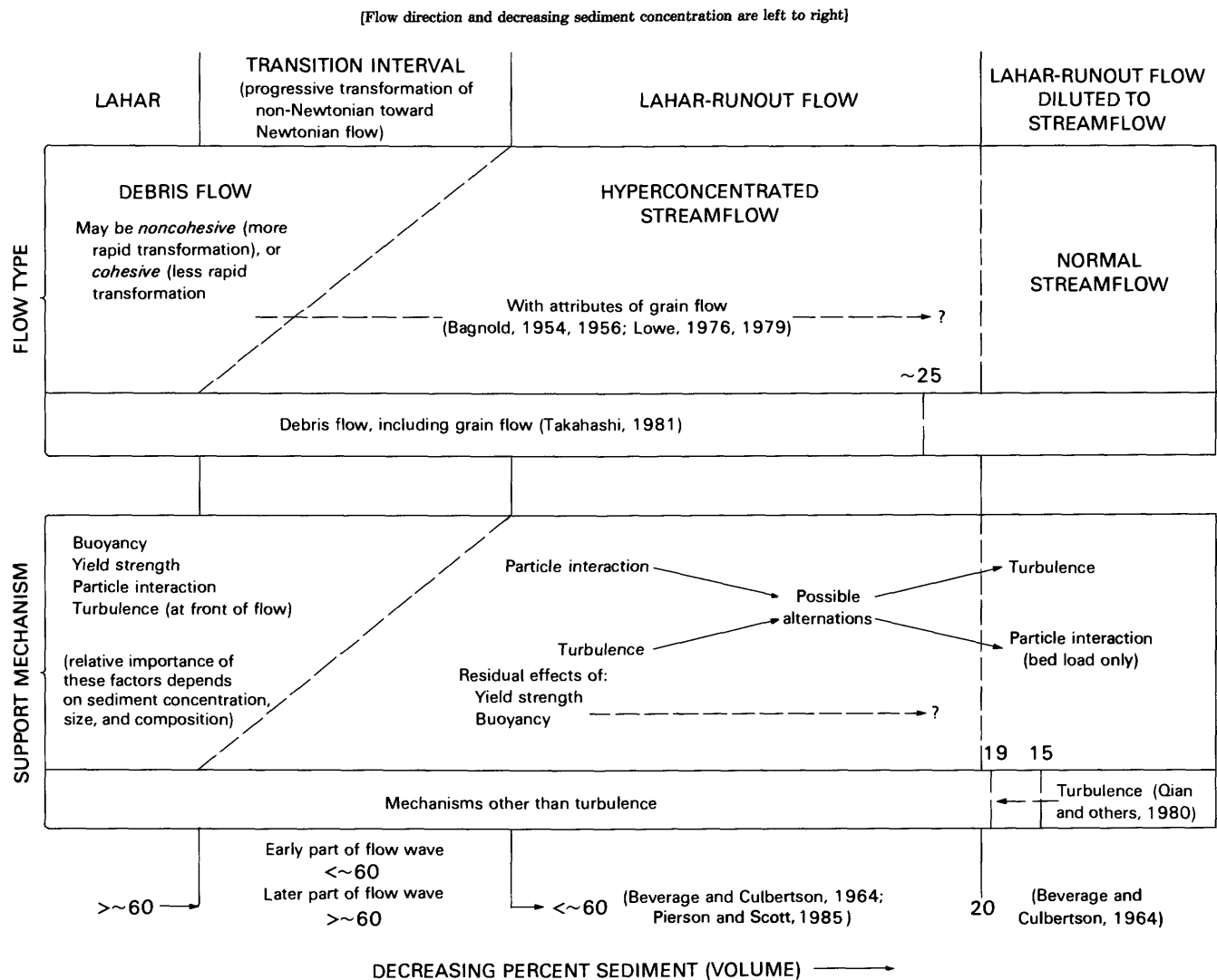
The physical threshold in sediment content between debris flow and hyperconcentrated flow can be defined because of the rapid decline in strength with small increases in water content near the threshold (Pierson and Scott, 1985). The continuous spectrum of textural change (figs. 38–41) records the approach to the transition and the continued dilution beyond it, suggesting that the multiple physical support mechanisms in debris flow and hyperconcentrated streamflow (table 9) are part of a continuum. Transitional behavior has been hypothesized by Hampton (1975), Carter (1975), and Middleton and Hampton (1976), and Lowe (1979 and 1982). Multiple support mechanisms have been postulated by Daido (1971) and Lowe (1979), and were observed by Lawson (1982) in small-scale flows.

Dilatant fluid flow and turbulent flow both occur within the hyperconcentrated range, but their relative importance is controversial. Although end-member grain flow (Lowe, 1976, 1979) probably did not occur, the question is whether momentum was transferred mainly by the collisions or near-collisions of particles (dilatant flow) or by the entraining fluid (turbulence). The importance of turbulence in some hyperconcentrated flows has been doubted. Nordin (1963) noted that in streams of the arid Southwest, turbulence probably was not an effective support mechanism above concentrations of approximately 370,000 mg/L. Beverage and Culbertson (1964) considered the effects of viscosity,

temperature, buoyancy, and Bagnold dispersive stress from grain collisions as possible substitutes for the role of turbulence as a support mechanism in hyperconcentrated flow. They did not define the relative importance of these other factors, but did note that the increased viscosity and density of the flow result in the need for less turbulence to support the coarser fractions of the load. The hyperconcentrated flow in the arid Southwest (Beverage and Culbertson, 1964), the 1980 runout flow (Ted Conradi, local resident, oral commun., 1980) and the 1982 runout flow (R. L. Dinehart, written commun., 1982) all had a smooth appearance that reflected a significant damping of large-scale turbulence.

Turbulence was well developed at the fronts of the 1980 and 1982 runout flows, as indicated by the coarse-tail grading of low-density clasts. Reported observations of standing waves—the surface expressions of the bed forms known as antidunes, which indicate an upper regime flow—show that turbulence also could have been effective during later parts of the 1982 runout flood wave (observations by R. L. Dinehart, S. A. Gustafson, K. K. Lee, and W. W. Larson, all U.S. Geological Survey, written commun., 1982). At Kid Valley, waves developed approximately an hour after the streamflow peak. About 45 minutes later, large rocks appeared to be rolling on the water surface, which was probably shallow flow on the berm surface. At Tower Road, large standing waves (over 1.8 m in height)

TABLE 9.—Sequential changes in flow type and particle support mechanisms during the transformation from lahar, to lahar-runout flow, to normal streamflow



were observed at 0020 to 0030 hours and at 0044 hours on March 20, during the lag between peak streamflow discharge and peak concentration (fig. 42). The forms were sporadically present throughout the remainder of the streamflow recession at that station. At Highway 99, flow near the peak was very smooth and velocity appeared lower than that of comparable storm runoff. Standing waves developed late in the recession. At Castle Rock, where concentrations did not approach hyperconcentrated levels, flow was continually turbulent, “with the look of boils” in contrast to the slick, oily appearance of the upstream flow.

The nature of the deposits, compared to the plane-bedded or crossbedded berms resulting from normal floods, is the strongest evidence that turbulence was of subordinate importance during the main wave of

sediment transport. Scour structures that reflect turbulent erosion of the bed are rare within the runout deposits. Bedding inclined to the flow, which would record dune forms developed during the main flux of sediment, is absent. Massive berms like the one shown in figure 38 are generally typical. Antidunes were sufficiently common throughout the passage of the flood wave, however, to suggest that at least local transformation to turbulent flow may have occurred. Alternating body transformations (Fisher, 1983) may account for the dichotomy of evidence; such an alternation in laminar and turbulent behavior has been hypothesized in submarine sediment gravity flows (Middleton, 1970). At least, variations in support mechanisms, such as increased turbulence through bar crossings in the generally braided post-1980 channel, are probable.

Evidence from the deposits of the transition interval suggests that the waning debris flow graded transformed to flow resembling grain flow through much of the interval, and that, as a sediment-support mechanism, particle collisions were progressively less effective as water content increased and a residual yield strength derived from the fine-sediment content declined. Hampton (1975) reported that the grain flow mechanism is operative in fine-grained debris flows, in addition to particle support by strength and buoyancy. The concentrations in the runout flow imply the presence of an interstitial fluid within the sand that had a high concentration of silt and clay and thus an enhanced viscosity and yield strength. In fact, some Chinese investigators establish the lower boundary of hyperconcentrated flow at the point where an incipient yield strength first appears (Hua Guo-xiang, Chengdu Univ. of Science and Technology, oral commun., 1985). The interval of high (>250,000 mg/L) but relatively constant fine-material concentration during the peak in sand concentration (fig. 42) is probably the period during which grain flow was most effective as a sand-transport mechanism. During that interval the coarse phase increased greatly without an accompanying large increase in silt and clay, and dispersive stress was an important support mechanism supplementing the yield strength provided by the finer phase.

### CONCLUSIONS ON LAHAR TEXTURE AS RELATED TO ORIGIN AND BEHAVIOR

The interpretation of a stratigraphic record of lahar deposits far from a volcano is fundamental to the long-term analysis of lahar magnitude and frequency. These aspects are discussed in the companion volume to this report (Scott, in press). Less obvious is the extent to which lahar origin and behavior are revealed by the stratigraphic record. For example, the most common lahar in the watershed proves to have been the middle segment of a lahar flood wave beginning and ending as a streamflow surge.

Two general categories of lahars that inundated flood plains many tens of kilometers from Mount St. Helens are apparent from the textural data: (1) common lahars that have a clay content of clearly less than 3 percent, and (2) rare lahars that have a clay content of about 3 percent or more. The common lahars formed mainly, if not entirely, from flow transformations; consequently they consisted mainly of volcanic materials previously subject to progressive or selective sorting, which had removed some or most of the clay in the hydrothermally altered volcanic rocks. Hydraulic sorting in stream channels is the most efficient sorting process. Sorting

also can be explosion induced, as by the winnowing of elutriated fines from a deflating, air-mobilized pyroclastic surge.

Significant lahars of meteorologic origin probably have not occurred since Ape Canyon time. Intense rainfall acting on ash-mantled slopes is a common way lahars are produced and may have been an effective mechanism during that eruptive stage, when large volumes of pumice were produced. The series of lahars of that age in the river system contains much pumice, but the larger flows in that sequence probably originated through the transformation of streamflow surges produced from the melting of snow and ice by pyroclastic flows.

### LAHARS FORMED BY FLOW TRANSFORMATIONS

The three types of lahar-forming flow transformations recognized in the modern eruptive period have probably operated to produce many of the large lahars originating from the northwest half of Mount St. Helens. This conclusion is strengthened by good geologic evidence of older flood surges and by necessarily less certain evidence of air- or gas-mobilized surges and their associated avalanches, and of avalanches without associated dispersed phases.

### FLOOD SURGES TRANSFORMED TO LAHARS

The location and length of channels where bulking occurred can be inferred from the textures of lahars formed from water surges. Particle shapes indicate that the two largest lahars in the system were formed of stream alluvium well beyond the base of the volcano. Other evidence, discussed in the companion volume (Scott, in press) and including the character of megaclasts in the deposits, shows that the two large flows formed by breakouts through natural dams of volcanic origin. Mapping of the flow deposits (Scott and Janda, 1982) shows that the largest single flow completed the transformation to a lahar only after more than 20 km of flow from ancestral Spirit Lake, the most probable source of the water surge.

The most likely way for smaller lahars to be generated in the present eruptive period, as inferred from the observed lahar behavior to date, particularly that of the second South Fork lahar and the March 1982 flow, is by transformation of eruption-induced snowmelt surges. Such surges include meltwater surges produced by heat, tephra, pumiceous pyroclastic flows, and hot avalanches from the dome. These surges may undergo much of their bulking on the slopes or shortly beyond the base of the

volcano and, with the exception of those associated with tephra or pumiceous pyroclastic flows, cannot be readily identified from particle shape or composition. Lahars generated in this way doubtless have been common in previous periods, but few of these have inundated flood plains (and thus have been preserved in the stratigraphic record) more than 50 km from the crater. No large lahars of a post-Ape Canyon age have a pumice content clearly indicating an origin associated with snowmelt by tephra or a pumiceous pyroclastic flow. The relatively small and locally pumiceous second lahar (PC 2) in the Pine Creek sequence is a possible example of that flow type, but the content of rounded clasts shows that most bulking occurred beyond the base of the volcano.

Between the size extremes of lake-breakout lahars and those formed from most other types of water surges are lahars probably resulting from large lithic pyroclastic flows formed from major dome disruptions, and their associated snowmelt. Observations at other volcanoes show that lahars of significant size have formed this way, in addition to those resulting elsewhere from pumiceous pyroclastic flows (C. G. Newhall, U.S. Geological Survey, oral commun., 1985). The bulking factors of these flows may be similar to those of flows formed by catastrophic ejection, and bulking will occur at least partly on the cone. A large proportion of prismatic jointed dome rocks (and pieces of disaggregated blocks) may be diagnostic, and the flow may be nearly monolithologic or at least have a dominant lithology near the volcano. Lahars in this category include a thick unit of probable Swift Creek age in the upper South Fork Toutle River (unit 6 of the Disappointment Creek section; Scott, in press), and numerous flow units in the sequence of Pine Creek age south of the volcano. (See Crandell and Mullineaux, 1973.)

Why, considering the vast volume of lahar deposits in 100 km of the Toutle-Cowlitz River system, was the pre-1980 Spirit Lake not a lahar-aggraded marsh? The lake formed during Smith Creek time as the expanding alluvial apron of the cone impinged against Harrys Ridge (Crandell, 1987). The radial flow pattern and the probability of channel shifting on alluvial surfaces lead to the inference that many flows have entered the lake. Most of these were probably only partly bulked with sediment, and major flows did not transform to lahars through bulking until they reached the lower slopes of the cone or beyond. Lahars issuing fully formed from a crater, like those formed as extensions of block-and-ash flows from dome collapse, have contributed only minor volumes beyond the mountain. Thus, Spirit Lake probably has impounded many water surges and dilute muddy flows, but has not been filled by lahars. It has

been a source of flood surges, either through water displacement or through outlet blockage (by flows with higher yield strengths than lahars) and subsequent breaching. The blockage provided by the alluvial apron of the volcano would normally have been broad, stable, and armored with coarse sediment.

#### CATASTROPHICALLY EJECTED SURGES AND AVALANCHES TRANSFORMED TO LAHARS

In texture and in composition and shape of component clasts, lahars formed by pyroclastic surge transformation may be like lahars formed from snowmelt surges. Textural likenesses reflect the similar results of sorting by hydraulic and explosion-induced mechanisms. The lahars originating with the initial May 18 eruption, including the 1980 South Fork lahar, illustrate the potential of catastrophic ejection to produce an approximately symmetrical ring of large lahars around the volcano. This is a likely origin for the larger lahars in the system that have relatively low bulking factors near the volcano and that may have a low content of prismatic jointed dome rocks.

This origin is more probable for older lahars that are associated with evidence of major explosive events. As in 1980, the volcano would probably have been saturated with water at the time of any previous major explosive eruption. Also as in 1980, relatively cool, water-saturated material may have been ejected peripheral to hot lateral blasts. The evidence for lahars of this origin in the Kalama eruptive period includes their association with deposits closely analogous to those of the 1980 lateral blast. Depending on the nature and energy of the catastrophic ejection, lahars may have formed from surge deflation or avalanche continuation. The presence of texturally similar, nonpumiceous lahars in all or most drainages implies a major, central explosive eruption. The Kalama-age lahars seem to be symmetrical; texturally similar flows of that age occur in all major drainages of the volcano, but uniform timing of the flows has not been demonstrated and the symmetry may reflect the central position of the dome of that period.

#### LAHARS FORMED FROM SLOPE FAILURES OF VOLCANIC DEPOSITS NOT SELECTIVELY SORTED

The lahars with a clay content of approximately 3 percent or more obtained much of that clay directly from hydrothermally altered volcanic rocks. This alteration implies a nearly continuously operating hydrothermal

system that would also have provided much of the water in any catastrophically ejected material. In the lower part of the modern crater are exposed predominantly dacite domes of pre-Castle Creek age (C. A. Hopson, U. Calif., Santa Barbara, written commun., 1980) that are altered to varying degrees.

The 1980 North Fork lahar was produced directly from the surface of the debris avalanche, representing the failed north flank of the mountain, and contains from 3 to 5 percent clay. The clay content of the lahar corresponds closely with the average clay content of the surficial debris avalanche, measured by Voight and others (1981) as an average of 4 percent. A similar relation between lahar origin and clay content was described by Crandell (1971) at Mount Rainier. There, however, the critical clay content was approximately 5 percent, but this higher value is partly due to sampling procedure. Lahars with more clay were ascribed by Crandell to slides of hydrothermally altered parts of the volcano; those with less were ascribed to eruptions producing block-and-ash flows or to interactions of a snowpack with pyroclastic and lava flows. Possible reasons for the somewhat lower clay content of lahars formed directly from hydrothermally altered material at Mount St. Helens include the relative youthfulness of the volcano and the occurrence of less intense or less continuous alteration.

Analogues of the 1980 North Fork lahar are relatively rare in the record of flows in the Toutle River system. The two flows of Smith Creek age are texturally comparable in clay content (where their mean grain size and facies are similar). All other flows of post-Ape Canyon age that extend far from the volcano's base fall clearly in the low-clay category. The relatively high-clay Smith Creek flows are logically interpreted as the result of a slope failure on the cone, with possible derivation via the intermediate stage of a debris avalanche. The flows may record explosive behavior (see discussion on origin of the Osceola Mudflow in Crandell, 1971), but more passive origins are also possible.

#### SUMMARY OF THE GENERAL RELATION OF LAHAR ORIGIN TO MAGNITUDE

Lahar magnitude is analyzed quantitatively in Scott (in press). Of three general sizes of lahars originating after Ape Canyon time in drainages of the northwest half of Mount St. Helens, (1) the largest lahars have formed from lake-breakout flood surges bulked by stream alluvium; (2) most intermediate-size lahars have probably originated (a) from meltwater floods produced by lithic pyroclastic flows derived from major dome

explosions, and (b) from catastrophic ejection of saturated cone material, either by transformation of voluminous but dilute pyroclastic surges, gravity transformations of large volumes of basal avalanches that continued as lahars, or the continuation of explosively induced avalanches; and (3) a probably large number of smaller lahars have resulted from eruption-induced snowmelt. Pumice-rich lahars of intermediate size were associated with large pumiceous pyroclastic flows during Ape Canyon time and probably formed by bulking of their associated meltwater surges. The larger of the two flows ascribed to possible slope failure in the Smith Creek period also falls in the intermediate category.

#### INTERPRETATIONS OF LAHAR DYNAMICS BASED ON TEXTURE

The rate of downstream transformation to a lahar-runout flow is strongly influenced by the amount of clay in a lahar, partly because the more granular, less cohesive low-clay debris flows have greater permeability and greater miscibility with overrun streamflow. The 1980 North Fork lahar, with 3 to 5 percent clay, traveled more than 100 km to the Columbia River without transforming but nevertheless showed continuous, gradual textural change in the direction of transformation.

The modern lahars that transformed attenuated more rapidly in peak discharge than did the 1980 North Fork lahar, and Scott (in press) showed that the older flow PC 1, which transformed, also attenuated rapidly. Because the typical lahar in the river system is of the low-clay variety and transformed to a lahar-runout flow, lahar flood routing and flow models should incorporate this behavior. The lahars are not simply waves of a constant mixture of mud, sand, and gravel moving through the system. At Mount St. Helens, they may be visualized more accurately as a flow wave beginning and ending as a streamflow surge, with only the middle segment consisting of debris flow.

A corollary, that the relatively high-clay lahars will move the longest distances, is true at Mount St. Helens if lahars are defined in the strict sense (that is, as debris flow). Lahars of equivalent initial magnitudes will move untransformed as debris flows for distances roughly proportional to their cohesiveness. The two largest lahars from the northwestern sector of the mountain were of the low-clay variety and did transform; even with the consequently more rapid attenuation in peak discharge, however, their distal runout flows probably exceeded, in magnitude and extent, the distal phase of the largest high-clay flow.

## REFERENCES CITED

- Bagnold, R. A., 1954, Experiments on a gravity-free dispersion of large solid spheres in a Newtonian fluid under shear: *Proceedings Royal Society London*, A225, p. 49-63.
- 1956, The flow of cohesionless grains in fluids: *Royal Society London Philosophical Transactions*, A249, p. 235-297.
- 1973, The nature of saltation and of "bed load" transport in water: *Royal Society of London Proceedings, Series A*, v. 332, p. 443-471.
- Baker, V. R., 1978, Large-scale erosional and depositional features of the Channeled Scabland, in Baker, V. R., and Nummedal, D., eds., *The Channeled Scabland, a guide to the geomorphology of the Columbia Basin*, Washington: Washington, D.C., National Aeronautics and Space Administration, p. 81-115.
- Bates, R. L., and Jackson, J. A., eds., 1980, *Glossary of geology*: Falls Church, Va., American Geological Institute, 751 p.
- Bemmelen, R. W. van, 1949, *The geology of Indonesia*, v. 1A, General geology of Indonesia and adjacent archipelagoes: The Hague, Government Printing Office, 732 p.
- Beverage, J. P., and Culbertson, J. K., 1964, Hyperconcentrations of suspended sediment: *Proceedings of American Society of Civil Engineers, Journal of the Hydraulics Division*, v. 190, no. HY6, p. 117-128.
- Bridge, J. S., 1981, Hydraulic interpretation of grain-size distributions using a physical model for bedload transport: *Journal of Sedimentary Petrology*, v. 51, p. 1109-1124.
- Brugman, M. M., and Meier, M. F., 1981, Response of glaciers to the eruptions of Mount St. Helens, in Lipman, P. W., and Mullineaux, D. R., eds., *The 1980 eruptions of Mount St. Helens*, Washington: U.S. Geological Survey Professional Paper 1250, p. 743-756.
- Carter, R. M., 1975, A discussion and classification of subaqueous mass-transport with particular application to grain-flow, slurry-flow, and fluxoturbidites: *Earth Science Reviews*, v. 11, p. 145-177.
- Chorley, R. J., 1959, The shape of drumlins: *Journal of Glaciology*, v. 3, p. 339-344.
- Costa, John E., 1984, Physical geomorphology of debris flows, in Costa, J. E. and Fleisher, P. J., eds., *Developments and applications of geomorphology*: Berlin, Springer-Verlag, p. 269-317.
- Crandell, D. R., 1971, Postglacial lahars from Mount Rainier Volcano, Washington: U.S. Geological Survey Professional Paper 677, 73 p.
- 1980, Recent eruptive history of Mount Hood, Oregon, and potential hazards from future eruptions: U.S. Geological Survey Bulletin 1492, 81 p.
- 1987, Deposits of pre-1980 pyroclastic flows and lahars from Mount St. Helens Volcano, Washington: U.S. Geological Survey Professional Paper 1444, 94 p.
- Crandell, D. R., Booth, B., Kusumadinata, K., Shimosuru, D., Walker, G. P. L., and Westercamp, D., 1984, *Source-book for volcanic-hazards zonation*: Paris, United Nations Educational, Scientific and Cultural Organization, 97 p.
- Crandell, D. R., and Mullineaux, D. R., 1973, Pine Creek volcanic assemblage at Mount St. Helens, Washington: U.S. Geological Survey Bulletin 1383-A, 23 p.
- Cummings, John, 1981, Chronology of mudflows in the South Fork and North Fork Toutle River following the May 18 eruption, in Lipman, P. W., and Mullineaux, D. R., eds., *The 1980 eruptions of Mount St. Helens*, Washington: U.S. Geological Survey Professional Paper 1250, p. 479-486.
- Daido, A., 1971, On the occurrence of mud-debris flow: *Bulletin of the Disaster Prevention Research Institute, Kyoto University*, v. 21, pt. 2, no. 187, p. 109-135.
- Davis, M. J., and Graeber, E. J., 1980, Temperature estimates of May 18 eruption of Mount St. Helens made from observations of material response [abs.], *Eos*, v. 61, p. 1136.
- Denlinger, R. P., Scott, K. M., and Pierson, T. C., 1984, Flow process and its effect on resistance in grain-supported lahars [abs.]: *Eos*, v. 65, p. 142.
- Dinehart, R. L., 1983, Patterns of sediment concentration in hyperconcentrated flows at Mount St. Helens [abs.]: *Eos*, v. 64, p. 707.
- Dinehart, R. L., Ritter, J. R., and Knott, J. M., 1981, Sediment data for streams near Mount St. Helens, Washington, v. 1, 1980 water-year data: U.S. Geological Survey Open-File Report 81-822, 87 p.
- Enos, Paul, 1977, Flow regimes in debris flow: *Sedimentology*, v. 24, p. 133-142.
- Fairchild, L. H., and Wigmosta, Mark, 1983, Dynamic and volumetric characteristics of the 18 May 1980 lahars on the Toutle River, Washington: *Proceedings of the Symposium on Erosion Control in Volcanic Areas; Seattle and Vancouver, Washington, July 6-9, 1982*, Technical Memorandum of Public Works Research Institute, Ministry of Construction, Government of Japan, no. 1908, p. 131-153.
- Fisher, R. V., 1971, Features of coarse-grained, high-concentration fluids and their deposits: *Journal of Sedimentary Petrology*, v. 41, p. 916-927.
- 1979, Models for pyroclastic surges and pyroclastic flows: *Journal of Volcanology and Geothermal Research*, v. 6, p. 305-318.
- 1983, Flow transformations in sediment gravity flows: *Geology*, v. 11, p. 273-274.
- Fisher, R. V., and Heiken, Grant, 1982, Mt. Pelée, Martinique—May 8 and 20, 1902, pyroclastic flows and surges: *Journal of Volcanology and Geothermal Research*, v. 13, p. 339-371.
- Fisher, R. V., and Schmincke, H.-U., 1984, *Pyroclastic rocks*: Berlin, Springer-Verlag, 472 p.
- Fisher, R. V., Smith, A. L., and Roobol, M. J., 1980, Destruction of St. Pierre, Martinique, by ash cloud surges, May 8 and 20, 1902: *Geology*, v. 8, p. 472-476.
- Fisher, R. V., and Waters, A. C., 1969, Bedforms in base-surge deposits—Lunar implications: *Science*, v. 165, p. 1349-1352.
- Flaxman, E. M., 1974, Potential errors in peak discharge estimates obtained by indirect methods: U.S. Department of Agriculture, Soil Conservation Service, Technical Note (Engineering) no. 5, 15 p.
- Flint, R. F., 1971, *Glacial and Quaternary Geology*: New York, Wiley and Sons, 892 p.
- Folk, R. L., 1966, A review of grain-size parameters: *Sedimentology*, v. 6, p. 73-93.
- 1980, *Petrology of sedimentary rocks*: Austin, Texas, Hemphill Publishing Company, 182 p.
- Foxworthy, B. L., and Hill, Mary, 1982, Volcanic eruptions of 1980 at Mount St. Helens—The first 100 days: U.S. Geological Survey Professional Paper 1249, 125 p.
- Friedman, G. M., 1962, On sorting, sorting coefficients and the lognormality of the grain-size distribution of sandstone: *Journal of Geology*, v. 70, p. 737-753.
- Friedman, G. M., and Sanders, J. E., 1978, *Principles of sedimentology*: New York, Wiley and Sons, 792 p.
- Gilkey, K. E., 1983, Sedimentology of the North Fork and South Fork Toutle River mudflows generated during the 1980 eruption of Mount St. Helens: Santa Barbara, Calif., University of California, M.A. thesis, 254 p.
- Hampton, M. A., 1975, Competence of fine-grained debris flows: *Journal of Sedimentary Petrology*, v. 45, p. 834-844.
- Harrison, S., and Fritz, W. J., 1982, Depositional features of March 1982 Mount St. Helens sediment flows: *Nature*, v. 299, p. 720-722.
- Heidel, S. G., 1956, The progressive lag of sediment concentration with flood waves: *American Geophysical Union Transactions*, v. 37, no. 1, p. 56-66.

- Hoblitt, R. P., Miller, C. D., and Vallance, J. W., 1981, Stratigraphy of the deposit produced by the May 18 directed blast, in Lipman, P. W., and Mullineaux, D. R., eds., The 1980 eruptions of Mount St. Helens, Washington: U.S. Geological Survey Professional Paper 1250, p. 401-419.
- Inman, D. L., 1952, Measures for describing the size distribution of sediments: *Journal of Sedimentary Petrology*, v. 22, no. 3, p. 125-145.
- Janda, R. J., 1981, Hydrologic phenomena associated with explosive Cascade volcanism [abs.]: *Eos*, v. 62, no. 45, p. 1082.
- Janda, R. J., Scott, K. M., Nolan, K. M., and Martinson, H. A., 1981, Lahar movement, effects, and deposits, in Lipman, P. W., and Mullineaux, D. R., eds., The 1980 eruptions of Mount St. Helens, Washington: U.S. Geological Survey Professional Paper 1250, p. 461-478.
- Johnson, A. M., 1970, *Physical processes in geology*: San Francisco, Freeman, Cooper and Co., 577 p.
- \_\_\_\_\_, 1979, Field methods for estimating rheological properties of debris flows: Unpublished manuscript, 36 p.
- Johnson, A. M., and Hampton, M. A., 1969, Subaerial and subaqueous flow of slurries: Final Report, U.S. Geological Survey, available from Branner Library, Stanford University, Stanford, California.
- Kellerhals, Rolf, and Bray, D. I., 1971, Sampling procedures for coarse fluvial sediments: *Proceedings of American Society of Civil Engineers, Journal of the Hydraulics Division*, v. 97, no. HY8, p. 1165-1180.
- Lawson, D. E., 1982, Mobilization, movement and deposition of active subaerial sediment flows, Matanuska Glacier, Alaska: *Journal of Geology*, v. 90, p. 279-300.
- Leopold, L. B., Wolman, M. G., and Miller, J. P., 1964, *Fluvial processes in geomorphology*: San Francisco, W.H. Freeman and Co., 522 p.
- Lipman, P. W., and Mullineaux, D. R., eds., 1981, The 1980 eruptions of Mount St. Helens, Washington: U.S. Geological Survey Professional Paper 1250, 894 p.
- Lisle, T. E., Lehre, A. K., Martinson, H. A., Meyer, D. F., Nolan, K. M., and Smith, R. D., 1983, Stream channel adjustments after the 1980 Mount St. Helens eruptions: *Proceedings of Symposium on Erosion Control in Volcanic Areas; Seattle and Vancouver, Washington, July 6-9, 1982*, Technical Memorandum of Public Works Research Institute, Ministry of Construction, Government of Japan, no. 1908, p. 31-72.
- Lombard, R. E., Miles, M. B., Nelson, L. M., Kresh, D. L., and Carpenter, P. J., 1981, The impact of mudflows of May 18 on the lower Toutle and Cowlitz Rivers, in Lipman, P. W., and Mullineaux, D. R., eds., The 1980 eruptions of Mount St. Helens, Washington: U.S. Geological Survey Professional Paper 1250, p. 693-699.
- Lowe, D. R., 1976, Grain flow and grain flow deposits: *Journal of Sedimentary Petrology*, v. 46, p. 188-199.
- \_\_\_\_\_, 1979, Sediment gravity flows—Their classification and some problems of application to natural flows and deposits: *Society of Economic Paleontologists and Mineralogists Special Publication* 27, p. 75-82.
- \_\_\_\_\_, 1982, Sediment gravity flows—II, Depositional models with special reference to the deposits of high-density turbidity currents: *Journal of Sedimentary Petrology*, v. 52, p. 279-297.
- Major, J. J., 1984, *Geologic and rheologic characteristics of the May 18, 1980 southwest flank lahars at Mount St. Helens*, Washington: University Park, Pa., Pennsylvania State University, M.S. thesis, 225 p.
- Malde, H. E., 1968, The catastrophic Late Pleistocene Bonneville Flood in the Snake River Plain, Idaho: U.S. Geological Survey Professional Paper 596, 52 p.
- Malin, M. C., and Sheridan, M. F., 1982, Computer-assisted mapping of pyroclastic surges: *Science*, v. 217, p. 637-640.
- Mandl, G., de Jong, L. N. J., and Maltha, A., 1977, Shear zones in granular material; an experimental study of their structure and mechanical genesis: *Rock Mechanics*, v. 9, p. 95-144.
- Middleton, G. V., 1970, Experimental studies related to problems of flysch sedimentation, in Lajoie, J., ed., *Flysch sedimentology in North America*: Geological Association of Canada Special Paper 7, p. 253-272.
- \_\_\_\_\_, 1976, Hydraulic interpretation of sand size distributions: *Journal of Geology*, v. 84, p. 405-426.
- Middleton, G. V., and Hampton, M. A., 1976, Subaqueous sediment transport and deposition by sediment gravity flows, in Stanley, D. J., and Swift, D. J. P., eds., *Marine sediment transport and environmental management*: New York, Wiley and Sons, p. 197-218.
- Moore, J. G., 1967, Base surge in recent volcanic eruptions: *Bulletin Volcanologique*, v. 30, p. 337-363.
- Moore, J. G., and Albee, W. C., 1981, Topographic and structural changes, March-July 1980—photogrammetric data, in Lipman, P. W., and Mullineaux, D. R., eds., The 1980 eruptions of Mount St. Helens, Washington: U.S. Geological Survey Professional Paper 1250, p. 123-141.
- Moore, J. G., and Melson, W. G., 1969, Nuées ardentes of the 1968 eruption of Mayon Volcano, Philippines: *Bulletin Volcanologique*, v. 33, p. 600-620.
- Moore, J. G., and Rice, C. J., 1981, Chronology and character of Mt. St. Helens explosive eruptive phase of May 18, 1980 [abs.]: *Eos*, v. 62, no. 45, p. 1081-1082.
- Moore, J. G., and Sisson, T. W., 1981, Deposits and effects of the May 18 pyroclastic surge, in Lipman, P. W., and Mullineaux, D. R., eds., The 1980 eruptions of Mount St. Helens, Washington: U.S. Geological Survey Professional Paper 1250, p. 421-438.
- Mullineaux, D. R., 1986, Summary of pre-1980 tephra-fall deposits erupted from Mount St. Helens, Washington State, USA: *Bulletin of Volcanology*, v. 48, p. 17-26.
- Mullineaux, D. R., and Crandell, D. R., 1962, Recent lahars from Mount St. Helens, Washington: *Geological Society of America Bulletin*, v. 73, p. 855-870.
- \_\_\_\_\_, 1981, The eruptive history of Mount St. Helens, in Lipman, P. W., and Mullineaux, D. R., eds., The 1980 eruptions of Mount St. Helens, Washington: U.S. Geological Survey Professional Paper 1250, p. 3-15.
- Naylor, M. A., 1980, The origin of inverse grading in muddy debris flow deposits—A review: *Journal of Sedimentary Petrology*, v. 50, p. 1111-1116.
- Neall, V. E., 1976a, Lahars as major geological hazards: *Bulletin of the International Association of Engineering Geology*, no. 14, p. 233-240.
- \_\_\_\_\_, 1976b, Lahars—Global occurrence and annotated bibliography: Publication of Geology Department, Victoria University of Wellington, New Zealand, no. 5, 18 p.
- Nordin, C. F., Jr., 1963, A preliminary study of sediment transport parameters, Rio Puerco near Bernardo, New Mexico: U.S. Geological Survey Professional Paper 462-C, 21 p.
- Orwig, C. E., and Mathison, J. M., 1982, Forecasting considerations in Mount St. Helens affected rivers: *Proceedings of Conference, Mount St. Helens—Effects on Water Resources*, Oct. 7-8, 1981, Jantzen Beach, Oreg., Washington Water Research Center, p. 272-292.
- Pierson, T. C., 1980, Erosion and deposition by debris flows at Mt. Thomas, North Canterbury, New Zealand: *Earth Surface Processes*, v. 5, p. 227-247.
- \_\_\_\_\_, 1985, Initiation and flow behavior of the 1980 Pine Creek and Muddy River lahars, Mount St. Helens, Washington: *Geological Society of America Bulletin*, v. 96, p. 1056-1069.

- Pierson, T. C., and Scott, K. M., 1985, Downstream dilution of a lahar: transition from debris flow to hyperconcentrated streamflow: *Water Resources Research*, v. 21, p. 1511-1524.
- Qian Yiying, Yang Wenhai, Zhao Wenlin, Cheng Xiuwen, Zhang Longrong, and Xu Wengui, 1980, Basic characteristics of flow with hyperconcentration of sediment, in Li Boning, chairperson, *Proceedings of the International Symposium on River Sedimentation*, March 24-29, 1980, Beijing, China: Beijing, Guanghai Press, p. 175-184.
- Rice, C. J., and Watson, D. K., 1981, Satellite observations of Mount St. Helens: *Eos*, v. 62, no. 28, p. 577-578.
- Rose, W. I. Jr., Pearson, T., and Bonis, S., 1977, Nuée ardente eruption from the foot of a dacite lava flow, Santiaguito Volcano, Guatemala: *Bulletin Volcanologique*, v. 40, no. 1, p. 23-38.
- Rosenbaum, J. G., and Waitt, R. B. Jr., 1981, Summary of eyewitness accounts of the May 18 eruption, in Lipman, P. W., and Mullineaux, D. R., eds., *The 1980 eruptions of Mount St. Helens*, Washington: U.S. Geological Survey Professional Paper 1250, p. 53-67.
- Schieferdecker, A. A. G., ed., 1959, *Geological nomenclature*: Gorinchem, Netherlands, Royal Geological and Mining Society, 521 p.
- Schmid, R., 1981, Descriptive nomenclature and classification of pyroclastic deposits and fragments—Recommendations of the IUGS Subcommittee on the Systematics of Igneous Rocks: *Geology*, v. 9, p. 41-43.
- Schmincke, H.-U., 1967, Graded lahars in the type sections of the Ellensburg Formation, south-central Washington: *Journal of Sedimentary Petrology*, v. 37, p. 438-448.
- Scott, K. M., 1967, Downstream changes in sedimentological parameters illustrated by particle distribution from a breached rockfill dam, in *Symposium on river morphology*, General Assembly of Bern, 1967, Reports and discussions: International Association of Scientific Hydrology Publication 75, p. 309-318.
- \_\_\_\_\_, 1971, Origin and sedimentology of 1969 debris flows near Glendora, California: U.S. Geological Survey Professional Paper 750-C, p. 242-247.
- \_\_\_\_\_, 1982, Erosion and sedimentation in the Kenai River, Alaska: U.S. Geological Survey Professional Paper 1235, 35 p.
- \_\_\_\_\_, 1984, Flow transformations and textural variation in lahars at Mount St. Helens, Washington (abst.): *Geological Society of America Abstracts with Programs*, v. 16, no. 6, p. 649.
- \_\_\_\_\_, 1985a, Lahars and flow transformations at Mount St. Helens, Washington, U.S.A.: *Proceedings of International Symposium on Erosion, Debris Flow, and Disaster Prevention*, Tsukuba, Japan, p. 209-214.
- \_\_\_\_\_, 1985b, Origin, behavior, and sedimentology of catastrophic lahars at Mount St. Helens, Washington: *Geological Society of America Abstracts with Programs*, v. 17, no. 7, p. 711.
- \_\_\_\_\_, in press, Magnitude and frequency of lahars and lahar-runout flows in the Toutle-Cowlitz River system: U.S. Geological Survey Professional Paper 1447-B.
- Scott, K. M., and Gravlee, G. C., 1968, Flood surge on the Rubicon River, California—Hydrology, hydraulics, and boulder transport: U.S. Geological Survey Professional Paper 422-M, 40 p.
- Scott, K. M., and Janda, R. J., 1982, Preliminary map of lahar inundation during the Pine Creek eruptive period in the Toutle-Cowlitz River system, Mount St. Helens, Washington: U.S. Geological Survey Water Resources Investigations Report 82-4067.
- Sharp, R. P., and Nobles, L. H., 1953, Mudflow of 1941 at Wrightwood, southern California: *Geological Society of America Bulletin*, v. 64, p. 547-560.
- Sheridan, M. F., 1979, Emplacement of pyroclastic flows—A review: *Geological Society of America Special Paper 180*, p. 125-136.
- Sheridan, M. F., and Wohletz, K. H., 1981, Hydrovolcanic explosions—The systematics of water-pyroclast equilibrium: *Science*, v. 212, p. 1387-1389.
- \_\_\_\_\_, 1983, Hydrovolcanism—Basic considerations and review: *Journal of Volcanology and Geothermal Research*, v. 7, p. 1-27.
- Sparks, R. S. J., 1976, Grain size variations in ignimbrites and implications for the transport of pyroclastic flows: *Sedimentology*, v. 23, p. 147-188.
- Sparks, R. S. J., Self, S., and Walker, G. P. L., 1973, Products of ignimbrite eruptions: *Geology*, v. 1, p. 115-118.
- Sparks, R. S. J., and Walker, G. P. L., 1973, The ground surge deposit; a third type of pyroclastic rock: *Nature, Physical Science*, v. 241, p. 62-64.
- Takahashi, T., 1981, Debris flow: *Annual Review of Fluid Mechanics*, v. 13, p. 57-77.
- U.S. Army Corps of Engineers, 1984, *Sedimentation study, Mount St. Helens, Cowlitz and Toutle Rivers*: Portland District, 67 p.
- Varnes, D. J., 1978, Slope movement types and processes, in Schuster, R. L., and Krizek, R. J., eds., *Landslides—Analysis and control*: National Research Council Transportation Research Board Special Report 176, p. 11-33.
- Visher, G. S., 1969, Grain size distributions and depositional processes: *Journal of Sedimentary Petrology*, v. 39, p. 1074-1106.
- Voight, Barry, Glicken, Harry, Janda, R. J., and Douglass, P. M., 1981, Catastrophic rockslide avalanche of May 18, in Lipman, P. W., and Mullineaux, D. R., eds., *The 1980 eruptions of Mount St. Helens*, Washington: U.S. Geological Survey Professional Paper 1250, p. 347-377.
- Voight, Barry, Janda, R. J., Glicken, Harry, and Douglass, P. M., 1983, Nature and mechanics of the Mount St. Helens rockslide-avalanche of 18 May 1980: *Geotechnique*, v. 33, p. 243-273.
- Waitt, R. B., Jr., 1981, Devastating pyroclastic density flow and attendant air fall of May 18—Stratigraphy and sedimentology of deposits, in Lipman, P. W., and Mullineaux, D. R., eds., *The 1980 eruptions of Mount St. Helens*, Washington: U.S. Geological Survey Professional Paper 1250, p. 439-458.
- Waitt, R. B., Jr., Pierson, T. C., MacLeod, N. S., Janda, R. J., and Holcomb, R. T., 1983, Explosive eruption, avalanche, flood, and lahar at Mount St. Helens on 19 March 1982—Amplification of eruptive effects by a winter snowpack: *Science*, v. 221, p. 1394-1397.
- Walker, G. P. L., 1971, Grain-size characteristics of pyroclastic deposits: *Journal of Geology*, v. 79, p. 696-714.
- \_\_\_\_\_, 1983, Ignimbrite types and ignimbrite problems: *Journal of Volcanology and Geothermal Research*, v. 7, p. 65-88.
- Waters, A. C., and Fisher, R. V., 1971, Base surges and their deposits—Capelinhos and taal volcanoes: *Journal of Geophysical Research*, v. 75 p. 5596-5614.
- Winner, W. E., and Casadevall, T. J., 1981, Fir leaves as thermometers during the May 18 eruption, in Lipman, P. W., and Mullineaux, D. R., eds., *The 1980 eruptions of Mount St. Helens*, Washington: U.S. Geological Survey Professional Paper 1250, p. 315-320.
- Wohletz, K. H., and Sheridan, M. F., 1979, A model of pyroclastic surge, in Chapin, C. E., and Elston, W. E., eds., *Ash-flow tuffs*: *Geological Society of America Special Paper 180*, p. 177-194.
- Wolman, M. G., 1954, A method of sampling coarse river-bed material: *American Geophysical Union Transactions*, v. 35, p. 951-956.
- Wright, J. V., Smith, A. L., and Self, S., 1980, A working terminology of pyroclastic deposits: *Journal of Volcanology and Geothermal Research*, v. 8, p. 315-336.
- Yesenov, U. Ye., and Degovets, A. S., 1979, Catastrophic mudflow on the Bol'shaya Almatinka River in 1977: *Soviet Hydrology; Selected Papers*, v. 18, p. 158-160.

---

---

## APPENDIX

---

---

## EQUATIONS USED IN CALCULATING LAHAR VELOCITY AND STATISTICS OF GRAIN SIZE DISTRIBUTIONS

### VELOCITY

The mean velocity of the 1980 South Fork lahar at peak stage was calculated locally from the tilt of the superelevated flow surface at a channel bend and the radius of curvature of the bend (Johnson, 1979, p. 27):

$$\bar{u} = (Rg \cos S \tan B)^{1/2}$$

where:  $\bar{u}$  = mean velocity  
 $R$  = radius of curvature of bend  
 $g$  = acceleration of gravity  
 $S$  = angle of channel slope  
 $B$  = angle of tilt of flow surface measured perpendicular to flow direction

Velocity was also determined by measuring the vertical distance of runup against valley walls and bedrock projections where flow impinged at a high angle:

$$\bar{u} = (2gh)^{1/2}$$

where:  $\bar{u}$  = mean velocity  
 $h$  = height of runup

The uncertainties and qualifications of the results of these techniques are discussed by Fairchild and Wigmosta (1983) and Pierson (1985). Regardless of whether the derived velocity determinations are absolutely accurate, they clearly document the abrupt downstream decline in relative velocity and discharge that accompanied flow deflation.

### GRAIN SIZE STATISTICS

The statistics of the grain size distributions are described by the graphically derived measures of Folk (1980). With cumulative frequency plotted on probability paper as percentage of grains finer than the limit of each phi class, mean grain size is defined as the graphic mean,

$$M_z = (\phi_{16} + \phi_{50} + \phi_{84})/3$$

Standard deviation is defined as the graphic standard deviation,

$$\sigma_G = (\phi_{16} - \phi_{84})/2$$

Standard deviation can also be defined as the inclusive graphic standard deviation,

$$\sigma_I = (\phi_{16} - \phi_{84})/4 + (\phi_5 - \phi_{95})/6.6$$

Skewness is defined as the graphic skewness,

$$Sk_G = \frac{\phi_{16} + \phi_{84} - 2\phi_{50}}{\phi_{16} - \phi_{84}}$$

Skewness can also be defined as the inclusive graphic skewness,

$$Sk_I = \frac{\phi_{16} + \phi_{84} - 2\phi_{50}}{2(\phi_{16} - \phi_{84})} + \frac{\phi_5 + \phi_{95} - 2\phi_{50}}{2(\phi_5 - \phi_{95})}$$

Kurtosis is defined as the graphic kurtosis,

$$K_G = \frac{\phi_{95} - \phi_5}{2.44(\phi_{75} - \phi_{25})}$$